

INVESTIGATION OF NOVEL NRF2 PARTNERS, RAC3 AND IQGAP1

by

JUNG-HWAN KIM

A Dissertation submitted to the
Graduate School-New Brunswick
Rutgers, The State University of New Jersey
in partial fulfillment of the requirements

for the degree of

Doctor of Philosophy

Graduate Program in Pharmaceutical Science

written under the direction of

Professor Ah-Ng Tony Kong, Ph.D.

and approved by

New Brunswick, New Jersey

May, 2009

ABSTRACT OF THE DISSERTATION

Investigation of Novel Nrf2 Partners, RAC3 and IQGAP1

By JUNG-HWAN KIM

Dissertation Director:

Professor Ah-Ng Tony Kong

Nuclear factor-erythroid-related factor 2 (Nrf2) is essential for the antioxidant responsive element (ARE)-mediated expression of a group of detoxifying and antioxidant genes, which detoxify carcinogens and protect against oxidative stress. In the current study, we investigated the novel Nrf2 partners RAC3/AIB1/SRC-3 and IQGAP1 on Nrf2 signaling. Here, we found that overexpression of RAC3, a nuclear co-regulator, induced Heme oxygenase-1 through Nrf2 transactivation in HeLa cells. Next, we conducted the interaction study between the RAC3 and Nrf2 proteins using co-immunoprecipitation assay (Co-IP) and Fluorescence Resonance Energy Transfer (FRET) analysis. The results showed that RAC3 bound to Nrf2 protein directly in the nucleus. Subsequently, we identified the domains of Nrf2 and RAC3 of their interaction using GST-pull down assay. The results showed that both N-terminal RAC-pas B and C-terminal RAC3-R3B3 were tightly bound to Neh4 and Neh5 transactivation domains. Furthermore, chromatin immunoprecipitation (ChIP) showed that RAC3 tightly bound to the ARE enhancer

region of the HO-1 promoter via Nrf2 binding. The data suggested that Nrf2 activation can be modulated and directly controlled via interacts with RAC3 protein in the HeLa cells. Next, we investigated IQGAP1, a calmodulin binding protein, as a novel Nrf2 partner isolated using One-strep tag pull-down method in HeLa cells. Initially, we tested the effect of calcium on Nrf2/ARE-luciferase activity and heme oxygenase-1 (HO-1) protein induction in HeLa cells. The results showed that Nrf2/ARE-luciferase activity and expression of HO-1 were increased by treatment of 3.8 mM of CaCl₂, suggesting calcium may be one of the important factors in Nrf2 signaling. Next, we investigated a function of IQGAP1 on Nrf2 signaling by co-transfection with EGFP-Nrf2 and Dsredm-IQGAP1 constructs in HeLa cells. The results showed that Dsredm-IQGAP1 transfection strongly increased the HO-1 expression and the stability of EGFP-Nrf2, which was abolished by siIQGAP1. Furthermore, IP study showed that the Nrf2-IQGAP1 complex was disrupted by CaCl₂ treatment suggesting Nrf2 might be liberated from IQGAP1 protein by calcium to be an active form. These results inferred that IQGAP1 may play a pivotal role in Nrf2 signaling in conjunction with intracellular calcium level. Taken together, our results suggest that both RAC3 and IQGAP1 may play an important role in Nrf2 transactivation and its signaling pathway, respectively.

PREFACE

This thesis is submitted for the Degree of Doctor of Philosophy in Pharmaceutical Sciences at Rutgers, The State University of New Jersey. It serves as documentation of my research work carried out between September 2003 and May 2009 under the supervision of Dr. Ah-Ng Tony Kong at Department of Pharmaceutics, Ernest Mario School of Pharmacy, Rutgers, The State University of New Jersey. To the best of my knowledge, this work is original, except where suitable references are made to previous work.

The thesis contains one major work and two supplementary works (suppl. 1 and 2). The major work is provide the functional roles of both RAC3 and IQGAP1 in Nrf2 signaling, which is responsible for the induction of antioxidant and phase II genes response to oxidative/chemical stresses. Suppl. 1 and 2 describes the combination effect of chemopreventive agents on prostate cancer and MRP2 (multidrug resistance protein 2), respectively. Suppl. 1 is already published in *Carcinogenesis* and others works are intended to be submitted to the peer-reviewed journals.

Jung-Hwan Kim

May 2009

ACKNOWLEDGEMENT

First of all, I would like to thank my advisor, Dr. Ah-Ng Tony Kong. Without his support, I wouldn't be able to achieve my Ph.D degree. I'm also indebted to Drs. Suzie Chen, Nanjoo Suh and Don Chen, who serve on my thesis committee for their valuable comments. And, I want to express my gratitude to my previous mentors Dr. Kyoung-Ja Kim in Soonchunhyang University, Dr. Young-Joon Surh in Seoul National University, and Dr. Jae-Young Koh in University of Ulsan College of Medicine, South Korea. And I also appreciate Dr. Kwang-Kyun Park in Yeonsei University, Drs. Kui-Lea Park, Soon-Young Han and Tae-Sung Kim in Korea Food and Drug Administration, Dr. Hyung-Sik Kim in Pusan National University in South Korea.

It is my pleasure to acknowledge all the Dr. Kong's past and present colleagues, Vidya Hebbar, Woo-Sik Jeong, Changjiang Xu, Wenge Li, Mohit Raja Jain, Xiaoling Yuan, Tin Oo Khor, Siwang Yu, Auemduan Prawan, Chi Chen, Rong Hu, Young-Sam Keum, Sujit Nair for their valuable help on my work. I also appreciate Ms. Hui Pung for her administrative support.

Lastly, I would like to thank my mom, dad, brother and two sisters for their invaluable sacrifice.

DEDICATION

To my parents

TABLE OF CONTENTS

ABSTRACT OF THE DISSERTATION	ii
PREFACE	iv
ACKNOWLEDGEMENT	v
DEDICATION	vi
LIST OF TABLES	xi
LIST OF FIGURES	xii
ABBREVIATIONS.....	xv
1.1. INTRODUCTION	1
1.2. MATERIALS AND METHODS	10
1.2.1. Materials	10
1.2.2. Cell Culture.....	11
1.2.3. Construction of Plasmids.....	11
1.2.4. Fusion Protein Purification and GST Pull-down Assay	14
1.2.5. Western Blot Analysis.....	16
1.2.6. Reverse Transcriptase PCR (RT-PCR)	16
1.2.7. Transient Transfection and Reporter Gene Activity Assays	17
1.2.8. Stable Transfection to HeLa Cells	19
1.2.9. Co-Immunoprecipitation (IP)	19
1.2.10. Fluorescence Resonance Energy Transfer (FRET) Analysis.....	21
1.2.11. Chromatin Immunoprecipitation (ChIP) Assay	22
1.2.12. Nrf2 Partner Pull-down with One-strep Tactin System.....	25
1.2.13. Epifluorescence	26

1.2.14. Statistics	26
1.3. RESULTS	26
1.3.1. RAC3 suppresses Nrf2/ARE activity	26
1.3.2. Different effect of RAC3 in Human Embryonic Kidney 293 (HEK293) cells ...	28
1.3.3. Expression of Heme oxygenase-1 (HO-1) was increased by RAC3	29
1.3.4. Nrf2 directly binds RAC3.....	29
1.3.5. N-terminal pasB and C-terminal RAC3 (R3B3) regions bind to Nrf2.....	31
1.3.6. PasB and R3B3 regions of RAC3 bind to N-terminal transactivation domains Neh5 of Nrf2.....	32
1.3.7. RAC3 binds to ARE region in heme oxygenase-1	33
1.3.8. Ca^{2+} activates Nrf2/ARE-luciferase activity and induces Heme oxygenase-1 expression	34
1.3.9. Fourteen Nrf2-partner candidates were isolated and identified from the One- STrEP™ purification system and LTQ_Orbitrap LC/MS/MS equipment, respectively	35
1.3.10. IQGAP1 enhances Nrf2 stability and HO-1 expression.....	35
1.3.11. Silencing of IQGAP1 makes Nrf2 unstable and that results in inhibition of heme oxygenase-1 expression.....	36
1.3.12. The two endogenous Nrf2 and IQGAP1 bind together	37
1.3.13. Nrf2-IQGAP1 complex was disrupted by calcium.....	37
1.3.14. Calcium stimulates the expression of heme oxygenase-1 in early time	38
1.4. DISCUSSION	38
1.5. SUMMARY	80

SUPPL. 1: INHIBITION OF EGFR SIGNALING IN HUMAN PROSTATE CANCER

PC-3 CELLS BY COMBINATION TREATMENT WITH BETA-PHENYLETHYL ISOTHIOCYANATE AND CURCUMIN	82
2.1 ABSTRACT	83
2.2 INTRODUCTION	84
2.3 MATERIALS AND METHODS	86
2.3.1. Materials	86
2.3.2. Cell Lines	86
2.3.3. MTT Assay	87
2.3.4. Luciferase Assay	87
2.3.5. Determination of DNA Fragmentation	88
2.3.6. Western Blotting	88
2.3.7. Immunofluorescence	89
2.4 RESULTS	89
2.4.1. Combination treatment with curcumin and PEITC has an additive inhibitory effect on cell survival signaling pathways in PC-3 C4 cells	89
2.4.2. EGFR signaling and NF- κ B signaling are activated by EGF	90
2.4.3. PEITC has an enhanced inhibitory effect on EGFR phosphorylation when it is combined with curcumin in EGF-stimulated PC-3 C4 cells	91
2.4.4. Combination treatment with PEITC and curcumin significantly inhibits EGFR signaling in PC-3 cells	92
2.5. DISCUSSION	93
 SUPPL. 2: RESVERATROL INHIBITS GENISTEIN-INDUCED MULTI-DRUG RESISTANCE PROTEIN 2 (MRP2) EXPRESSION IN HEPG2 CELLS	107

3.1. ABSTRACT	108
3.2. INTRODUCTION	109
3.3. MATERIALS AND METHODS	112
3.3.1. Materials	112
3.3.2. Cell culture	112
3.3.3. Cell proliferation assay	113
3.3.4. Luciferase assay	113
3.3.5. Western blotting	114
3.3.6. RNA extraction and RT-PCR	114
3.3.7. Immunofluorescence	115
3.3.8. DNA-Protein pull-down assay	116
3.4 RESULTS	117
3.4.1. Toxicity of genistein and resveratrol in HepG2-C3 cells	117
3.4.2. Effects of genistein and resveratrol on MRP2-Luciferase activity	117
3.4.3. Inhibition of genistein-induced MRP2 protein by resveratrol	118
3.4.4. Suppression of genistein-induced MRP2 mRNA by resveratrol	118
3.4.5. Inhibition of genistein-induced MRP2 vacuoles by resveratrol	119
3.4.6. Inhibitory effect of resveratrol on genistein- or rifampicin-induced binding activity between RXR α and MRP2 promoter DNA	119
3.5 DISCUSSION	120
REFERENCES	135
CURRICULUM VITAE	150

LIST OF TABLES

Table 1. Identified Nrf2 partners from LC/MS/MS	79
---	----

LIST OF FIGURES

Fig.1-1. Schematic diagram showing the different structures of segmented domains of His-Nrf2 and GST-RAC3 for GST pull-down assay.	47
Fig.1-2. Nrf2/ARE-luciferase activity was suppressed by RAC3 and recovered by siRAC3.	49
Fig.1-3. RAC3 silencing increases Nrf2/luciferase activity.	51
Fig.1-4. Transient transfection of RAC3 shows different results in Nrf2/ARE luciferase between HeLa and HEK293 cells.	53
Fig.1-5. HO-1 protein and its mRNA were induced by transient transfection with Nrf2 and RAC3 and decreased by siRAC3.	54
Fig.1-6. Nrf2 binds directly to RAC3 protein.	56
Fig.1-7. pasB and R3B3 domains of RAC3 bind to Nrf2.	58
Fig.1-8. pasB and R3B3 regions in RAC3 strongly bind to N2 containing Neh5 domain of Nrf2.	60
Fig.1-9. Fluorescence Resonance Energy Transfer (FRET) signals were strong between pasB and R3B3 regions in RAC3 and N2 containing Neh5 domain of Nrf2.	62
Fig.1-10. RAC3 and Nrf2 bind to the ARE enhancers in 5'-flanking region of hemeoxygenase-1 (HO-1) promoter.	63
Fig.1-11. Cartoon shows a possible interaction between Nrf2 and RAC3 in the ARE enhancer region of hemeoxygenase-1 (HO-1) promoter (upper) by direct interactions between specific domains (lower).	65
Fig.1-12. Verification of conditions for Nrf2-partner candidate pull-down with One-	

strep tactin system.....	66
Fig.1-13. Purification and identification of novel Nrf2 partners.....	68
Fig.1-14. IQGAP1 enhances expression of Nrf2 and induction HO-1 expression.	70
Fig.1-15. The stability of Nrf2 is increased by IQGAP1.....	72
Fig.1-16. siIQGAP1 suppresses HO-1 expression and ARE-luciferase activity. .	74
Fig.1-17. Nrf2 escapes from the IQGAP1 by calcium.	76
Fig.1-18. Calcium, in early time, stimulates the expression of HO-1 protein.	77
Fig.1-19. A schematic representation of possible mechanisms of Nrf2 activation through IQGAP1 protein in the presence of calcium.....	78
Fig.1-20. The schematic representation shows the summary for the possible mechanisms of Nrf2 activation through RAC3 and IQGAP1 protein.....	81
Fig. 2-1. Combined effects of PEITC and curcumin on cell death and NF- κ B signaling pathways in PC-3 human prostate cancer cells.....	98
Fig. 2-2. Effects of EGF on EGFR signaling in PC-3 C4 cells.....	100
Fig. 2-3. Inhibition of EGFR phosphorylation by PEITC, curcumin, and their combination after stimulation of PC-3 C4 cells with EGF.....	102
Fig. 2-4. Additive inhibition of EGFR signaling in PC-3 parental cells by combination of PEITC and curcumin.	104
Fig. 2-5. A schematic representation of possible mechanisms for the combined effect of PEITC and curcumin on EGFR signaling and apoptosis in PC-3 cells.	106
Fig.3-1. Chemical structures of genistein and resveratrol.....	124

Fig.3-2. Cytotoxicity of genistein and resveratrol in HepG2-C3 cells	125
Fig.3-3. Resveratrol inhibits genistein-induced MRP2-luciferase activity.	126
Fig.3-4. Resveratrol inhibits genistein-induced MRP2 protein.	128
Fig.3-5. Resveratrol suppresses genistein-induced <i>MRP2</i> mRNA.	129
Fig.3-6. Genistein-induced apical MRP2 vacuoles were repressed by Resveratrol.	131
Fig.3-7. Resveratrol suppresses RXR α binding in the MRP2 promoter.	133

ABBREVIATIONS

Nrf2, Nuclear factor-erythroid 2-related factor 2

RAC-3, Receptor-associated coactivator 3

AIB-1, Amplified in breast cancer-1 protein

SRC-3, Steroid receptor coactivator protein 3

NCoA-3, Nuclear receptor coactivator 3

TRAM-1, Thyroid hormone receptor activator molecule 1

ACTR, Activator of retinoid and thyroid receptors

pCIP, CBP-interacting protein. Neh, Nrf2-ECH homology

TAD, transactivation domain

CARM1, Coactivator-associated arginine methyltransferase

PRMT1, Protein arginine methyl-transferase 1

p/CAF, p300/CBP-associated factor

GST, glutathione S-transferase

NQO1, NAD(P)H: quinone oxidoreductase 1

UGT, UDP-glucuronosyltransferase

γ GCS, γ -glutamylcystein synthetase

ARE/EpRE, Anti-oxidant responsive element/electrophile response element;

Keap1, Kelch-like ECH-associated protein 1

HO-1, Heme oxygenase-1

MAPK, Mitogen-activated protein kinase

IQGAP1, IQ motif containing GTPase activating protein 1

1.1. Introduction

Mammalian cells have developed efficient machinery to maintain the balance of redox status from the extracellular environment and/or intracellular oxidative electrophilic stresses. When cells are exposed to sub-lethal levels of oxidative stresses, defensive battery of genes can be triggered rapidly to protect the cells as an adaptive response. However, at time failure of the antioxidant machinery or prolonged oxidative stress leads to tissue damage or aberrant modification of macromolecules resulting in certain diseases including cancers.

Onset of human cancer can be occurred by insult of chemical carcinogens which are the most important factor in carcinogenesis. Of course other factors such as virus infection and UV/radioactive irradiation may also lead to various types of cancers. Many research works have shown that many carcinogens can obtain their carcinogenic activity during the biotransformation. This reaction is referred to as metabolic activation, which is, basically, processed by a large number of cytochrome p450 superfamilies (CYPs). If reactive metabolites were not eliminated from the body properly, these will attack the critical cellular macromolecules such as DNA, RNA and protein and cause abnormal cell conditions.

In order to counteract such undesired effects, human body tissues/cells have developed an elaborate detoxification system, so called phase II metabolism, which can increase the solubility of reactive chemicals through enzymatic conjugation, such as glucuronidation, glutathione conjugation and sulfation and thereby facilitate the elimination of harmful carcinogens from the body. In this regard, the induction of phase II enzymes has been considered as one of the successful strategies for cancer prevention

(17).

Defense system, against to the oxidative stresses and chemical insults, can be activated by expression of detoxifying enzymes including phase II drug metabolizing detoxifying enzymes, such as glutathione S-transferase (GST), NAD(P)H: quinone oxidoreductase 1(NQO1), UDP-glucuronosyltransferase (UGT) (15, 123, 190) and anti-oxidant enzymes, such as heme oxygenase-1 (HO-1) (3) and γ -glutamylcystein synthetase (γ GCS) (119) as well as multidrug ABC transporters, such as MRP1 and MRP2 (multidrug-resistance-associated protein 1 or 2) (52, 168).

These genes are generally controlled and regulated by the nuclear factor-erythroid 2-related factor 2 (Nrf2)(95, 119, 168), a transcription factor belonging to the Cap “n” Collar (CNC) family and posses a highly conserved basic leucine zipper (bZIP) region (83). As defense machinery against oxidative stress, detoxification and antioxidant related genes are coordinately regulated through a *cis*-acting enhancer element called anti-oxidant responsive element/electrophile response element [ARE/EpRE, 5'-(A/G)TGACNNNGC (A/G)-3] at their 5'-flanking regions (87, 104, 144). Originally, activator protein 1 (AP-1), a transcription factor, was considered as ARE binding molecule because of the high similarity between the ARE and the TPA response element (TRE; TGACTCA). However, subsequent studies showed that overexpression of AP-1 molecules did not activate but rather inhibited the ARE (166).

Moi *et al.* in 1994, cloned and characterized Nrf2 based on its binding affinity to NF-E2/AP-1 repeat in the promoter of beta-globin gene (122). Later, Itoh *et al.* suggested that Nrf2/small Maf might be able to activate gene expression directly through the ARE and demonstrated that disruption of *nrf2* (+/-) mice showed a significant reduction of GSTs

and NQO1 level, compared with wild type nrf2 (+/+) mice (63).

Subsequently, a pivotal role of Nrf2 in managing of oxidative or electrophilic stress has been shown in Nrf2 knockout mice studies. In the absence of Nrf2 gene, induction of detoxifying enzymes against oxidative stress are dramatically abolished and the Nrf2 knockout mice are much more sensitive to oxidative stress-induced lung injury and more susceptible to carcinogens (16, 38, 96).

Human Nrf2, basically, is homologous to mouse and chicken and contains six highly conserved domains, Neh1 (Nrf2 ECH homology 1) to Neh6 (64). The Neh1 has a CNC-type basic leucine zipper for DNA binding and dimerization with other transcription factors. In addition, a functional NLS (nuclear localization signal) has been identified in this domain (66). Neh2 is a Keap1 binding domain, which controls Nrf2 negatively by allowing Nrf2 to be targeted by the Cullin 3-based E3 ubiquitin ligase complex for ubiquitination involved proteasomal degradation (64, 81). Neh3 is a C-terminal domain, which is responsible for transcriptional activation by recruiting a coactivator (130). Neh4 and Neh5 are transactivation domains, which interact with CBP (CREB-binding protein) and BRG1 (Brahma-related gene 1) (73, 189). Lastly, Neh6 domain has highly concentrated serine residues and functions as a degron in the nucleus for destabilization of Nrf2 under oxidative conditions (120).

Understanding of the Nrf2 regulation has been progressed by the cloning of Keap1 (Kelch-like ECH-associated protein 1) gene. Keap1 is basically comprised three major domains, Broad complex, Tramtrack, and Bric-a-brac (BTB) in the N-terminal, intervening region (IVR) in the central, and kelch repeats in the C-terminal. The kelch repeats of keap1 directly bind to the Neh2 domain of Nhe2 (82, 124). It is, to date,

widely accepted that Keap1 protein functions as a negative regulator by modulating as a molecular sensor or switch on Nrf2 signaling under intracellular redox conditions. Under normal condition, Nrf2 forms a dimer with Keap1 in the cytoplasm. However, under oxidative stress condition, Nrf2-Keap1 complex can be disrupted to allow Nrf2 to translocate into the nucleus for the transcription of detoxifying genes by binding to the ARE enhancer (82, 124).

Although many studies have shown that chemopreventive agents can lead to the nuclear accumulation of Nrf2, resulting in induction of Nrf2-dependent gene (6, 53, 137, 161), precise mechanisms on Nrf2 transactivation triggered by chemicals or oxidative/electrophile stresses are still unclear. Several mechanisms have been questioned how Nrf2 escape from the Keap1 protein under chemical/oxidative stresses.

One of plausible models on this mechanism is cysteine sensor model that cysteine-rich Keap1 protein directly sensing chemical/oxidative stress via thiol modification on its cysteine residues, which may cause a conformational change, resulting in release of Nrf2 from the Nrf2-Keap1 complex. Human Keap1 is a cysteine-rich (27 cysteine residues) protein that serves as a sensor in Nrf2 signaling by interacting with the ETGE motif in the Neh2 domain of Nrf2 (161). To date, three key cysteine residues (C151, C273 and C288) were identified and studied for their functional roles in Nrf2 signaling (33, 37, 102, 110, 187, 188). Based on these studies, thiol modification in Keap1 protein may be critical for sensing of Nrf2 signaling.

Under basal conditions, Keap1 plays a role not only in sequestration of Nrf2 in the cytoplasm, but also in targeting of Nrf2 for ubiquitin-mediated proteasomal degradation (128). Keap1 may function as a molecular switch for maintaining of Nrf2 to

certain level under normal or stressed conditions through degradation process. Ubiquitin-mediated protein degradation plays a critical role in managing many cellular events, such as cell cycle, cell growth/differentiation, and cellular response to stress. Ubiquitination is a post-translational modification processed by a set of three enzymes, E1 (ubiquitin activating enzymes), E2 (ubiquitin conjugating enzyme) and E3 (ubiquitin ligase), allowing ubiquitin conjugation to substrates thereby facilitating proteasomal degradation. Basically, this process is achieved through the coordinated action by these enzymes.

Initially, ubiquitin is joined to a cysteine residue on E1 through a thioester bond. Next, ubiquitin is translocated from E1 to E2 by transthioylation, and lastly, ubiquitin in E2 is transferred to lysine residues of a substrate by E3 ligase which is responsible for substrate specificity and proteasomal degradation (28, 58, 136). Based on previous reports by four different groups, Keap1, especially BTB (Bric-a-brac, Tramtrack, Broad-complex) domain, was proved to be an adaptor protein for Keap1-Cul3-Rbx1(ROC1) based E3 ubiquitin ligase complex for Nrf2 degradation (30, 44, 81). Two cysteines (C273 and C288) in the IVR are required for Keap1-mediated Ubiquitination of Nrf2, whereas one cysteine (C151) in the BTB is required to release Nrf2 protein from Keap1 (33, 196).

Nrf2 is a very unstable protein under basal condition since Keap1 is actively targeting Nrf2 for sequestration and ubiquitin-mediated proteasomal degradation. Here, we have one question. If Nrf2 is so fragile by Keap1-Cul3-mediated proteasomal degradation, how Nrf2 protein can be ready for the activation response to oxidative/chemical stresses. It is suggesting that specific machinery may exist for maintaining of stable form of Nrf2 which is responsible for the speedy execution against oxidative/chemical stresses. In this study, we propose that IQGAP1 protein may serve

as a nest of Nrf2 in normal condition and subsequently Nrf2 can be released from the IQGAP1 through increased intracellular calcium signals triggered by oxidative/chemical stresses.

As an critical aspect of chemoprevention, many dietary phytochemicals as potent Nrf2 inducers include sulforaphane (cruciferous vegetables), curcumin (turmeric), and genistein (soy product), epigallocatechin-3-gallate (EGCG; green tea), zerumbone (Zingiber zerumbet Smith), resveratrol (grapes), caffeic acid phenethyl ester (conifer trees), cafestol and kahweol (coffee), cinnamonyl-based compounds (cinnamon), zerumbone (ginger), garlic organosulfur compounds (garlic), lycopene (tomato), carnosol (rosemary), and avicins (Bentham plant). Besides phytochemicals, certain synthetic chemicals such as retinoic acid (the oxidized form of vitamin A), oltipraz, 2-indol-3-yl-methylenequinuclidin-3-ols (an indole analogue), and the synthetic triterpenoid 2-cyano-3,12-dioxooleana-1,9(11)-dien-28-oic acid (CDDO) and its derivative 1-[2-cyano-3,12-dioxooleana-1,9(11)-dien-28-oyl] imidazole (CDDO-Im) are also potent Nrf2 inducers (reviewed in ref. (98) and (94)).

So far, several mechanisms on Nrf2 transactivation have been reported. Nrf2 transactivation activity can be triggered by some kinases, such as mitogen-activated protein kinases (MAPKs) (128), protein kinase C (PKC) (61), and phosphoinositide-3-kinase (PI3K) (127). In addition, among the Maf basic leucine zipper (bZip) transcription regulator, small Mafs (MafF, MafK and MafG) play an important role in Nrf2 transactivation. These proteins contain leucine-zipper motifs, which allow heterodimerization with Nrf2 and binding to the ARE DNA sequence region (8). The CREB binding protein (CBP), a nuclear co-activator, has been implicated in Nrf2

signaling through binding directly to the two transactivation domains (Neh4 and Neh5) of Nrf2 (73). Furthermore, a member of p160 protein cofactor family, ARE-binding protein-1 (ARE-BP-1), was previously speculated as an Nrf2/ARE binding protein (194).

The Receptor-associated coactivator 3 (RAC3), also called steroid receptor coactivator (SRC-3/ACTR/AIB1/p/CIP/TRAM-1), is a member of the p160 family including SRC-1 (NCoA-1) and SRC-2 (TIF2/GRIP1/NCoA2), and plays a pivotal role in cell growth (171, 192), and mammary gland development (182). This coactivator family interacts not only with steroid hormone receptors, such as estrogen receptor (ER), progesterone receptor, and thyroid receptor (49, 159, 185), but also with several transcriptional factors including activator protein 1 (AP-1), nuclear factor-kappa B (NF- κ B), and signal transducer and activator of transcription (STAT) (5, 99, 176). Furthermore, it recruits the other nuclear co-regulates and chromatin modification factors, such as CREB binding protein (CBP/p300), p300/CBP-associated factor (p/CAF), protein arginine methyltransferases 1 (PRMT1), and coactivator associate arginine methyltransferase 1 (CARM1), which confer the transcription of target genes (19, 21, 84, 117, 184).

The RAC3, like the other family members, share common structural domains. These include the N-terminal bHLH (basic helix-loop-helix) domain, the Pas (Per/ARNT/Sim) domain, the transcriptional activation domains for interaction with CBP/p300, PRMT1 and CARM1, LXXLL motifs (where L is leucine and X is any amino acid), and the poly glutamate (poly Q) domain. In general, the bHLH domain is considered to be involved in the interaction with many transcription factors, while the Pas domains (PasA and PasB) are known to be involved in potential protein-protein

interactions (100).

RAC3 was first identified as a gene highly expressed and amplified in many breast and ovarian cancer cell lines (4). Recent data suggest that RAC3 can play an important role in cell growth in breast and prostate cancer cell lines (183, 192). Furthermore, in the transgenic mice model, overexpressed RAC3 caused mammary hypertrophy, hyperplasia, abnormal postweaning involution and showed high malignant tumor incidence potentially via stimulating the PI3K/AKT/mTOR signaling pathway (162). In contrast, the study using the RAC3 knockout mice showed lower incidence of ras-related mammary gland tumorigenesis (91), exhibited growth retardation as well as showed abnormal adult body size (171, 182). Based on these reports, unlike other p160 coactivators, RAC3 may potentially play a role in cell growth and tumorigenesis.

Previously Zhu *et al.* proposed (194) that ARE-binding protein-1 was a member of p160 family, the identity of this molecule was still unknown. However, based on recent data from our lab, it suggested that RAC3 might be the p160 which directly interact with Nrf2 protein since Gal4-luciferase activity was induced by cotransfection with Nrf2 (1-370) and RAC3 in HepG2 cells. But it is still not clear how RAC3 modulates the Nrf2 signaling, since Gal4-luciferase reporter system just inform the binding interaction between two molecules, and also, functional domains from the two proteins are not verified (108). If RAC3 interacts and regulates Nrf2 signaling, it is quite interesting how oncogenic RAC3 can regulate cytoprotective Nrf2 protein. Thus, we investigated the role of RAC3 on Nrf2 signaling and functional domains of Nrf2 and RAC3 in HeLa cell.

Although, so far, several proteins have been implicated for the Nrf2 signaling, the precise molecular mechanisms of Nrf2 signaling events remained. Therefore, a screening

for potential Nrf2 interacting partners may be necessary to better understand the molecular mechanisms of Nrf2-related gene transcription. Here, we isolated several possible Nrf2 partners using One-STrEP-tag purification system (IBA GmbH, Germany). This system was designed to purify the complex bound to one-strep tagged protein under physiological condition. After purification of the protein complex, we identified fourteen Nrf2 partners using powerful LTQ_Orbitrap LC/MS/MS equipment. Among the newly isolated Nrf2 partners, we investigated IQGAP1 (IQ motif containing GTPase activating protein 1) protein on Nrf2 signaling.

IQGAP1, like other IQGAP family such as IQGAP2 and IQGAP3, share conserved protein structure including calmodulin-binding IQ motifs and the GTPase activating protein (GAP) homology domain (175). IQGAP1 was first identified as a Rac and Cdc 42 binding protein coupled with actin. It is widely accepted that IQGAP1 inhibits its GTPase activity by recruiting Cdc42 and Rac1 (51, 93). IQGAP protein interacts with numerous cellular signaling molecules and coordinates various cellular events in actin and tubulin cytoskeletons through four major domains (reviewed in ref. (11): CHD, calponin homology domain [for actin binding (12)]; WW, WW domain [for ERK2 binding (142)]; IQ, IQ motifs [for calmodulin (107), myosin light chain (174) and S100B binding (115)]; GRD, GAP-related domain [for CDC42 and Rac1 binding (51, 116)]; dCT, distal C-terminal domain [for E-cadherin, β -catenin (93) and CLIP-170 binding (43, 93)].

Calcium and calmodulin are implicated on various cellular functions, ranging from muscle contraction to the cell cycle. Previous report indicates that calcium and calmodulin regulate the mitogen-activated protein kinase (MAPK) signaling pathway

(142). The MAPK has been implicated on the Nrf2 signaling. IQGAP1 may play an important role in calcium related signal transduction of Nrf2 pathways. Although IQGAP1 scaffolds many signaling molecules associated with integration of skeletal molecules, such as actin and microtubules, the precise molecular mechanism is still unclear. Our current study provides a potential clue that IQGAP1 may involve in Nrf2 scaffolding for Nrf2's target gene regulation.

Here, we investigated the function of RAC3 and IQGAP1 on Nrf2 signaling.

1.2. Materials and Methods

1.2.1. Materials

Minimum essential medium (MEM), fetal bovine serum (FBS) and penicillin/streptomycin antibiotics mixture and Dynabead G were obtained from Invitrogen. The anti-Nrf2 (C-20, H-300), anti-RAC3 (M-397), anti-GFP (B-2), anti-Dsred, anti-IQGAP (H-109), (C-20), anti-Keap1 (E-20), and anti-Maf F/G/K (H-100), anti-HO-1 (C-20), anti-GAPDH, anti-Lamin A, anti-Actin and secondary antibodies were purchased from Santa Cruz Biotechnology. Anti-HA was obtained from Zymed Laboratories. ECL femto signal substrate and M-PER mammalian cell lysis buffer were obtained from Pierce Biotech Inc. Transfection reagent jetPEI was purchased from Polyplus-Trasfection (Bioparc, Illkirch, France). Polypropylene column was from Qiagen and cover glass bottomed culture dishes were purchased from MatTek Corporation (Ashland, MA, USA). Polyvinylidene difluoride (PVDF) membrane was from Millipore. Sulforaphane (SFN) and MG132 were purchased from Alexis (San Diego, CA, USA). Sulforaphane was purchased from Alexis (San Diego, CA, USA). Protease inhibitor cocktail was obtained

from Roche Molecular Biochemicals. Mammalian expression vectors, pEGFP-C1, pDsredm-C1, pEYFP-C1, and pECFP-C1, were obtained from Clontech. pET28b(+) and pGEX4T3 vector were from Novagen and GE Healthcare Life Sciences, respectively. pRNATin-H1.2/Hygro vector for siRAC3 constructs was purchased from Genscript (NJ, USA). All other chemicals used were of analytical grade or the highest grade available.

1.2.2. Cell Culture

HeLa or HEK293 cells were maintained at 37°C in a humidified atmosphere of 5% CO₂/95% air in MEM or DMEM medium supplemented with 10% heat-inactivated fetal bovine serum (FBS) and 50 U/ml of penicillin/streptomycin mixture (Gibco BRL, Grand Island, NY), respectively. The cells were grown to 60–80% confluency and trypsinized with 0.05% trypsin containing 2 mM EDTA.

1.2.3. Construction of Plasmids

Full-length wild type human Nrf2 cDNA (NM 006164, 605 aa) was purchased from I.M.A.G.E consortium (Open Biosystems, Huntsville, AL). For the expression of Nrf2 in HeLa cells, Nrf2 cDNA was subcloned into pEGFP-C1 vector (Clontech) for the expression of EGFP-Nrf2. For GST pull-down studies, Nrf2 cDNA and its segments were subcloned into pET28b (+) vector (Novagen) for the expression of His-Nrf2 fusion protein in BL21 StarTM (DE3) *E. coli* (Invitrogen). The wild type of Nrf2 and its segments were amplified and sub-cloned into the vector using XhoI-BamHI digestions. The cloned plasmids were designated as follow: His-Nrf2₁₋₆₀₅, His-N1₁₀₈₋₆₀₅, His-N2₁₈₀₋₆₀₅, His-N2a₂₁₅₋₆₀₅, His-N2b₂₅₅₋₆₀₅, His-N2c₂₉₈₋₆₀₅, His-N3₃₃₃₋₆₀₅, and His-N4₄₀₃₋₆₀₅. For FRET analyses, Nrf2₁₋₆₀₅, N1₁₀₈₋₆₀₅, N2₁₈₀₋₆₀₅, and N2a₂₁₅₋₆₀₅ were sub-cloned into pEYFP-C1

vector (Clontech).

For construction of RAC3 plasmids, pSG5-RAC3-HA, for mammalian expression with full-length (AF010227, 1417 aa), and pGEX2T-bHLH, pGEX2T-pasA, pGEX2T-pasB, pGEX2T-R1 plasmids, for bacterial expression, were described previously (177). To prepare different segments of GST-RAC3 proteins, different fragments of RAC3 were amplified and sub-cloned into pEGX2T (for full length RAC3) and pGEX4T3 (for segmented RAC3) vectors by BamHI/bglII-EcoRI/MfeI and BamHI-XhoI digestions respectively. The cloned plasmids were designated as follow: GST-RAC3₁₋₁₄₁₇, GST-bHLH₁₋₁₀₅, GST-PasA₉₂₋₂₀₄, GST-PasB₂₀₃₋₄₀₈, GST-R1₁₋₄₀₈, GST-R2₄₀₁₋₁₄₁₇, GST-R2A₄₀₁₋₁₄₁₇, GST-R3₉₀₂₋₁₄₁₇, GST-B3A₁₀₁₇₋₁₄₁₇, GST-R3B₁₁₆₀₋₁₄₁₇, GST-R3B1₁₂₁₀₋₁₂₈₄, GST-R3B2₁₁₉₅₋₁₄₁₇, GST-B3B3₁₂₁₀₋₁₄₁₇, GST-R3B4₁₂₃₅₋₁₄₁₇, and GST-R3C₁₂₈₅₋₁₄₁₇.

For FRET analyses, CFP-RAC3 and its different segments were subcloned into pECFP-C1 vector by KpnI-BamHI/bglIII (for CFP-RAC3) and XhoI-BamHI (for CFP-pasA, CFP-pasB, and CFP-R3B3) digestion respectively. Fig. 1-1 also shows each proposed proteins which were designated as amino acid lengths.

For RAC3 silencing experiments, three different small interference RNAs (siRNAs) for RAC3 were designed by Genscript siRNA Target Finder and synthesized DNA duplexes were inserted into pRNATin-H1.2/Hygro vector (Genscript, NJ, USA). The sequences for each siRAC3 constructs were as follow: pRNATin-siRAC3-I, 5'-GAT CCC GTA TGT CTG TCC ATA TAA TCC TTT GAT ATC CGA GGA TTA TAT GGA CAG ACA TAT TTT TTC CAA A-3'; pRNATin-siRAC3-II, 5'-GAT CCC GTT TGT TAC AGG ATT TCG GAA GTT GAT ATC CGC TTC CGA AAT CCT GTA ACA AAT TTT TTC CAA A-3' and pRNATin-siRAC3-III, 5'-GAT CCC GTC ATA GGT TCC ATT

CTG CCG GTT GAT ATC CGC CGG CAG AAT GGA ACC TAT GAT TTT TTC CAA A-3'. The duplexes were synthesized, and high pressure liquid chromatography-purified by Integrated DNA Technologies. Synthesized DNA was annealed to form double strands followed by BamHI and XhoI restriction enzymes digestions and directly ligated to pRNAT-CMV3.2/neo/cGFP vector.

To identify and purify the Nrf2-unknown partner complexes using Strep-tactin bead, pEGFP-Nrf2-One-strep plasmid was constructed. Nrf2 gene (NM 006164, 605 aa) was first amplified with specifically designed primers (forward: 5'-AAA CTC GAG ATG ATG GAC TTG GAG CTG CCG CCG CCG GGA C-3' and reverse: 5'-AAA GGA TCC TTA TTT TTC GAA CTG CGG GTG GCT CCA CGA TCC ACC TCC CGA TCC ACC TCC GGA ACC TCC ACC TTT CTC GAA CTG CGG GTG GCT CCA GTT TTT CTT AAC ATC TGG CTT CTT AC-3') for tagging One-strep tag (SAWSHPQFEK-(GGGS)₂GGASHPQFEK) in the C-terminal of Nrf2. Then, Nrf2-One-strep gene was amplified using the Platinum *pfx* DNA polymerase kit (Invitrogen) following manufacturer's instruction. Briefly, cDNA (0.5 µg) was denatured at 95°C for 2 min and cycled 24 times at 94°C for 15 sec, 55°C for 15 sec, and 68°C per min/per kb. The PCR reaction ended with 10 min incubation at 68°C. The amplified PCR product was cut with BamHI and XhoI restriction enzymes and subcloned into pEGFPC3 vector. For the control, one-strep tag was also linked to the C-terminal of EGFP gene. Based upon the results of LC/MS/MS profile, IQGAP1 was subcloned into the pDsredm-C1 vector (clontech). This candidate cDNAs was purchased from the I.M.A.G.E clone consortium (Invitrogen) and amplified using PCR method with specifically designed primers containing appropriate restriction enzyme sites. Amplified IQGAP1 gene was cut by

XhoI/ApaI restriction enzymes, and then subcloned into the pDsredm-C1 vector. All PCR reaction conditions were the same as previous experiment. For IQGAP silencing experiments, two different siIQGAP DNA duplex were inserted into pRNAT-CMV3.2/neo/cGFP vector (Genscript, NJ, USA). The sequences for pRNAT-siIQ-1 and -2 were 5'-GAT CCT AAA TCA GAG TAC TCA TCC ACT TGA TAT CCG GTG GAT GAG TAC TCT GAT TTA CGC-3' and 5'-GAT CCT TCT ACG GTC AAT AGC TTC ATT TGA TAT CCG ATG AAG CTA TTG ACC GTA GAA CGC-3' respectively. The duplexes were synthesized, and purified by high pressure liquid chromatography (Integrated DNA Technologies). Synthesized DNA were annealed to form double strand and cut with BamHI and XhoI restriction enzyme sites and ligated into pRNAT-CMV3.2/neo/cGFP vector.

1.2.4. Fusion Protein Purification and GST Pull-down Assay

For purification of the GST-RAC3 and its segments, pGEX2T- or pGEX4T-based RAC3 constructs were transformed into BL21 Star™ (DE3) *E. coli* (Invitrogen) and cultured in ampicillin (50 µg/ml) containing 5 ml of liquid LB media overnight at 37°C in orbital shaker. Then 50 ml of the same media were added and incubated until OD₆₀₀ reached 0.6. These are then cultured for another 4 h by adding 1 mM Isopropyl β-D-1-thiogalactopyranoside (IPTG) to induce GST-RAC3 proteins. Cultured bacteria were then centrifuged at 7,000 rpm for 3 min at 4 °C. The pellets were suspended and sonicated in phosphate buffered saline (PBS) containing 10 mM EDTA and protease inhibitor cocktail (Roche) on ice. After bacterial lysis, lysates were centrifuged at 12,000 rpm for 5 min at 4°C. The supernatants were then applied to Polypropylene column (Qiagen) loaded with 1 ml of 50% slurry glutathione (GSH) sepharose bead (GE Healthcare Life Sciences) and

incubated for 5 min at 4°C on a rotator. After incubation, beads were washed 3 times with 20 volumes of PBS (containing 0.1% triton X-100) in the cold room. After washing, beads were suspended with 1 ml of incubation buffer [25 mM Tris-phosphate (pH 7.8), 2 mM DTT, 2 mM 1,2-diaminocyclohexane-N,N,N',N'-tetraacetic acid, 10% glycerol and 1% Trion X-100] and kept at 4°C before GST pull-down assay. The same volume of purified GST and GST-RAC3 proteins were subjected to SDS-PAGE and stained with commassie brilliant blue to verify the purity of proteins and to determine the bead volumes for GST pull-down assay.

For the purifications of His-Nrf2 and its segments, pET28b(+)-based Nrf2 constructs were transformed into BL21 Star™ (DE3) *E. coli* and cultured in 5 ml LB media containing 50 µg/ml kanamycin for overnight at 37°C in orbital shaker. After adding of 5 ml LB media into 50 ml LB bacterial media, bacteria were incubated until OD₆₀₀ reached 0.6. Then IPTG was added for 1 h for the induction of six-histidine (His₆)-tagged fusion protein (His-Nrf2). The rest of the procedures are the same as described above. His-Nrf2 proteins were purified using Ni-NTA agarose system according to the manufacturer's instructions (Qiagen).

To study the binding interactions between RAC3 and Nrf2 proteins, purified GST-RAC3-bead and His-Nrf2 protein samples were mixed in 500 µl incubation buffer [25 mM Tris-phosphate (pH 7.8), 2 mM DTT, 2 mM 1,2-diaminocyclohexane-N,N,N',N'-tetraacetic acid, 10% glycerol and 1% Trion X-100] and incubated overnight at 4°C. After incubation, the beads were vigorously washed 5 times with 10 volume of washing buffer (PBS with 0.1% tween 20, pH7.2). Then the beads were mixed with 200 µl of 2xSDS buffer, boiled for 5 min and subjected to SDS-PAGE and Western blot

analysis. For the control of equal loading, the same samples were run on SDS-PAGE, stained with commassie brilliant blue and blotted with antibodies against c-terminal or His-tag of Nrf2.

1.2.5. Western Blot Analysis

HeLa cells were plated on 100 mm culture dishes at $\sim 2.0 \times 10^6$ cells/plate for 16 h prior to plasmid transfection. After transfection, cells were scraped and treated with RIPA lysis buffer (150 mM NaCl, 0.5% Triton X-100, 50 mM Tris-HCl, pH 7.4, 25 mM NaF, 20 mM EGTA, 1 mM DTT, 1 mM Na_3VO_4 , and protease inhibitor cocktail) for 30 min on ice followed by centrifugation at $14,800 \times g$ for 15 min. The protein concentration of the supernatant was measured by using the BCA reagent. Protein (20 μg) was electrophoresed on 4-15% gradient Tris-HCl gel (Biorad) and electrotransferred onto polyvinylidene difluoride (PVDF) membrane in Tris-glycine buffer (pH 8.4) containing 20% methanol. The membrane was then blocked with 5% fat-free dry milk in phosphate-buffered saline (PBS) containing 0.1% Tween-20 (PBS-T) for 1 h. Membranes were probed with primary antibodies and horseradish peroxidase-conjugated secondary antibody by standard Western blot procedures. The proteins were then visualized with the femto signal chemiluminescent substrate (Pierce) using the image analyzer (Biorad).

1.2.6. Reverse Transcriptase PCR (RT-PCR)

Total RNA from HeLa cells and primary cultured human liver cells was isolated with Trizol method (Invitrogen, Carlsbad, CA). Total RNA samples were converted to single-stranded cDNA by the Superscript First-Strand Synthesis System III (Invitrogen) and the resulting cDNA was amplified by the PCR supermix kit (Invitrogen). PCR

conditions are as follows: 94°C for 2 min followed by cycles of denaturation at 94°C for 20 sec, annealing at 55°C for 30 sec, extension at 72°C for 45 sec, and a final extension at 72°C for 5 min. The 5' and 3' primers for each gene amplification were used as follow: *HO-1* (574 bp), 5'-CTT CTT CAC CTT CCC CAA CA-3' and 5'-ATT GCC TGG ATG TGC T TTC-3'; *NQO1* (500 bp), 5'-GCC GCA GAC CTT GTG ATA TT-3' and 5'-AAG TGA TGG CCC ACA GA AAG-3'; *GSTA1* (506 bp), 5'-GGC TGC AGC TGG AGT AGA GT-3' and 5'-GCA GGT TGC TGA TTC TGG TT-3'; *UGT1A1* (539 bp), 5'-TAA GTG GCT ACC CCA AAA CG-3' and 5'-TCT TGG ATT TGT GGG CTT TC-3'; *UGT1A3* (539 bp), 5'-TAA GTG GCT ACC CCA AAA CG-3' and 5'-TCT TGG ATT TGT GGG CTT TC-3'; *GAPDH* (590 bp), 5'-ACC CAG AAG ACT GTG GAT GG-3' and 5'-AGG GGT CTA CAT GGC AAC TG-3'. *GAPDH* was used for the internal control. PCR products were resolved on 1.5% agarose gels and visualized under UV lamps.

1.2.7. Transient Transfection and Reporter Gene Activity Assays

To analyze the ARE-luciferase activity, HeLa cells were plated in 6-well plates at $\sim 4.0 \times 10^5$ cells/well and cultured for 16 h prior to transfection. The cells were then transfected with different constructs (pSG5-RAC3-HA, pEGFP-Nrf2, pRNATin-siRAC3s or pHOGL3/9.1; provided by Dr. Anupam Agarwal, as described previously (78)) in the presence of ARE-luciferase reporter construct for 20-24 h. ARE-luciferase reporter construct containing 41 bp (-754 to -714) from murine GSTY α was generously provided by Dr. William Fahl (University of Wisconsin, Madison, WI) as described previously (172). The amount of plasmids in different experiments was indicated in the respective figures and legends. The transfection procedures were followed manufacturer's instructions (Bioparc, Illkirch, France). In brief, plasmids mixture in 100 μ l of NaCl (150

mM) and jetPEI transfection reagent in 100 μ l of NaCl (150 mM) were mixed and incubated for 25 min at room temperature. The ratio between plasmid and jetPEI was 1:4. After incubation, two hundred microliters of the mixtures were applied to the HeLa cells for 24 h. After transfection, medium was replaced by fresh medium for the following drug treatments. Cells were treated with 10 μ M MG132 or 25 μ M sulforaphane for 6 h. Then cells were washed once with PBS, scraped, and incubated in 200 μ l of reporter lysis buffer (Promega) on ice for 10 min. After centrifugation at 12,000 rpm for 5 min at 4°C, 10 μ l of cell lysate was mixed with luciferase substrate (Promega), and the ARE-luciferase activity was measured using a Sirius luminometer (Berthold Detection System). Luciferase activity was normalized against β -galactosidase activity. The β -galactosidase activity was determined as described previously (149).

For Nrf2 partner pull-down study using One-strep tactin system, HeLa cells (50 % confluence) were plated in twenty of 15 cm culture dishes per group and cells were cultured overnight. Then, cells were transfected with pEGFP-Nrf2-One-strep or pEGFPC3-One-strep plasmid for 24 h. Twelve micrograms of plasmid were mixed with jetPEI reagent (Polyplus-Trasfection™, Illkirch, France) in a ratio 1 μ g DNA to 4 μ l jetPEI. Before the cells were harvested, GFP expression was checked for the transfection efficiency under the blue filtered fluorescence microscopy. Then, the cells were immediately washed once with ice cold PBS (phosphate buffered saline, pH 7.4, w/o EDTA), scrapped and proceeded to the Nrf2 partners pull-down experiment as described below. For reporter gene activity assay, HeLa cells were plated in 6-well plates at $\sim 4.0 \times 10^5$ cells/well. Sixteen hour after plating, cells were transfected using the jetPEI reagent according to the manufacturer's instructions. For each well, 500 ng of pEGFP-Nrf2 or

500 ng of pDsredm-IQGAP1, pRNAT-iIQGAP1, 200 ng of ARE-Luciferase construct (172) were added into 100 μ l of NaCl (150 mM). The various amounts of plasmids were also applied for certain experiments as indicated in the figure legend. In addition, jetPEI reagent was added into another tube of 100 μ l of NaCl (150 mM). The two different tubes were mixed vigorously and incubated at room temperature for 25 min. After that, the cells were incubated with transfection complexes for 20-24 h at 37°C incubator. After transfection, cells were washed once with PBS, scraped, and lysed in 200 μ l of reporter lysis buffer (Promega) on ice for 10 min. After centrifugation at 12,000 rpm for 5 min at 4°C, 10 μ l of lysate was mixed with luciferase substrate (Promega), and the ARE-luciferase activity was measured using a Sirius luminometer (Berthold Detection System). Luciferase activity was normalized by measuring the conventional β -gal activity by the transfection with pCDNA3.1/hisB/lacZ plasmid coding galactosidase.

1.2.8. Stable Transfection to HeLa Cells

HeLa cells were transfected with pRNATin-H1.2/Hygro basic vector or pRNATin-siRAC3-II constructs using a jetPEI reagent (Polyplus-Trasfection, Bioparc, Illkirch, France). Cells were cultured in fresh medium containing 0.8 mg/ml G418 24 h after transfection. Cell colonies were selected for growth in the presence of G418 by limited dilution. Selected colonies were checked for their RAC3 protein levels by Western blot analysis. Obtained clone 6 (siRAC3-II₆) was presented in this study.

1.2.9. Co-Immunoprecipitation (IP)

HeLa cells were plated in 100 mm dishes at $\sim 2.0 \times 10^6$ cells/plate and cultured for 16 h prior to transfection. After cell stabilization, the cells were transfected with 2 μ g of

pEGFP-Nrf2 and/or 2 μ g of pSG5-RAC3-HA for 24 h using jetPEI transfection reagent. The total amount of plasmids was adjusted with pcDNA3.1 control vector. After transfection, cells were lysed with M-PER mammalian lysis buffer (Pierce) containing protease inhibitors. Commercially available M-PER lysis buffer was designed for whole cell lysis for certain cell lines. However, this buffer could only break cellular membrane in HeLa cells (data not shown). In other words, M-PER can be used to fractionate cytosol and nucleus. So, we used this property of M-PER for current study. In brief, the cells were first lysed to release cellular membrane with M-PER lysis buffer for 10 min on ice. Then the samples were centrifuged at 12,000 rpm for 1 min at 4°C to obtain the nuclear fraction. The pellets were gently washed once with the same buffer and resuspended with the same buffer. Then the nuclear pellets in the buffer were sonicated and centrifuged at 12,000 rpm for 10 min at 4°C. For proteins from the whole cell lysis, the cells were first sonicated in the M-PER buffer to suspend the proteins. Protein concentration from the fractionated samples was measured by the BCA reagent. Two hundred micrograms of protein samples were precleaned with 50 μ l of TrueBlotTM anti-rabbit IgG IP beads (ebioscience, San Diego, CA) for 30 min. Then the supernatants were incubated with anti-RAC3 (2 μ g, M-397) for 1 h at 4°C and followed by the pull-down step by adding TrueBlotTM anti-rabbit IgG IP beads to the samples for 1 h. After reaction, the beads were washed 3 times with 500 μ l of M-PER buffer at 4°C. Then the beads were mixed with 200 μ l of 2xSDS sample buffer and boiled for 5 min. And then samples were subjected to Western blot analysis and blotted against GFP-Nrf2 using anti-GFP antibody. To pull-down the His-tagged Nrf2 from HeLa cells, Ni-NTA agarose beads were used instead of Ig IP beads.

For IQGAP study in Nrf2 signaling, HeLa cells were plated on 100 mm dishes and cultured until over 95% confluence. Then, the cells were treated with CaCl_2 (3.8 mM) or EGTA (5 mM) or BAPTA (10 μM) for different time intervals. Next, cells were harvested and lysed with M-PER (Pierce) buffer for cytosolic extract. Four hundred micrograms of cytosolic samples were subjected to immunoprecipitation (IP) assay using anti-IQGAP1 (H-109) or Dsred (C-20) antibodies. In this experiment, Dynabead G beads (Invitrogen) were used for IP. The Procedures were followed by the manufacture's protocol. Briefly, four micrograms of antibodies were incubated with Dynabead protein G for 10 min to make antibody-bead complex first. Then, this complex was incubated with cytosolic lysates for 10 min at room temperature. After washing the IP complexes, IP samples were suspended with 200 μl of 2xSDS sample buffer and 20 μl of aliquots were subjected to Western blotting using anti-Nrf2 (C-20) antibody or IQGAP1 (H-109).

1.2.10. Fluorescence Resonance Energy Transfer (FRET) Analysis

Hela cells were cultured in glass bottom dishes (MatTek, Ashland, MA) and co-transfected with pECFP-RAC3 or its segments (pECFP-pasA, -pasB, or -R3B3) and pEYFP-Nrf2 or its segments (pEYFP-N1, -N2, or -N2a). After 24 h transfection, the cells were examined under the Zeiss LSM510 laser scanning confocal microscope (Zeiss, Thornwood, NY) with a 63x objective. We used a sensitized emission method for the FRET assay (163). Three channels were used to detect the donor (ECFP, excitation at 457 nm and emission at 475-525 nm), acceptor (EYFP, excitation at 543 nm and emission at 475-525 nm) and FRET (excitation at 457 nm and emission at 545-600 nm) signals. The FRET signal was corrected by subtracting the crosstalk from each single ECFP or EYFP signal according to Trinkle-Mulcahy's method (163). The net FRET was calculated

according to the following formula:

$$\text{Net FRET} = \text{FRET signal} - [(\alpha \times \text{YFP signal}) + (\beta \times \text{CFP signal})]$$

$$\alpha_{\text{crosstalk for YFP only}} = (\text{CFP}_{\text{ex}} / \text{YFP}_{\text{em}}) / (\text{YFP}_{\text{ex}} / \text{YFP}_{\text{em}})$$

$$\beta_{\text{crosstalk for CFP only}} = (\text{CFP}_{\text{ex}} / \text{YFP}_{\text{em}}) / (\text{CFP}_{\text{ex}} / \text{CFP}_{\text{em}})$$

In our present system, α and β were measured as 20% and 21% respectively. Data were analyzed by LSM510 SP2 software (Zeiss, version 3.2).

1.2.11. Chromatin Immunoprecipitation (ChIP) Assay

HeLa cells were plated in 100 mm culture dishes at 50% confluency overnight. Then the cells were transfected with pEYFP-Nrf2 (3.5 μg) and pSG5-RAC3-HA (3.5 μg) using jetPEI reagent for 22 h. For control, pcDNA3.1 was used. Transfection protocol was the same as the method described above in the ARE-reporter assay. After transfection, the cells were washed twice with cold PBS and fixed with 10 ml of 1% formaldehyde for 10 min at room temperature. To stop the cross-linking, five hundred microliters of glycine (1.25 M) were added to the plates for 5 min and washed briefly with cold PBS. Then the cells were scrapped in ice-cold PBS and centrifuged at 12,000 rpm for 1 min at 4°C. Cells were harvested and then suspended with 500 μl of SDS lysis buffer (1% SDS, 10 mM EDTA, 50 mM Tris-HCl, pH 8.1, protease inhibitors cocktail). The Samples were sonicated using Biorupers system (Cosmo bio, Japan) for 15 min (30 sec ON/30 sec OFF mode) on ice water bath, and centrifuged at 12,000 rpm for 5 min at 4°C. Each sample

(150 μ l) was mixed with 1,350 μ l of ChIP dilution buffer (0.01% SDS, 1.1% Triton X-100, 1.2 mM EDTA, 16.7 mM Tris-HCl, pH 8.1, 167 mM NaCl, protease inhibitor cocktail). Then sixty microliters of TrueBlotTM anti-rabbit IgG IP beads (ebioscience, San Diego, CA) were added to the samples and incubated for 1 h at 4°C in a rotary shaker. After precleaning step, the samples were centrifuged at 2,000 rpm for 1 min at 4°C and the supernatants were transferred to new tubes. The samples in the new tubes were mixed with 15 μ l of anti-Nrf2 (H-300) or anti-RAC3 (M397) antibodies and incubated for 6 h in the cold room. To pulldown the DNA-protein complex, sixty microliters of TrueBlotTM anti-rabbit IgG IP beads were added and incubated for 1 h after primary antibody incubation. After incubation, the samples were washed once with the following washing buffers for 15 min sequentially using low salt washing buffer (0.1% SDS, 1% Triton X-100, 2 mM EDTA, 20 mM Tris-HCl, pH 8.1, 150 mM NaCl); high salt washing buffer (0.1% SDS, 1% Triton X-100, 2 mM EDTA, 20 mM Tris-HCl, pH 8.1, 500 mM NaCl); LiCl buffer (0.25 M LiCl, 1% NP-40, 1% deoxycholate, 1 mM EDTA, 10 mM Tris-HCl, pH 8.1); and TE buffer (10 mM Tris-HCl, 1 mM EDTA, pH 8.0.). Then the samples were eluted with 200 μ l of freshly prepared 2x elution buffer (1% SDS, 0.1M NaHCO₃). For reverse-cross linking, sixteen microliters of 5 M NaCl were added to the samples and incubated for 8 h at 65°C and followed by DNA purification using Qiagen PCR purification kit. The DNA samples were eluted with 50 μ l of ultrapure water (Invitrogen). Then the samples were run on DNA electrophoresis gel to check the DNA sizes of between 200 and 1000 base pairs (bp) after reverse cross-linking. PCR was performed with 5 μ l of ChIP DNA samples, using the following primers for two different regions of AREs (for A region: 5'-GGC GCC TTG GGA ATG CTG AGT CGCG-3' and 5'-GCT

TTA ATG GTA GGC AGG AGG AAG TG-3'; for B region: 5'-CCC TGC TGA GTA ATC CTT TCC CGA-3' and 5'-TGG AGT CTG GAG TCG GGA CAT-3'). The expected PCR products were 200 bp and 242 bp respectively. The PCR reactions were performed using HotstarTaq Master Mix (Qiagen) with the following reaction conditions (initial activation step: 95°C for 15 min; three steps for cycling: 95°C for 30 sec, 55°C for 30 sec, 72°C for 40 sec, 34 cycles; final extension: 72°C for 1 min).

For Nrf2 partner pull-down study using One-strep tactin system, HeLa cells (50 % confluence) were plated in twenty of 15 cm culture dishes per group and cells were cultured overnight. Then, cells were transfected with pEGFP-Nrf2-One-strep or pEGFPC3-One-strep plasmid for 24 h. Twelve micrograms of plasmid were mixed with jetPEI reagent (Polyplus-Trasfection™, Illkirch, France) in a ratio 1 µg DNA to 4 µl jetPEI. Before the cells were harvested, GFP expression was checked for the transfection efficiency under the blue filtered fluorescence microscopy. Then, the cells were immediately washed once with ice cold PBS (phosphate buffered saline, pH 7.4, w/o EDTA), scrapped and proceeded to the Nrf2 partners pull-down experiment as described below. For reporter gene activity assay, HeLa cells were plated in 6-well plates at $\sim 4.0 \times 10^5$ cells/well. Sixteen hour after plating, cells were transfected using the jetPEI reagent according to the manufacturer's instructions. For each well, 500 ng of pEGFP-Nrf2 or 500 ng of pDsredm-IQGAP1, pRNAT-iIQGAP1, 200 ng of ARE-Luciferase construct (172) were added into 100 µl of NaCl (150 mM). The various amounts of plasmids were also applied for certain experiments as indicated in the figure legend. In addition, jetPEI reagent was added into another tube of 100 µl of NaCl (150 mM). The two different tubes were mixed vigorously and incubated at room temperature for 25 min. After that, the cells

were incubated with transfection complexes for 20-24 h at 37°C incubator. After transfection, cells were washed once with PBS, scraped, and lysed in 200 µl of reporter lysis buffer (Promega) on ice for 10 min. After centrifugation at 12,000 rpm for 5 min at 4°C, 10 µl of lysate was mixed with luciferase substrate (Promega), and the ARE-luciferase activity was measured using a Sirius luminometer (Berthold Detection System). Luciferase activity was normalized by measuring the conventional β-gal activity by the transfection with pCDNA3.1/hisB/lacZ plasmid coding galactosidase.

1.2.12. Nrf2 Partner Pull-down with One-strep Tactin System

Scrapped HeLa cells from 20 plates above were lysed in 4 ml of lysis buffer [25 mM NaCl, 50 mM Tris-HCl, protein inhibitor cocktail (Roche, Indianapolis, IN) in 0.2% Triton-X100, and 7.5% glycerol, W/O EDTA, pH 7.4]. Cell lysis was done by four freezing/thawing cycles using liquid nitrogen. Every single thawing cycle, pipetting was performed to disrupt the cells. After lysis, all procedure was followed by One-STrEPTM purification system (IBA GmbH, Germany). Briefly, lysates were then centrifuged at 15,000 rpm for 20 min at 4°C. The supernatant was applied to the One-strep tactin bead column packed with 1 ml bead in polypropylene column with gravity flow rate. Next, columns were washed with 1 ml washing buffer (150 mM NaCl, 50 mM Tris-HCl, 0.2%, Triton-X100, pH 8.0) for 5 times and eluted with 500 µl elution buffer (150 mM NaCl, 50 mM Tris-HCl, 2.5 mM Desthiobiotin pH 8.0), repeated 4 times. Each small fraction was subjected to PAGE gel electrophoresis for silver staining to verify the elution of the Nrf2 complex. After silver staining of the gel, eluted samples were concentrated using Microcon YM50 (Millipore) by centrifugation for 20 min at 4°C. Concentrated samples were subjected to PAGE gel electrophoresis and then silver staining was processed using

Silver SNAP kit for the LC/MS/MS. After silver staining, candidate bands were excised and analyzed for protein identification using LTQ_Orbitrap LC/MS/MS equipment (Thermo Fisher Scientific, Waltham, MA) in the UMDNJ proteomic core facility. Mass data were analyzed using The Global Proteome Machine Organization Proteomics Database (Open Source Software, www.thegpm.org).

1.2.13. Epifluorescence

HeLa cells grown on cover glass were transfected with various plasmids and then fixed in 4% paraformaldehyde in PBS (pH 7.4), for 10 min. After brief washing the cells with PBS solution, slides were mounted in a medium (VECTASHIELD, Vector Laboratories Inc, Burlingame, CA, USA) containing an anti-fade agent and DAPI. Sample images were taken with a fluorescence microscope (Nikon, ECLIPSE E 600 system), and the images were processed using Photoshop 8.0 (Adobe Systems, San Jose, CA).

1.2.14. Statistics

Statistical analysis was performed student *t*-test using Sigma plot software (Ver. 7). The results were presented as mean \pm S.D (n=3) and P values < 0.05 were considered to be significant.

1.3. Results

1.3.1. RAC3 suppresses Nrf2/ARE activity

To check whether RAC3 protein affect the Nrf2 activity, HeLa cells were transiently transfected with EYPF-Nrf2 and/or HA-RAC3 constructs in the presence of

ARE-luciferase gene construct. The results show that ARE-luciferase activity was highly induced by EYFP-Nrf2 and decreased by cotransfection with EYFP-Nrf2 and HA-RAC3. Also, cells were treated with proteasome inhibitor (MG132, 10 μ M) and ARE inducer (Sulforaphane, 25 μ M) for 6 h after cotransfection with EYFP-Nrf2 and HA-RAC3 constructs. MG132 treatment was significantly suppressed ARE-luciferase activity in compare to HA-RAC3 transfection, whereas, sulforaphane treatment resuscitated ARE-luciferase activity has the same level as YFP-Nrf2 transfection only (Fig. 1-2A).

To confirm the inhibitory activity of RAC3 on Nrf2/ARE activity, we designed and constructed three siRAC3 constructs in plasmid based expression system. First, we screened the effective siRAC3 among siRAC3-I, siRAC3-II, and siRAC3-III. Western blot analysis results indicated that siRAC3-I, and siRAC3-II silenced overexpressed HA-RAC3 protein level to basal level. To check equal amount siRAC3 construct, expression level of GFP, which is constitutively expressing from the vector, was measured by blotting against anti-GFP antibody (Fig. 1-2B).

To support inhibitory function of RAC3 on Nrf2/ARE activity, different amount of HA-RAC3 and siRAC3-III constructs were transfected into HeLa cells in the presence of YFP-Nrf2 and ARE constructs. The results show that Nrf2/ARE-luciferase activities were inhibited by HA-RAC3 (Fig. 1-2C) and increased by siRAC3-III in a dose dependent manner (Fig. 1-2D). We also measured the Nrf2/ARE luciferase in established HeLa-siRAC3-II₆ cells (stably transfected with siRAC3-II construct) by transfecting the YFP-Nrf2 and ARE-luciferase constructs. The results shows that Nrf2/ARE luciferase activity was dramatically induced in RAC3 silenced HeLa-siRAC3-II₆ cells (Fig. 1-2A). To study the effect of siRAC3 on ARE in HO-1 promoter, HeLa cells were transiently

transfected with pmt-HO-1/-9.1 plasmid (containing the -9.1kb size of 5' flanking region in HO-1 promoter ligated to the luciferase gene) and YFP-Nrf2 or siRAC3-III. The results showed that siRAC3-III significantly induced HO-1 promoter-luciferase activity in the presence of Nrf2 (Fig. 1-3B).

1.3.2. Different effect of RAC3 in Human Embryonic Kidney 293 (HEK293) cells

Since the function of RAC3 might be different in different cells, so we verified the effect of RAC3 on Nrf2 signaling in human embryonic kidney 293 (HEK293) cells. Firstly, HeLa and HEK293 cells were transfected with different amount of YFP-Nrf2 construct in the presence of ARE plasmid for 24 h for Nrf2/ARE-luciferase assay. As results, Nrf2/ARE-luciferase activities were increased by the transfection of YFP-Nrf2 construct in both cells lines (Fig. 1-4A). Next, we evaluated the functional role of RAC3 in these cell lines in the presence of YFP-Nrf2 or pcDNA3.1-CBP constructs. Since CBP protein was considered as a partner of Nrf2 for the transcriptional activation, we also analyzed the Nrf2/ARE-luciferase activity by CBP protein with RAC3 in HeLa and HEK293 cells. The results showed that Nrf2/ARE-luciferase activity, in the HeLa cells, was significantly decreased by the transfection of RAC3 only, CBP and CBP plus RAC3 with dose dependent manner in the presence of YFP-Nrf2 and ARE constructs. However, no significant effects of RAC3 in Nrf2/ARE-luciferase activity were measured in HEK293 cells (Fig. 1-4B). The results suggest that different function of RAC3 may be occurred by the cell specificity. However, it was questioned why Nrf2/ARE-luciferase activity was not increased by CBP as Nrf2 co-activator. In this regard we, next, measured the Nrf2/ARE- induced protein or mRNA level after co-transfection with HA-RAC3 and

YFP-Nrf2 constructs in HeLa cells.

1.3.3. Expression of Heme oxygenase-1 (HO-1) was increased by RAC3

Based on results from the Fig.1-2, we assumed that RAC3 also could inhibit the expression of Nrf2-mediated target proteins, such as HO-1, NQO-1, GSTA1, UGT1A1 and UGT1A3. In this regard, we checked whether RAC3 had the same function as a suppressor in the expression of target protein or mRNA as shown in the Nrf2/ARE-luciferase activity. Surprisingly, Transfection of HA-RAC3 increased the HO-1 protein level (Fig.1-5A) and its mRNA level (Fig. 1-5B) with dose dependent fashion in the presence of YFP-Nrf2 construct. However, none of HA-RAC3 and YFP-Nrf2 affected the expression of *NQO-1* mRNA level. Furthermore, no expression of the different Nrf2 target genes, such as GSTA1, UGT1A1 and UGT1A3, were detected in HeLa cells (Fig.1-5B). To support these results, different sets of siRAC3 constructs were transfected into the HeLa cells in the presence of YFP-Nrf2 construct to show the inhibition of HO-1 induction. As expected, HO-1 protein was inhibited by siRAC3s (siRAC3-1<siRAC3-2<siRAC3-3) (Fig.1-5C), which was conflicting results against the Nrf2/ARE-luciferase assay (Fig. 1-2). These results suggest that Nrf2/ARE-luciferase system for the functional study of Nrf2 partner is not appropriate.

1.3.4. Nrf2 directly binds RAC3

Prior to the study of binding interaction between Nrf2 and RAC3 proteins, the overexpressed EGFP-Nrf2 and HA-RAC3 proteins were first measured after transfection of pEGFP-Nrf2 or pSG5-RAC3 in HeLa cells. The cells were treated with MG132 (proteasomal inhibitor) after transfection to enhance accumulated proteins by preventing

protein degradation. Western blot analysis showed that MG132 stabilized the overexpressed EGFP-Nrf2 and HA-RAC3 proteins as detected by anti-Nrf2(C-20) and anti-GFP (B-2) or anti-RAC3 (M397) and anti-HA (Zymed) antibodies for EGFP-Nrf2 and RAC3 proteins, respectively (Fig. 1-6A).

To examine the subcellular distribution of endogenous Nrf2, RAC3 and HO-1 proteins in HeLa cells, the cells were treated at MG132 (10 μ M) with different time intervals and fractionated into cytosol and nuclear fractions. Western blot analysis showed that majority of endogenous Nrf2 and RAC3 proteins were localized in the nucleus (Fig. 1-6B).

To investigate whether Nrf2 binds to RAC3 in HeLa cells, the cells were transiently cotransfected with EGFP-Nrf2 and HA-RAC3 constructs. After cotransfection, the cells were fractionated into cytosolic and nuclear or whole cell extracts and subjected to co-immunoprecipitation (Co-IP) assay against HA-RAC3 using anti-RAC3 (M-397) antibody and followed by Western blotting against GFP-Nrf2 using anti-GFP antibody. The results showed that GFP-Nrf2 and HA-RAC3 were tightly bound together (Fig. 1-6C).

To provide more evidence whether these two proteins bind directly together, *in vitro* GST pull-down experiment was conducted using human GST-RAC3 (full-length) and His-Nrf2 (full-length) proteins, which were overexpressed and purified from bacteria. GST-RAC3 protein was first purified using glutathione (GSH) sepharose beads and followed by incubation with purified His-Nrf2. Then GSH-protein-bead complexes were subjected to Western blot analysis against His-Nrf2 using anti-Nrf2 antibody (C-20). The results strongly suggested that RAC3 protein could bind to Nrf2 directly (Fig. 1-6D).

1.3.5. N-terminal pasB and C-terminal RAC3 (R3B3) regions bind to Nrf2

Previous studies using the Nrf2/ARE luciferase assay, co-IP method and GST pull-down assay, we concluded that Nrf2 activation could be modulated by direct binding to the RAC3 protein. We next investigated the possible binding region of RAC3 with Nrf2 protein. The different sizes of the purified GST-RAC3 polypeptides were incubated with His-Nrf2 protein followed by GST pull-down assay. The constructs of the different GST-RAC3 segments in pGEX2T or pGEX4T vector are shown in Fig. 1-1A.

First, we conducted GST pull-down assay by incubating with His-Nrf2 and different GST-RAC3 fragments (bHLH, pasA, pasB, R1, R2, R2A, and R3) (Fig. 1-1A). The samples were immunoblotted against Nrf2 using anti-Nrf2 (C-20) antibody. The results showed that His-Nrf2 strongly interacted with pasB and R3 of GST-RAC3 protein (Fig. 1-7A). R1 and R2 also showed some interactions with Nrf2 (Fig. 1-7A).

To find more specific region in R3 for His-Nrf2 binding, R3 of GST-RAC3 was dissected into three parts (R3A, R3B, and R3C; Fig. 1-1A) and followed by GST pull-down assay as described above. The results showed that R3A and R3B also interacted with His-Nrf2, whereas the short C-terminal protein (R3C) did not interact with His-Nrf2 (Fig. 1-7B).

To further investigate the binding of R3B segment to Nrf2, N-terminal of R3B was deleted to make R3B subsegments (R3B1, R3B2, R3B3, and R3B4; Fig. 1-1A) to find the specific region for His-Nrf2 binding. GST pull-down study showed that R3B3 was strongly bound to His-Nrf2, whereas the binding of R3B4 to His-Nrf2 was significantly reduced (Fig. 1-7C).

We next compared the binding ability between R3B1 and R3B3 to His-Nrf2. The

results showed that R3B1 had lower binding affinity to His-Nrf2 as compared to R3B3 (Fig. 1-7D). These results, taken together, suggest that pasB (92-204) and R3B3 (1210-1417) regions in RAC3 protein may play critical roles in Nrf2 activation.

1.3.6. PasB and R3B3 regions of RAC3 bind to N-terminal transactivation domains Neh5 of Nrf2

So far, we had found the critical regions of RAC3 binding to the full-length Nrf2 protein. However, the region of Nrf2 that may bind to RAC3 protein is not elucidated. We next investigated the Nrf2 region, which can bind to the RAC3 protein. Prior to the GST pull-down method, various His-Nrf2 segments (Fig. 1-1B) were constructed in pET28b(+) vector for bacterial expression.

The purified His-Nrf2 and its different size of segments (N1, N2, N2-a, N2-b, N2-c, N3, and N4; Fig. 1-1B) were incubated with pasB or R3B3 fragments (from above) conjugated with GSH bead. After incubation, the samples were immunoblotted against Nrf2 using anti-Nrf2 (C-20). Since Nrf2 antibody (C-20) recognizes the C-terminal epitope of human Nrf2, all Nrf2 segments can be detected in immunoblotting analysis. The results showed that both pasB and R3B3 of RAC3 strongly bound to N1 and N2 of Nrf2, but not the others (Fig. 1-8).

To corroborate the results from the GST pull-down study above, we next conducted fluorescence resonance energy transfer (FRET) assay to verify the interactions between Nrf2 and RAC3. This assay was designed to validate the molecules that are closely locating within 10 nm distance. Recently, cyan fluorescent protein (CFP)-yellow fluorescent protein (YFP) pair has been used for FRET assay to investigate the functional

interactions between two molecules. If, for example, CFP-tagging protein is closely co-localized with or bound to YFP-tagging protein, energy (457 nm) given to CFP-tagging protein can transfer to YFP-tagging protein to emit yellow fluorescent energy (545-600 nm). Based on this rationale, we constructed ECFP-RAC3 and its segments (ECFP-PasA, ECFP-pasB, and ECFP-R3B3) and EYFP-Nrf2 and its segments (EYFP-N2 and EYFP-N2a). Then, HeLa cells were cotransfected with ECFP-RAC3s and EYFP-Nrf2s with different combinations. FRET results showed that Net FRET signal was the strongest in pairs with ECFP-R3B3 and EYFP-Nrf2 or EYFP-N2 (Fig. 1- 9A,B).

1.3.7. RAC3 binds to ARE region in heme oxygenase-1

Based on the results above, we can suggest that RAC3 could regulate Nrf2 signaling via directly binding of its N-terminal pasB domain and C-terminal R3B3 region to the Neh4 and/or Neh5 domains (Fig. 1-1B) of Nrf2. Then, RAC3 protein might be detectable in the Nrf2-bound ARE DNA sequence. For this reason, we conducted chromatin immunoprecipitation (ChIP) assay to elucidate whether RAC3 protein is detectable in the ARE sequences binding with Nrf2. HeLa cells were transfected with EYFP-Nrf2 and/or HA-RAC3 constructs and the total cell-lysate samples were subjected to ChIP assay against the ARE enhancers in Heme oxygenase-1 (HO-1) promoter.

As described previously, the HO-1 5'-flanking region contains ARE enhancers (A, at -4.1 kb) and three ARE enhancers (B, at -9.1 kb). These two regions were amplified by PCR reaction after immunoprecipitation using anti-RAC3 (M-397) or anti-Nrf2 (C-20) antibodies. The PCR results showed that both regions A and B were strongly amplified in EYFP-Nrf2 plus HA-RAC3 transfection group from two different sets of antibody-treated groups (Fig. 1-10A). These results suggest that RAC3 can bind to Nrf2, which binds to

the ARE sequence in the 5'-flanking region of human HO-1.

1.3.8. Ca^{2+} activates Nrf2/ARE-luciferase activity and induces Heme oxygenase-1 expression

Prior to isolation of Nrf2 partner candidates using One-STrEPTTM purification system (IBA GmbH, Germany), HeLa cells were transfected with EGFP-Nrf2-One-strep (GFP-Nrf2-Os) or EGFP-One-strep (EGFP-Os) construct in the presence of ARE-luciferase plasmid to check for Nrf2 transcriptional activity. After transfection, HeLa cells were treated with 25 μM of sulforaphane, a naturally occurring ARE activator, for 6 h. The results show that EGFP-Nrf2-One-strep strongly induced the Nrf2/ARE-luciferase activity. Moreover its activity was enhanced by sulforaphane treatment (Fig. 1-12A). Thus, we used these constructs for the isolation of potential candidates of Nrf2 partners. To conduct the Nrf2-partner isolation, it is necessary to know whether divalent cations, such as Ca^{2+} or Mg^{2+} , are involved. This is because chelating agent, such as EDTA, in lysis buffer can interfere to make complex between Nrf2 and its partners if Ca^{2+} ion is critical for the Nrf2 signaling. Thus, we check whether Ca^{2+} could activate Nrf2/ARE-luciferase activity and endogenous hemoxygenase-1 (HO-1) induction. The result showed that Nrf2/ARE-luciferase activity (Fig. 1-12B) and HO-1 protein (Fig. 1-12C) were significantly induced by adding 3.8 mM of CaCl_2 in GFP-Nrf2 transfected cells, whereas higher concentrations of CaCl_2 at 11.8 mM did not activate Nrf2/ARE-luciferase activity and HO-1 expression. This might be due to the cytotoxicity.

1.3.9. Fourteen Nrf2-partner candidates were isolated and identified from the One-STrEP™ purification system and LTQ_Orbitrap LC/MS/MS equipment, respectively

Fig. 1-13A shows the One-STrEP™ purification system that was applied in this study (IBA GmbH, Germany). The key principle of this experiment is that One-strep tag in EGFP-Nrf2 protein can easily bind to strep-tactin bead and EGFP-Nrf2-One-strep bound partner complexes can then be eluted with desthiobiotin sequentially. The eluted protein complexes can be separated on SDS-PAGE gel and the gel will be stained with appropriate staining such as silver staining and followed by mass spectroscopic analysis. Representative bands can be excised for the identification of Nrf2 partner candidates using LTQ_Orbitrap LC/MS/MS equipment. Thus, we cut out the six representative bands (F1 to F6, Fig 1-13B) from the silver stained gel and each band from two groups was analyzed for protein identification. As a result, fourteen major Nrf2 binding proteins were identified. Among them, four were a known Nrf2 and ten were a new Nrf2 partner candidates that were identified (Table 1).

To check and verify the identified proteins, elution samples were subjected to Western blot analysis using anti-IQGAP1, anti-Keap1, and anti-Maf F/G/K antibodies. The results showed that all proteins were clearly detected as EGFP-Nrf2-One-strep partners (Fig. 1-13C). Based on these results, we investigated the interaction and functional significance between Nrf2 and IQGAP1, a calmodulin binding protein, as a newly identified Nrf2 partner on Nrf2 signaling.

1.3.10. IQGAP1 enhances Nrf2 stability and HO-1 expression

To verify the role of IQGAP1 in Nrf2 signaling, HeLa cells were transfected with EGFP-Nrf2 and Dsredm-IQGAP1 constructs for 24 h. Immunoblotting data showed that Dsredm-IQGAP1 stabilized the EGFP-Nrf2 resulting in strong induction of heme oxygenase-1 (Fig. 1-14A). Likewise, EGFP-Nrf2 was also stabilized by Dsredm-IQGAP1 expression shown in separate experiment (Fig. 1-15A). To support this finding, HeLa cells were cotransfected with EGFP-Nrf2 and Dsredm or EGFP-Nrf2 and Dsredm-IQGAP1 for 24 h in cover glass-bottomed dishes. Then the expressed proteins in the cells were analyzed for their subcellular localization and intensity of protein expressed under the fluorescent microscopy. Epifluorescence results showed that EGFP-Nrf2 protein, when transfected with EGFP-Nrf2 alone, was mostly expressed in the nucleus. In contrast, EGFP-Nrf2 was strongly increased its expression in the nucleus as well as in the cytoplasm by co-transfection with Dsredm-IQGAP1 plasmid (Fig. 1-14B). As a negative control for this experiment, HeLa cells were transfected with EGFP-Nrf2 and Dsredm-Keap1 to show the localization and stability of Nrf2 by the Keap1 protein. The Figure showed that Nrf2 was localized in the cytoplasm with Keap1 and the stability of Nrf2 in cytoplasm was dramatically decreased (Fig. 1-14B).

1.3.11. Silencing of IQGAP1 makes Nrf2 unstable and that results in inhibition of heme oxygenase-1 expression

To confirm the function of IQGAP1 on Nrf2 signaling, first we designed and constructed two possible small interference IQGAP1 RNAs (siIQGAP1s) in pRNAT vector (Genscript), which expresses GFP constitutively. To screen the effective siIQGAP1 constructs against IQGAP1, HeLa cells were transfected with each siIQGAP1 construct

(siIQGAP1-1 or siIQGAP1-2) with EGFP-Nrf2 plasmid for 24 h and subjected to Western blot analysis. The results showed that endogenous level of IQGAP1 was significantly decreased by siIQGAP1-2 transfection. Furthermore, expression of heme oxygenase-1 (HO-1) and EGFP-Nrf2 were also significantly decreased by siIQGAP1 (Fig. 1-16A). Densitometrical results showed that endogenous protein levels of HO-1 and IQGAP1 in EGFP-Nrf2 transfection were decreased to 40% and 50% by siIQGAP1-2 plasmid transfection (Fig. 1-16B). In the triple transfection (EGFP-Nrf2 plus Dsredm-IQGAP1 plus siIQGAP1-2) study also showed that siIQGAP1-2 inhibited the endogenous HO-1 and Dsredm-IQGAP1 as well as EGFP-Nrf2 expression (Fig. 1-16C). Likewise, siIQGAP1-2 also repressed the Nrf2/ARE-luciferase activity (Fig. 1-16D).

1.3.12. The two endogenous Nrf2 and IQGAP1 bind together

With the EGFP-Nrf2-One-strep tag purification system above, it can be postulated that IQGAP1 protein can bind to Nrf2 directly or indirectly. To support this result, we conducted immunoprecipitation (IP) assay. HeLa cells, in normal condition, were subjected to IP with anti-IQGAP1 (H-109) or anti-Dsred (C-20) antibodies and blotted against Nrf2 using anti-Nrf2 (C-20) antibody. The results showed that Nrf2 strongly bound to IQGAP1 protein (Fig. 1-17A). To verify the quality of fractionated samples, both cytosolic and nuclear extracts were subjected to Western blotting using IQGAP1 and Lamin A for cytosolic and nuclear extracts respectively (Fig. 1-17B).

1.3.13. Nrf2-IQGAP1 complex was disrupted by calcium

From the previous data, we can assume that IQGAP may play an important role in Nrf2 signaling in conjunction with calcium. To test the function of calcium on Nrf2-

IQGAP1 binding, HeLa cells were treated with 3.8 mM CaCl_2 (in control, 1.8 mM), 5 mM EGTA (calcium chelator) or 10 μM BAPTA (calcium chelator) for 30 min and subjected to immunoprecipitation shown in Fig. 1-17A. The results showed that binding affinity of Nrf2 to IQGAP1 was significantly decreased by treatment of CaCl_2 , whereas, treatment of either EGTA or BAPTA had no effect on this (Fig. 1-17A).

1.3.14. Calcium stimulates the expression of heme oxygenase-1 in early time

To show the affinity between Nrf2 IQGAP1 with different time intervals, HeLa cells were treated with 3.8 mM CaCl_2 for 0 to 6h. Next, cytosolic extracts were subjected to immunoprecipitation using anti-Dsred (C-20) or anti-IQGAP1 (H-109) and blotted against Nrf2 (C-20) or IQGAP1 (H-109) antibodies (Fig. 1-18A). In addition, the same cytosolic samples were subjected to Western blotting against HO-1 using anti-HO-1 (C-20) antibody (Fig. 1-18B). The results showed that Nrf2-IQGAP1 complex was disrupted in 30 min by treatment of CaCl_2 and resurrected after 1 h. Moreover, HO-1 protein was induced by single treatment of CaCl_2 . Induction of HO-1 was started in 30 min and time dependently increased up to 6 h. These results suggest that calcium may trigger the sequestration of Nrf2 from IQGAP1 in early time (< 30 min) resulted in HO-1 induction.

1.4. Discussion

Nrf2 is a key transcription factor for the regulation of ARE-mediated gene expression in response to oxidative and electrophilic insults. Although numerous papers were published on the mechanism of Nrf2-mediated induction of phase II detoxifying enzymes and antioxidant enzymes, the exact mechanisms of Nrf2 signaling is still not clear.

Although, previously, several interacting molecules, such as Keap1, CBP/p300, and small Maf proteins (MafF, MafG, and MafK), were identified as potential regulators of Nrf2 signaling, it is possible that other unknown partners could interact with Nrf2 for the regulation of antioxidant response. In this study, we demonstrated that the nuclear co-regulator RAC3, a p160 cofactor family, interacted with Nrf2 by binding between the two regions of RAC3 and the Neh5 domain of Nrf2 in HeLa cells.

From the previous report by Zhu and Fahl (194), it was proposed that ARE-binding protein-1 (ARE-BP-1), not identified protein, which might be a member of p160 coactivator could bind to the ARE sequence for the regulation of antioxidant genes, since MafK antibody ablated the binding ability of the ARE-binding protein-1 to the ARE sequence in gel-shift assay. In addition, they used SRC-1 or SRC-2 antibodies for the ablation between ARE-BP-1 and ARE sequence, however it was shown that they had no effect on that binding inhibition. Indeed, it remains to be determined whether RAC3, same as SRC-3, involved in the binding ability to the ARE sequence.

Meanwhile, recent publication from our lab elucidated the interaction between RAC3 and Nrf2 using Gal4-luciferase reporter system in HepG2 cells (108). This paper showed that Gal4-Nrf2 (1-370) chimera containing two transactivation domains (TAD), Neh4 and Neh5, interacted with RAC3 resulted in the induction of luciferase activity. However, enhancement of transactivation activity of Nrf2 by RAC3 may not be explained in this paper since Gal4-luciferase system is designed to find a binding partner that can be a transcriptional activator or suppressor. To know the functional role of RAC3 in Nrf2 signaling, it is necessary to verify the induction of Nrf2-induced target protein such as Heme oxygenase-1. Therefore, we investigated whether RAC3 is a coactivator or

corepressor of Nrf2 signaling.

First, we evaluated the function of RAC3 on Nrf2 transactivation signal by testing the Nrf2/ARE-luciferase activity. If this assay system is appropriate for the functional study of Nrf2 partners (co-activator or co-repressor), the expression of Nrf2-mediated target protein such as HO-1 would be consistent with results of Western blotting method and RT-PCR analysis. However, as results shown in the Fig. 1-2, Nrf2/ARE-luciferase assay was conflicted with Western blotting and RT-PCR results. Here, we postulate that short size of ARE-luciferase gene in reporter vector may not be sufficient for the Nrf2-partner interaction study, or co-transfection (RAC3 and Nrf2 construct) may not good tool since over-expression of one gene can be hindered by the other gene's over-expression. Therefore, in this study, we will exclude the results from the Nrf2/ARE-luciferase assay.

In this study, based on the Western blot analysis and RT-PCR, we showed that overexpression of RAC3 could induce the HO-1 protein and *HO-1* mRNA in HeLa cells. However, we found that the expression of *NQO-1* mRNA was not much changed by co transfection of YFP-Nrf2 and HA-RAC3 transfection. In addition, the mRNA levels of *GSTA1*, *UGT1A1* and *UGT1A3* were not expressed in HeLa cells.

Here, we investigated the interactionship between Nrf2 and RAC3 protein whether these molecules were direct or indirect interacting for the transactivation of Nrf2. Furthermore, we identified the possible interacting domains of two molecules.

From the GST pull-down assay in Fig 1-7, the interaction domains between RAC3 and Nrf2 were kind of surprising. The data suggest that R3B3 has much stronger binding affinity to Nrf2 than the pasB of RAC3 domain (Fig. 1-1A+B). Twenty amino acids,

¹²¹⁰MQPQQGFLNAQMVAQRSRELLS¹²³¹, might be indispensable for the binding of RAC3 to Nrf2 protein since cutting out this part caused significant loss of binding ability to Nrf2 (comparing R3B3 versus R3B4; Fig. 1-1A + Fig. 1-7C). From the Fig. 1-6 to 1-8, the N-terminal pasB and C-terminal R3B3 regions of RAC3 bind to both Nrf2-N1 and Nrf2-N2 but not Nrf2-N2a segments. The results suggest that Neh5 domain of Nrf2 may be indispensable for the RAC3 binding. But the possibility of Neh4 domain bind to RAC3 is still possible, because N1 is strongly binds to R3B3 rather than N2. To elucidate whether Neh4 domain can bind to both pasB and R3B3 regions of RAC3, different mutation methods will be needed in the future. It is possible that RAC3 may need both Neh4 and Neh5 domains of Nrf2 for the modulation of signaling. Katoh *et al.* (73) showed that both Neh4 and Neh5 domains of Nrf2 could cooperatively bind to CBP resulted in synergistic increase of Nrf2 transactivation. In addition, Shen *et al.* (152) showed that Nrf2 transactivation domain containing Neh4 and Neh5 could bind to CBP protein resulted in the activation of Nrf2 using the Gal4-luciferase system.

Like other p160 cofactors family, RAC3 also shares conserved domains (118). From the N-terminus, there is a basic helix-loop-helix (bHLH) domain and pasA/B (Per/Arnt/Sim) domains for the nuclear localization (103) and protein-protein interaction (118), respectively. In the middle region, there is an α -helical LXXLL motif where it can bind with steroid receptor (54). In the C-terminus, there are HAT domain for acetyltransferase activity, CBP binding domain and CARMI/PRMT1 interaction domain (100), which is also overlapping with our R3B3 region of Nrf2 (Fig. 1-1A). Based on these information, it may be speculated that pasB domain of RAC3 may bind to Nrf2 for the recognition and dimerization and this is followed by R3B3 (we named Nrf2 bind domain,

NBD) binding to Nrf2.

Numerous reports showed that RAC3, expresses not only in breast cancer cells (91, 162), but also in different types of cancers, such as prostate cancer (45), esophageal squamous cell carcinomas (181), pancreatic adenocarcinoma (55), hepatocellular carcinoma (170), colorectal carcinoma (179), and gastric cancers (146). Therefore, the oncogenic RAC3 may play an important role in tumorigenesis.

In this study of IQGAP1 on Nrf2 signaling, we have isolated and identified several possible Nrf2 signaling-partner proteins using One-strep tag purification system. Among the newly identified Nrf2 partners, IQGAP1, a scaffolding, actin binding and calmodulin binding protein, was further investigated on the Nrf2 signaling. Here, we found that calcium ion could play an important role in Nrf2 signaling. In that regards, we postulate that IQGAP1 protein may scaffold Nrf2 via calcium signaling, which lead to augmentation of Nrf2 stability to enhance the induction of phase II genes or antioxidant related genes.

Nrf2 has been considered as a key transcriptional factor for the regulation of ARE-mediated gene expression in response to oxidative and electrophilic insults. Although the several functional proteins, such as Keap1(82, 124), MAPKs (128), PKC (61), PI3K (127), CBP (73) as well as small Mafs (8), have been implicated on the Nrf2 transactivation activity. The precise mechanism of Nrf2 signaling is elusive.

Previously, it had been considered that Nrf2 might be regulated by Keap1 anchoring to the cytoskeleton, such as F-actin, in the perinuclear region (71). However this hypothesis is challenged by Velichkova and Hasson's theory (165). They propose that Keap1 does not anchor Nrf2 to the cytoskeleton. In response to oxidative stress, Nrf2

may be released not from the Keap1 anchored to the actin but instead from those Keap1 in the cytoplasm for its nuclear localization. Moreover, this notion has been supported by Watai *et al.* (173) suggesting that the complex between Keap1 and actin cytoskeleton or cytoplasmic scaffold may not be as simple and direct straightforward, since they show no clear-cut of co-localization between endogenous Keap1 and actin filaments (F-actin). In this regards, molecular mechanism based on the perinuclear localization of Keap1 may need to be further clarified.

Since the precise event of Nrf2 signaling can not be explained with restricted information, thus we explored to find potential new Nrf2 partners. To investigate new and novel Nrf2 partners, in the current study we applied One-strep tag purification system (IBA, GmbH, Germany). This system is designed to purify intact protein complexes under physiological conditions inside the cells. One-strep tag consists of two strep tag II sequences (SAWSHPQFEK) along the edges, which facilitate binding affinity between One-strep tag and streptavidin bead (Strep-Tactin bead).

Prior to purification of Nrf2 complex, we first checked the role of calcium ion in Nrf2 activation through the Nrf2/ARE-luciferase and Western blotting against HO-1 protein. If calcium ion plays a critical role in Nrf2-partner complex, then the complex could be affected by EDTA in cell lysis buffer. Based on these results in Fig. 1-12B and 1C, calcium ion is really involved in the Nrf2-partner complex, thus chelating agents, such as EDTA or EGTA, were not added in the cell lysis buffer during the critical purification step. From this information, we isolated many possible Nrf2 partner candidates and identified them using powerful LTQ_Orbitrap LC/MS/MS equipment. Although Table 1 shows only five representative identified proteins, nine newly identified

proteins (unpublished results) and some proteins having low rl (number of peptides found from the sequence only) values were not shown.

Calcium ion involvement was previously postulated from the preliminary results in our group (unpublished results). tBHQ-induced Nrf2/ARE-luciferase activity and HO-1 expression were dramatically abolished by treatment of EGTA (5 mM), a chelating agent of Ca^{2+} , in HT-29 cells and HepG2 cells (data not shown). Whereas Nrf2/ARE-luciferase activity and HO-1 expression were significantly increased by treatment of CaCl_2 in HeLa cells (Fig.1-12B/C and Fig. 1-18).

It has been reported that diallyl trisulfide (DATS), a garlic organosulfur compound, could increase the intracellular level of Ca^{2+} in the early hours of treatment (147). In addition, it is known that an increased level of intracellular Ca^{2+} is associated with GSH (reduced glutathione) level (70), and Calcium-dependent CaMK (calcium/calmodulin-dependent protein kinase) is implicated in stress-mediated cellular defense response (60).

Furthermore, microarray data reported by Lee et al. (97) showed that Nrf2^{+/+} mouse primary neuronal cultures had higher expression levels of genes encoding calcium homeostasis protein, such as, visinin-like 1, calbindin-28K, synaptotagmin-1, hippocalcin, and calmodulin III, compared with Nrf2^{-/-}, suggesting calcium may play an important role in Nrf2 signaling. Based on these previous reports, it is assumable that increased intracellular level of Ca^{2+} by inducers may play a critical role in Nrf2 signaling.

IQGAP1, as a scaffolding protein, can assemble with many proteins, such as calmodulin, actin, Cdc42, Rac1, E-cadherin, β -catenin, and CLIP-170, for different signaling pathways. As such IQGAP1 partners can be modulated by calmodulin

association with calcium ion (Reviewed in ref. (11)). Calcium ion, as a intracellular messenger, is distributed ubiquitously in the cells and play an important role in controlling numerous cellular events (7). The major mediator of Ca^{2+} signaling is calmodulin, which modulates the function of various downstream targets (24). A temporal rise of intracellular Ca^{2+} concentration induces a conformational change in calmodulin followed by its binding to specific domains on target proteins. For instances, in vitro association between IQGAP1 and Cdc42 was abrogated by calmodulin only in the presence of Ca^{2+} (69). whereas, interaction between calmodulin and IQGAP1 in the cells was enhanced by increase of Ca^{2+} concentration, with a concomitant decrease in the association of IQGAP1 with Cdc42 (57). Moreover, IQGAP is also regulating the cytoskeleton via a direct interaction with actin, via stimulating cross-linking of F-actin.

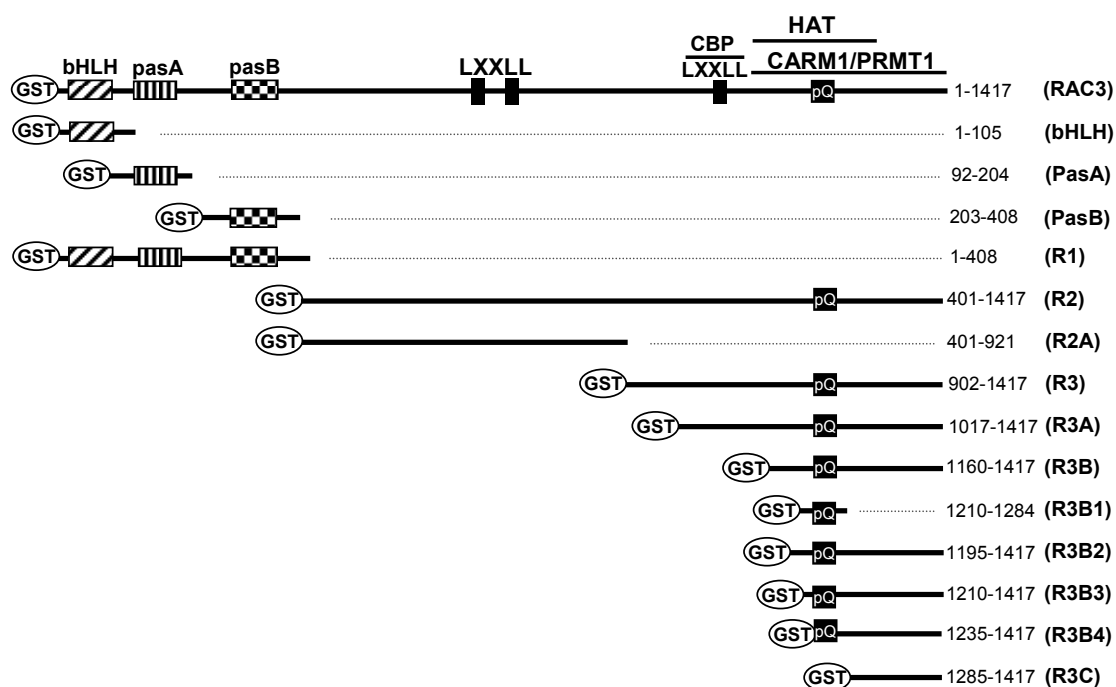
Likewise, as previously described above, cross-linking activity of IQGAP is enhanced by active Cdc42 (bound form to IQGAP1), and reduced by calmodulin in the presence of Ca^{2+} (42, 57, 113). Thus, IQGAP1 may provide a molecular link integrating Ca^{2+} /calmodulin signaling with Cdc42 and the cytoskeleton. In this study, Cdc42 was also isolated and identified from the Nrf2-partner purification system but not included in Table 1 due to the low rl values. The functional of Cdc42 on IQGAP-Nrf2 complex would need to be investigated. Although calmodulin interaction to the IQGAP1 has been implicated in different signaling pathways, the molecular functional role of calmodulin-associated IQGAP1 has not been fully understood.

It has been shown that chemical stress-induced ARE and phas II activites were inhibited by staurosporine, a potent non-specific protein kinase inhibitor (195), and that this inhibitory effect has been attributed to downregulation of the PKC signaling (9, 61).

Based on the role of protein kinases in Nrf2/ARE signaling, the previous paper in our lab suggested that CaMK might be a major functional kinase among other protein kinases, such as PKC, protein kinase A, protein kinase G and myosin light chain kinase. The results were shown that pretreatment with KN-93, a selective CaMK inhibitor, interfered with calmodulin/CaMK binding, resulted in significant inhibition of ARE activity (18).

Based on our results obtained above, we speculate that the intracellular calcium ion concentration $[Ca^{2+}]_i$ may dictate with the potency of calcium-binding protein to IQGAP1, resulting in Nrf2 transactivation. Here, we propose a novel function of IQGAP1 on Nrf2 signaling, in association with Ca^{2+} concentration (Fig. 1-19). For further study, association of Nrf2 to the IQGAP1 must be clarified whether Nrf2 can bind IQGAP1 directly or indirectly and what domain(s) they bind to each other. In addition, subcellular changes of Nrf2-IQGAP1 by stimulation of Ca^{2+} are also interesting.

A)



B)

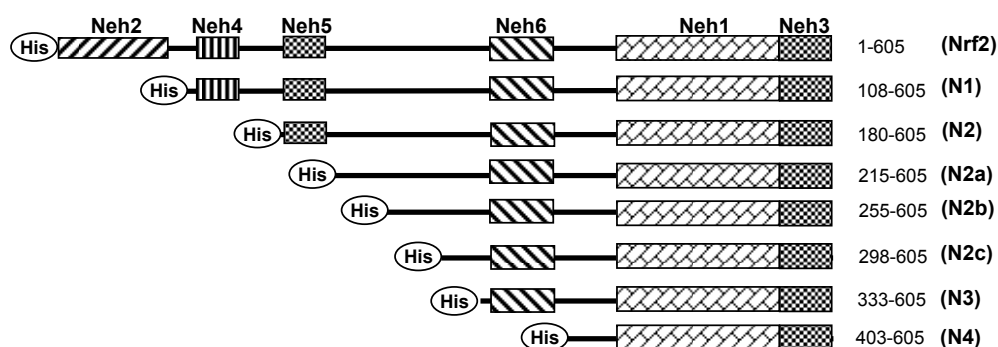


Fig.1-1. Schematic diagram showing the different structures of segmented domains of His-Nrf2 and GST-RAC3 for GST pull-down assay.

A) RAC3 and its segments were subcloned into the bacterial expression vector

pGEX2T or pGEX4T to introduce the N-terminal GST-tag. B) Nrf2 and its segments were subcloned into the bacterial expression vector pET28b(+) to introduce the N-terminal His-tag. The different sizes of the segments are indicated in the figure by amino acid (aa) number from the full length of Nrf2 and RAC3, respectively. All the domains from Nrf2 and RAC3 were previously reported (UniProt Q16236 and Q9Y6Q9).

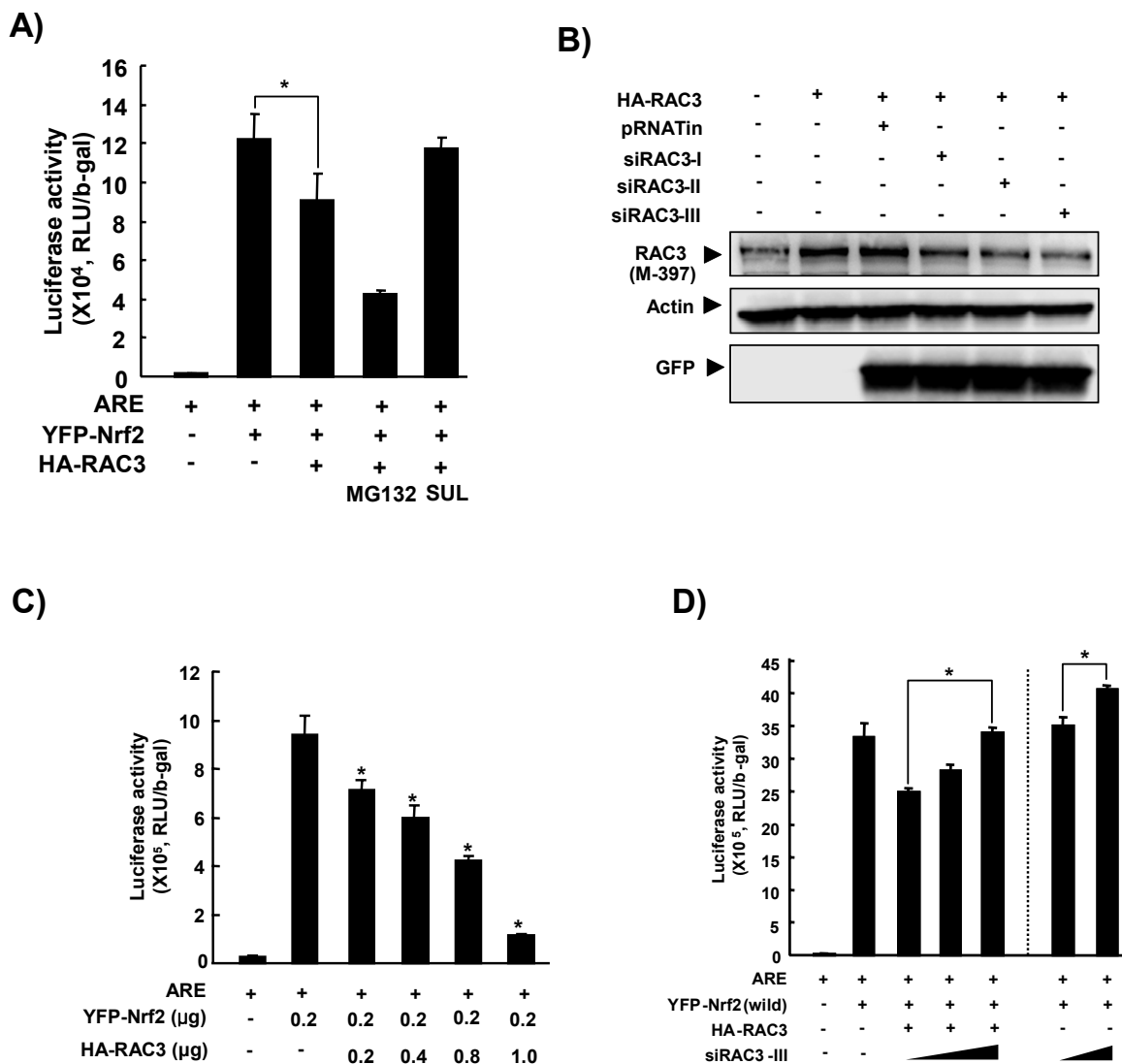


Fig.1-2. Nrf2/ARE-luciferase activity was suppressed by RAC3 and recovered by siRAC3.

A) HeLa cells were transfected with YFP-Nrf2 (0.5 μg) or HA-RAC3 (1 μg) construct for 20 h in the presence of ARE-luc and β-gal constructs using jetPEI reagent and treated with MG132 (10 μM), sulforaphane (25 μM), or tBHQ (100 μM) for 6 h. Cell lysates were subjected to luciferase reporter assay for Nrf2/ARE-

luciferase activity. B) For RAC3 protein silencing study, HeLa cells in 6-well plates were transfected with three designed siRAC3 (2 μ g) (siRAC3-I,-II,-III) and HA-RAC3 (1 μ g) constructs for 24 h. Then cells were lysed with RIPA buffer and subjected to Western blot analysis. For equal plasmid transfection, GFP from pRNATin was measured. C) To study the dose depend manners for Nrf2/ARE-luciferase activity by RAC3, cells in 6-well plates were transfected with YFP-Nrf2 (200 ng) with different amounts of HA-RAC3 (0.2-1 μ) in the presence of ARE (200 ng) and β -gal (100 ng) constructs for 24 h and followed by Nrf2/ARE-luciferase reporter assay. D) To test the dose depend manners for Nrf2/ARE-luciferase activity by siRAC3-III, cells in 24-well plates were transfected with different amounts of siRAC3-III (100, 200 or 300) in the presence of YFP-Nrf2 (200 ng), HA-RAC3, ARE (200 ng) and β -gal (100 ng) constructs for 24 h and followed by Nrf2/ARE-luciferase reporter assay. pcDNA3.1 was used for equal amount transfection for transfection study. Asterisks indicate statistical significance (t test, $p < 0.05$)

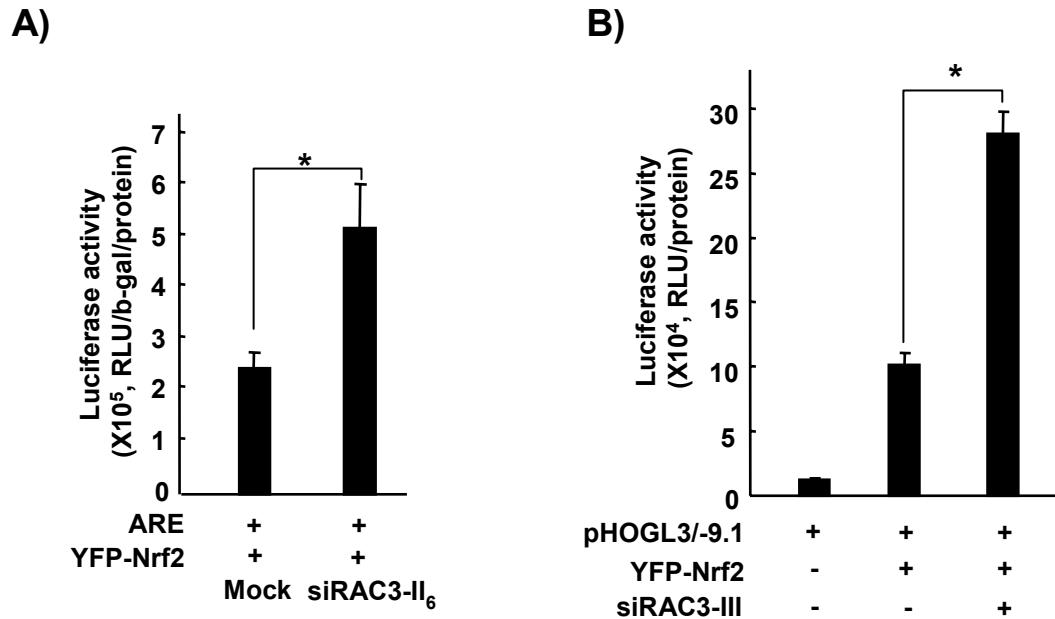
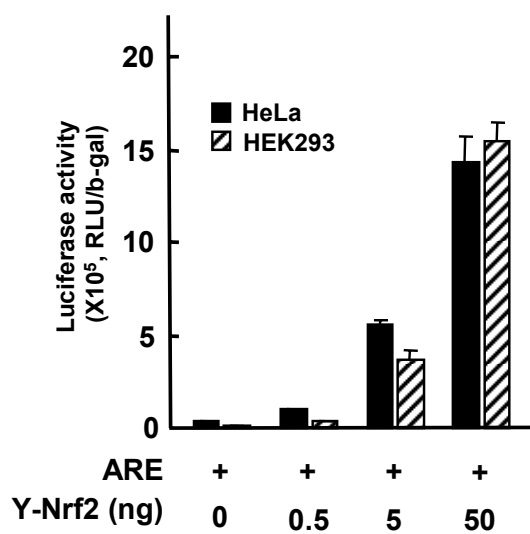


Fig.1-3. RAC3 silencing increases Nrf2/luciferase activity.

A) HeLa-siRAC3-II₆ cells, a stable transfectant with siRAC3-II, were plated in 6-well plates and transfected with YFP-Nrf2(0.5 µg) for 22 h in the presence of ARE (20 ng) and β-gal (0.5 µg) constructs. B) To study the effect of siRAC3 on ARE in HO-1 promoter, HeLa cells were plated in 6 well plates and transiently transfected with 100 ng of plasmid pHOGL3/9.1 containing the -9.1kb size of 5' flanking region in HO-1 promoter ligated to the luciferase gene and 0.5 µg of YFP-Nrf2 or 0.5 µg of siRAC3-III using jetPEI reagent for 24 h. Lysates were analyzed for luciferase activity. Luciferase activity was normalized against β-galactosidase activity. pcDNA3.1 was used for equal amount transfection for transfection study. Asterisks indicate statistical significance (*t* test, *p* < 0.05)

A)



B)

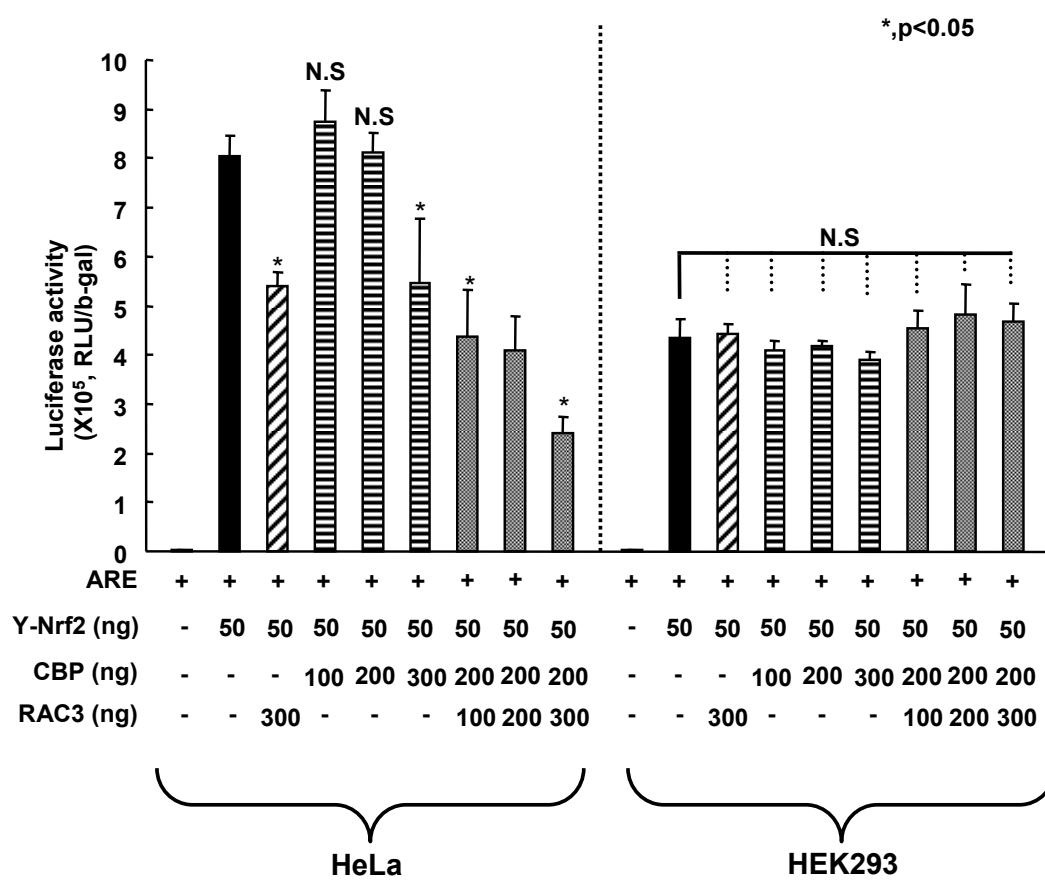


Fig.1-4. Transient transfection of RAC3 shows different results in Nrf2/ARE luciferase between HeLa and HEK293 cells.

A) To see the effect of Nrf2 on Nrf2/ARE luciferase activity in two different cells (HeLa and HEK293), the two different cells were transiently transfected with indicated amount of YFP-Nrf2 construct for 24 h. Then cell lysates were subjected to ARE-luciferase assay. B) To see the effect of RAC3 in HeLa and HEK293 cells, the two cells were transiently transfected with HA-RAC3 in the presence of different constructs indicated in the figure. Luciferase activity was normalized against β -galactosidase activity. pcDNA3.1 was used for equal amount transfection for transfection study. Asterisks indicate statistical significance (t test, $p < 0.05$). N.S, no significant

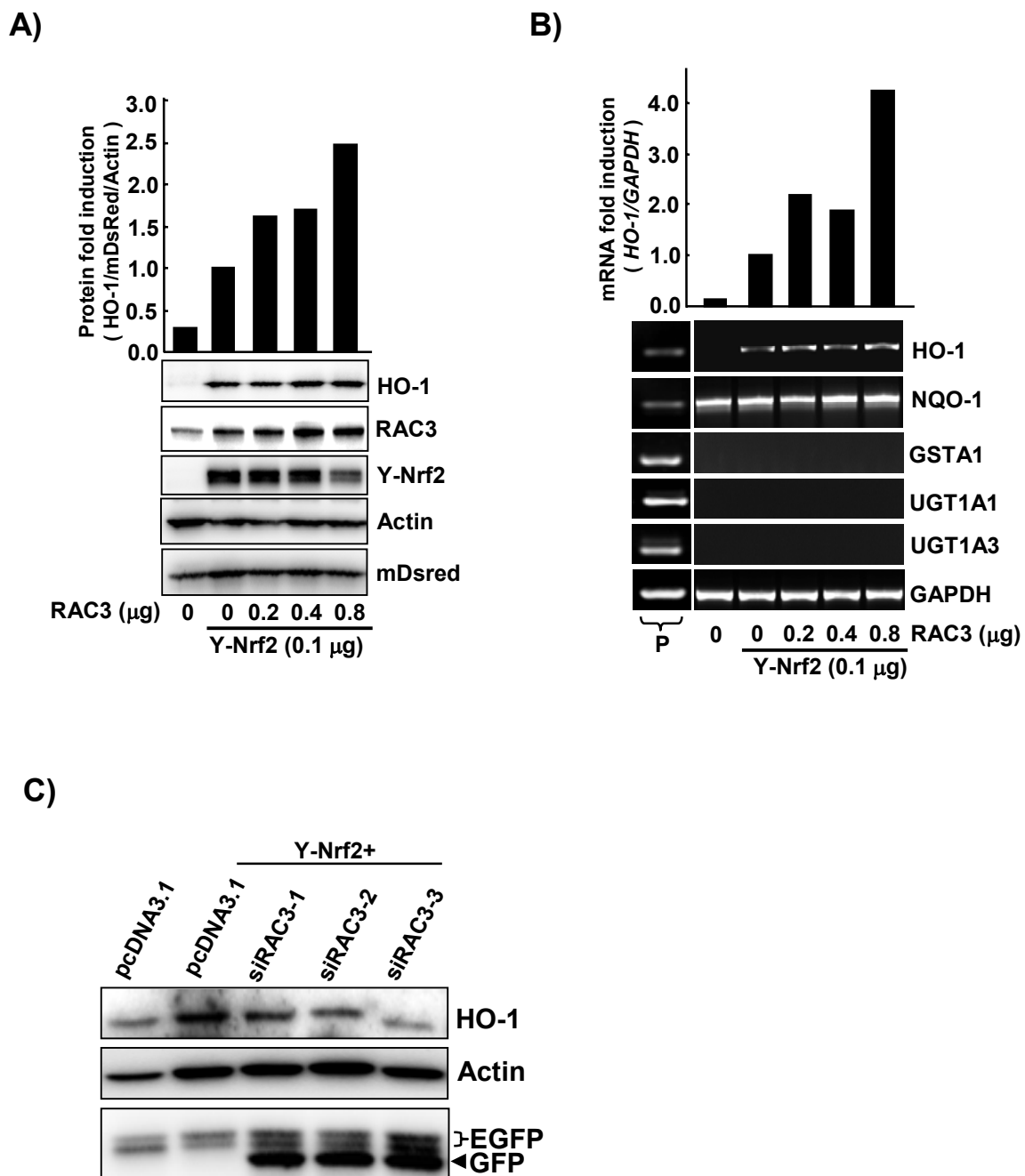


Fig.1-5. HO-1 protein and its mRNA were induced by transient transfection with Nrf2 and RAC3 and decreased by siRAC3.

A) HeLa cells were transfected with YFP-Nrf2 and HA-RAC3 constructs for 24 h. Amounts of constructs were indicated above. Then cell lysates (20 μ) were

subjected to Western blotting to measure HO-1 protein level. pcDNA3.1 was used for equal amount transfection. For transfection efficiency, pDsredm (10 ng) was transfected to each well. The relative fold induction of HO-1 was analyzed by densitometrical analysis (upper bar). B) To see the effect of RAC3 on *HO-1* mRNA expression, same samples from the duplicates from (A) was subjected to RT-PCR. Specifically designed primers used for the amplification of HO-1, NQO-1, GSTA1, UGT1A1, UGT1A3 and GAPDH. P, positive control from primary cultured human liver. The relative fold induction of *HO-1* mRNA was measured by densitometrical analysis (upper bar). C) To see the effects of siRAC3 constructs on HO-1 expression, HeLa cells were transfected with YFP-Nrf2 (0.8 µg) and three different siRAC3s (0.7 µg) for 24 h. EGFP protein from pEGFP empty vector (0.2 µg) was used for equal transfection. GFP protein expressed by siRAC3 construct was also used for equal transfection among siRAC3 constructs.

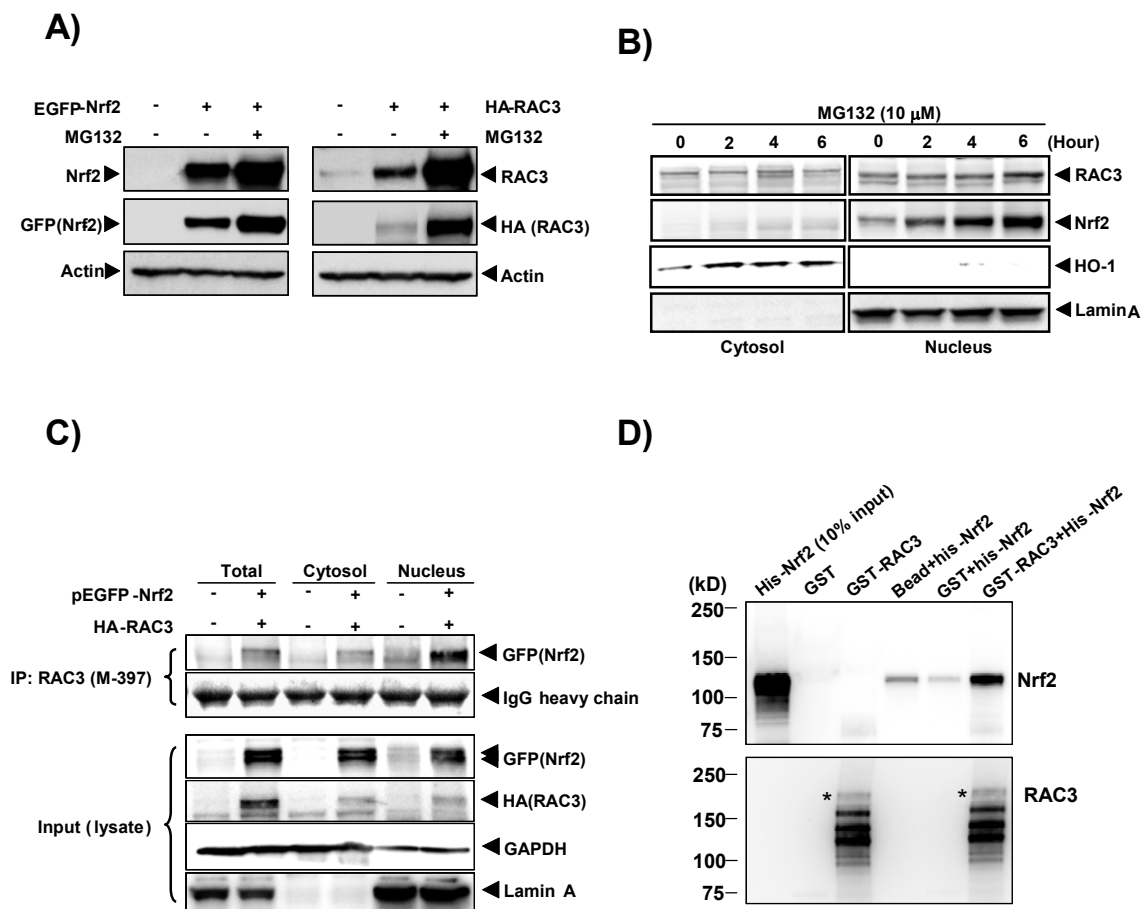


Fig.1-6. Nrf2 binds directly to RAC3 protein.

A) Prior to the Co-IP study with Nrf2 and RAC3, two constructs were verified by checking their EGFP-Nrf2 or HA-RAC3 overexpression in HeLa cells. The cells were transiently transfected with GFP-Nrf2 (3 μ g) or HA-RAC3 (3 μ g) using jetPEI reagent (Polyplus-Trasfection) for 24 h and followed by MG132, a proteasome inhibitor, treatment for 6 h. Protein samples (20 μ g) were subjected to Western blot analysis against overexpressed Nrf2 and RAC3 using anti-GFP or anti-Nrf2 (C-20) and anti-HA or anti-RAC3 (M-397) antibodies. Actin was used for equal loading control. B) To understand the subcellular localization of RAC3

and Nrf2 in HeLa cells, MG132 (10 μ M), a proteasome inhibitor, was treated for different time intervals and the cytosolic and nuclear fractions were isolated using M-PER buffer (Pierce). Fractionated samples (20 μ g) were subjected to Western blot analysis to measure endogenous level of proteins using specific antibodies as indicated on the figure. Lamin A was used as control indicator for nuclear fraction. C) To study whether Nrf2 can bind to RAC3 protein, HeLa cells in 6-well plates were transfected with EGFP-Nrf2 (2 μ g) and HA-RAC3 (2 μ g) constructs for 24 h to conduct co-immunoprecipitation (Co-IP) assay. Two hundred micrograms of protein from the different fractions were immunoprecipitated with anti-RAC3 (M-397) and blotted against EGFP-Nrf2 using anti-GFP antibody by Western blot analysis. Co-IP method is described in the Materials and Methods. GAPDH and Lamin A were used for the control standards of cytosol and nucleus. IgG heavy chain was used for equal bead loading control. D) To study whether Nrf2 can bind to RAC3 directly, purified His-Nrf2 and GST-RAC3 from bacterial expression system were incubated and GST-RAC3 was pull-downed with GSH-bead in vitro. Protein-bead complexes were subjected to Western blot analysis using anti-Nrf2 (C-20) antibody. The detail procedures are described in Materials and Methods.

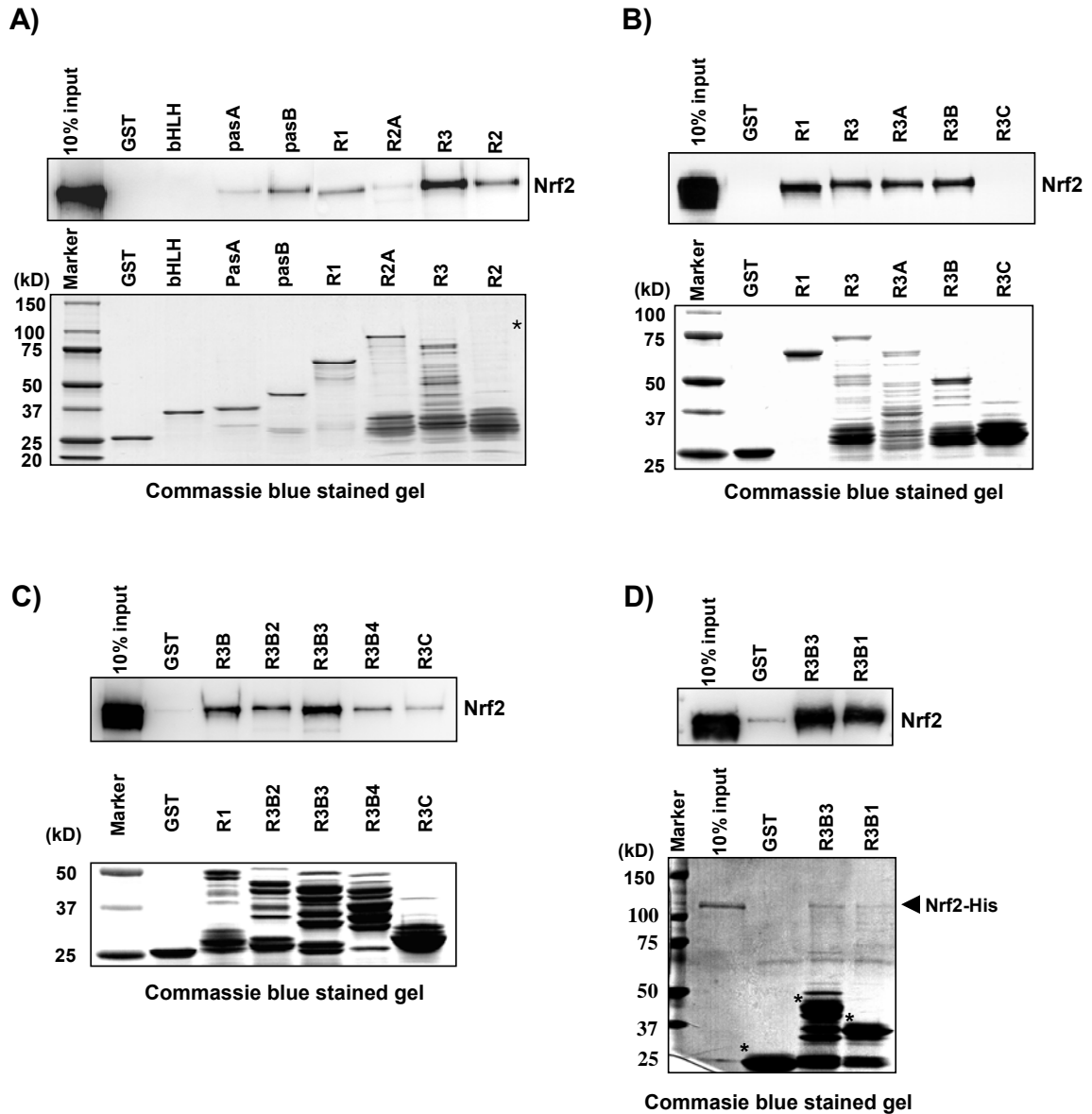


Fig.1-7. pasB and R3B3 domains of RAC3 bind to Nrf2.

A) Purified GST-RAC3 segments were incubated with His-Nrf2 protein and followed by GST pull-down assay. N-terminal segments (bHLH, pasA, pasB, and R1), central segment (R2A), and C-terminal segments (R2 and R3) were incubated with His-Nrf2 and followed by GST pull-down assay. Protein-bead complex samples were prepared for Western blot analysis blotting against His-

Nrf2 using anti-Nrf2 (C-20). Among the segments of GST-RAC3, pasB and R3 strongly bound to His-Nrf2 protein. B) To identify the Nrf2 binding domain in the R3 region of RAC3, N-terminal deleted segments of R3 (R3A, R3B, and R3C) were incubated with His-Nrf2 and followed by GST pull-down assay. Immunoblotting against His-Nrf2 was the same as above. In this study, R3B segment of GST-RAC3 strongly bound to His-Nrf2 protein. C) To identify the Nrf2 binding domain in R3B region of RAC3 based on the previous results in (B), N-terminal deleted segments of R3 (R3B2, R3B3, and R3B3) were incubated with His-Nrf2 and followed by GST pull-down assay and immunoblotted against His-Nrf2. In this study, R3B3 segment of GST-RAC3 bound strongly to His-Nrf2 protein. D) R3B3 and its C-terminal deletant R3B1 were incubated with His-Nrf2 protein to verify the binding region of RAC3. GST pull-down assay for this study was the same as in (A). Equal volume of purified His-Nrf2 was applied to the reactions, and the same amount of GST-RAC3 segments for the reaction were run on SDS-PAGE gel and stained with commassie brilliant blue shown in the bottom from each experiment. Asterisk indicates the expecting size of the proteins. Degraded GST-RAC3 segments are also shown in commassie blue stained gels.

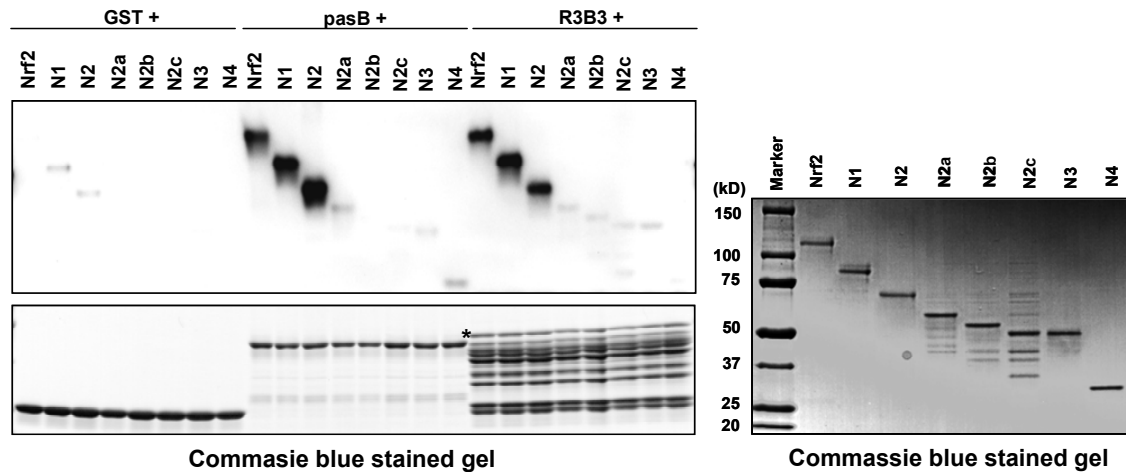
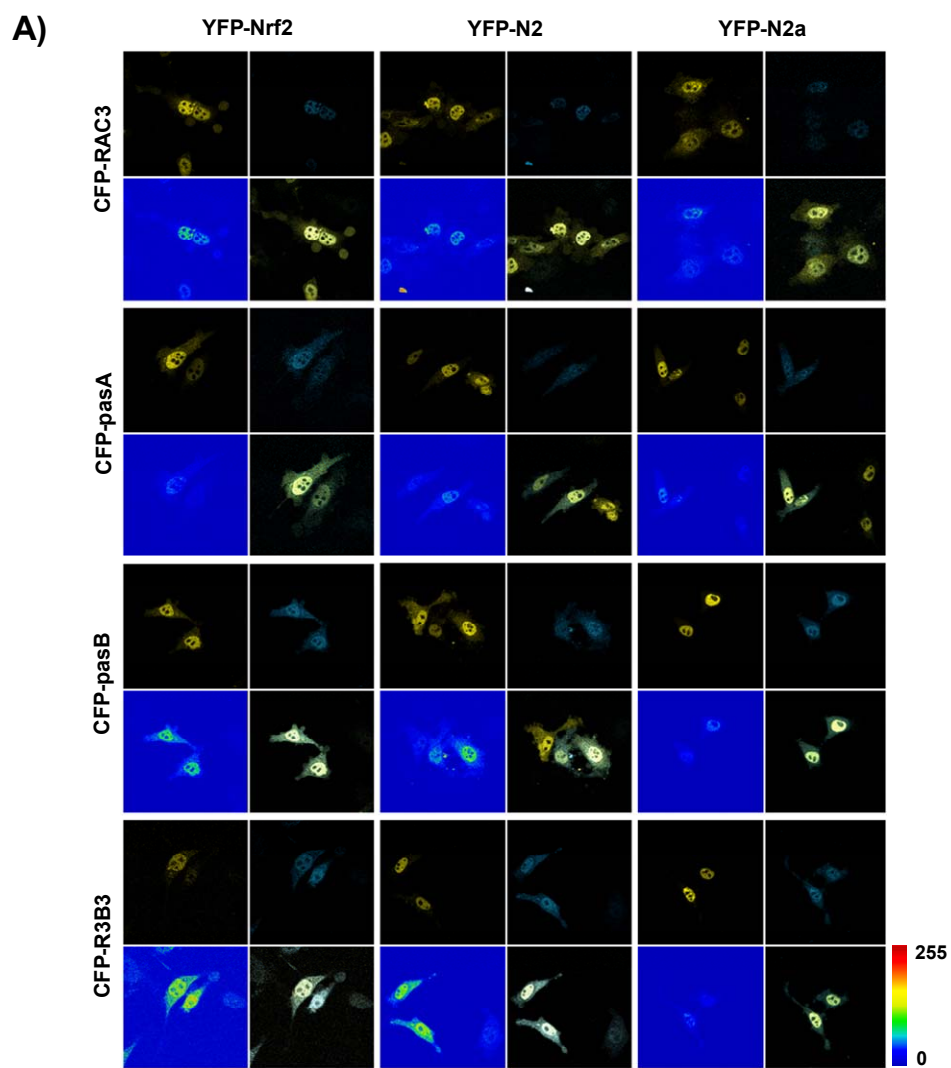


Fig.1-8. pasB and R3B3 regions in RAC3 strongly bind to N2 containing Neh5 domain of Nrf2.

To identify the binding domain of Nrf2 by pasB and R3B3 regions of RAC3, GST-pasB or GST-R3B3 were incubated with His-Nrf2 and its segments. GST pull-down procedures were the same as previous experiments described above. Equal amount of purified His-Nrf2 and its segments were run on SDS-PAGE gel and stained with commassie brilliant blue shown in the right panel in the figure. Also, the amount of GST, GST-pasA, and GST-R3B3 segments used in pull-down assay were run on SDS-PAGE gel and stained with commassie brilliant blue as shown in the bottom of left panel. Asterisk indicates the expecting size of proteins.



B)

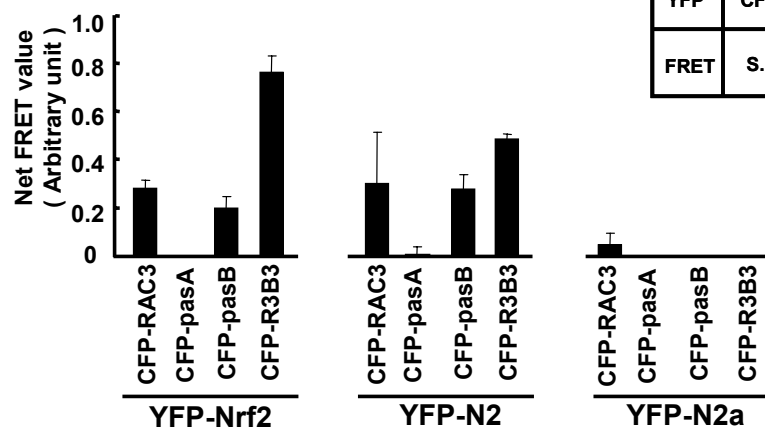


Fig.1-9. Fluorescence Resonance Energy Transfer (FRET) signals were strong between pasB and R3B3 regions in RAC3 and N2 containing Neh5 domain of Nrf2.

To analyze the potential interaction between Nrf2 and RAC3 proteins in HeLa cells, FRET signals were measured using the Zeiss LSM510 laser scanning confocal microscope (Zeiss, Thornwood, NY). Cells plated in glass bottom dishes and were co-transfected with EYFP-Nrf2 or its segments (EYFP-N2 and EYFP-N2a) and ECFP-RAC3 or its segments (ECFP-pasB and ECFP-R3B3) by different combinations using jetPEI transfection reagent for 24 h. Procedures for FRET assay were described in Materials and Methods. Florescent channels are shown in the figure. Intensity of FRET signal is shown by rainbow color. Net FRET values were measured by densitometric analysis from the three different FRET signals (bottom).

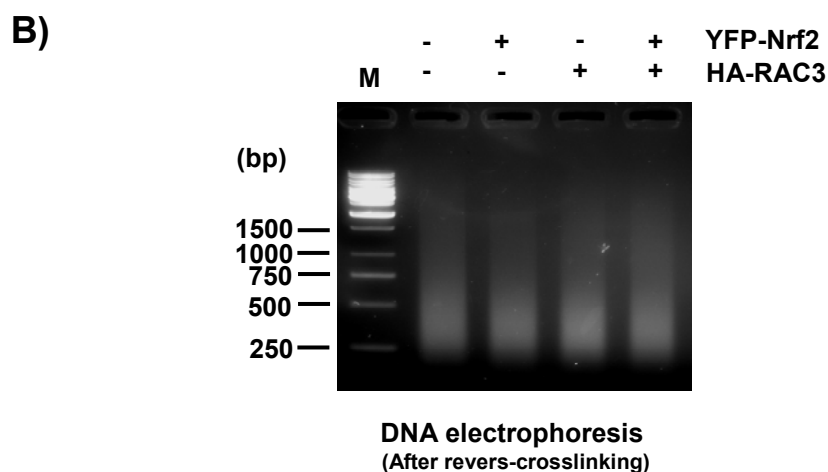
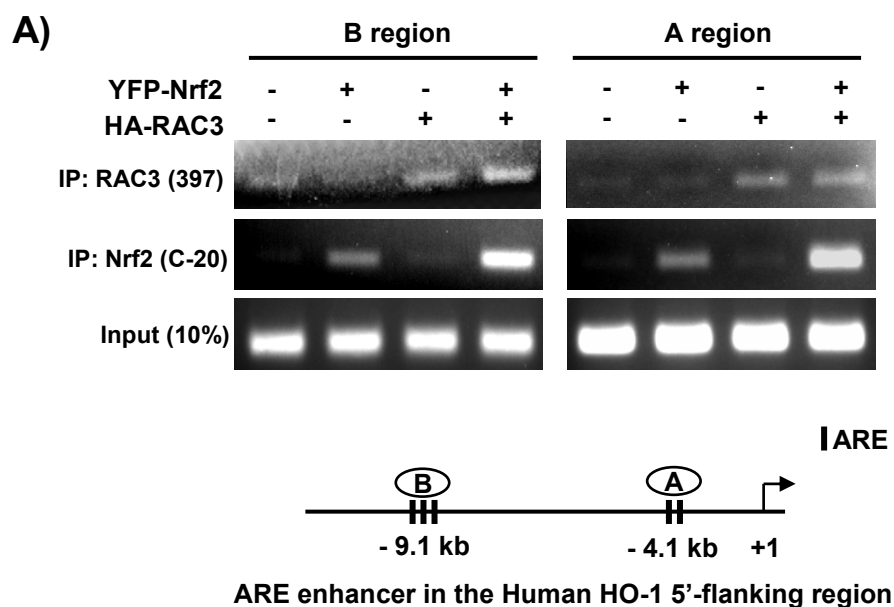


Fig.1-10. RAC3 and Nrf2 bind to the ARE enhancers in 5'-flanking region of hemeoxygenase-1 (HO-1) promoter.

A) To study whether RAC3 can bind to Nrf2/ARE enhancers in HO-1, Chromatin immunoprecipitation (ChIP) Assay was conducted. HeLa cells were plated in 100

mm culture dishes and transfected with EYFP-Nrf2 (3.5 g) and HA-RAC3 (3.5 g) constructs using jetPEI reagent for 22 h. Procedures for the ChIP assay are described in Materials and Methods. The ChIP DNA samples from anti-Nrf2 (C-20) or anti-RAC3 (M-397) were subjected to PCR reaction to amplify the two isolated ARE regions (-4.1 kb and -9.1 kb) using specific primers. Non-IP samples were used as input controls. B) ChIP DNA samples after sonication/reverse-crosslinking were run on DNA electrophoresis to show optimal DNA shearing patterns. M, 1Kb DNA ladder (Fermentas).

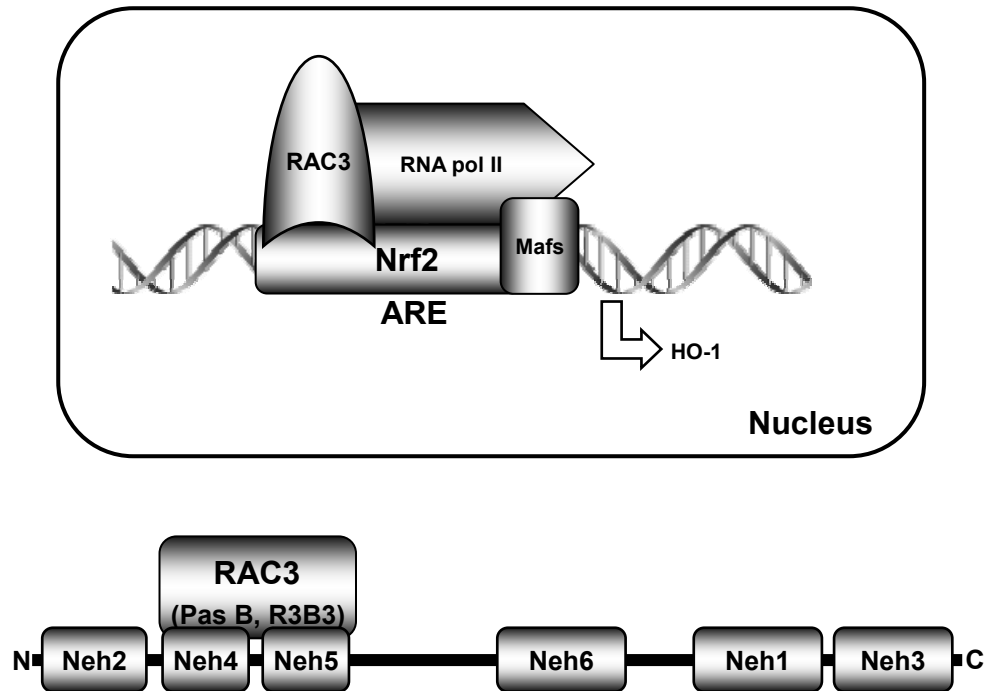


Fig.1-11. Cartoon shows a possible interaction between Nrf2 and RAC3 in the ARE enhancer region of hemeoxygenase-1 (HO-1) promoter (upper) by direct interactions between specific domains (lower).

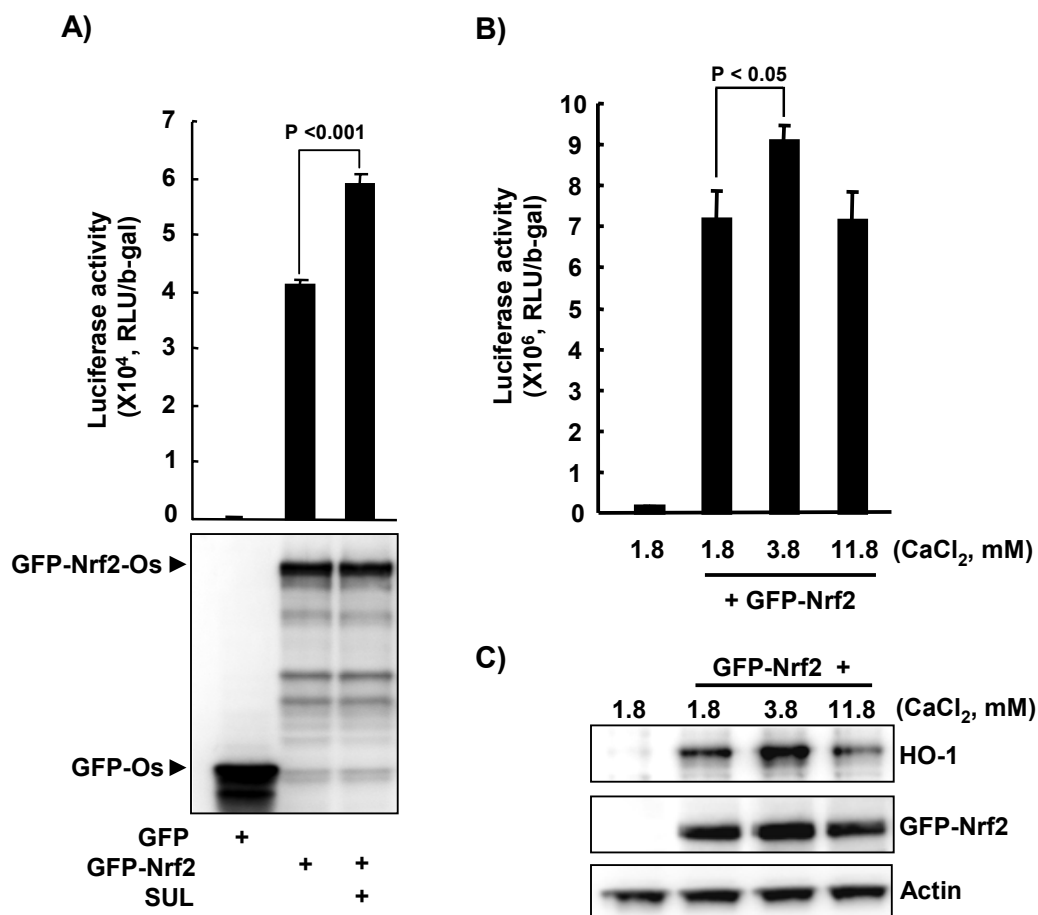


Fig.1-12. Verification of conditions for Nrf2-partner candidate pull-down with One-step tactin system.

(A) To verify the Nrf2-one-strep tag construct for this system, HeLa cells were transfected with pEGFP-Nrf2-Os and pGL2-ARE-Luc plasmids to examine the Nrf2 transcriptional activity. pEGFP-Os (without Nrf2) was also transfected as a control. After 24 h transfection, the cells were treated with 25 μ M SUL as an Nrf2 inducer for another 6 h. Then, cells were subjected to ARE-luciferase activity measurement. After

measurement of ARE-luciferase, the expression level of GFP-Nrf2-Os was also measured by Western blot analysis to show equal amount of Nrf2 with same samples. (B) To check the involvement of calcium ion on Nrf2 activity or Nrf2 partner complex, various concentrations of CaCl_2 were treated in HeLa cells for 6h after co-transfection with pEGFP-Nrf2 and pGL2-ARE-Luc. If Ca^{2+} is critical for Nrf2 partner complex, divalent chelators such as EDTA, may need to be avoided in the One-strep tactin buffer system. ARE-luciferase activity was then measured by ARE-Luciferase reporter assay. (C) Expression level of endogenous Heme oxygenase-1 (HO-1) was also analyzed with the same samples from A and B by Western blot analysis. GFP-Nrf2-Os, GFP-Nrf2-One-Strep; GFP-Os, GFP-One-strep; SUL, sulforaphane

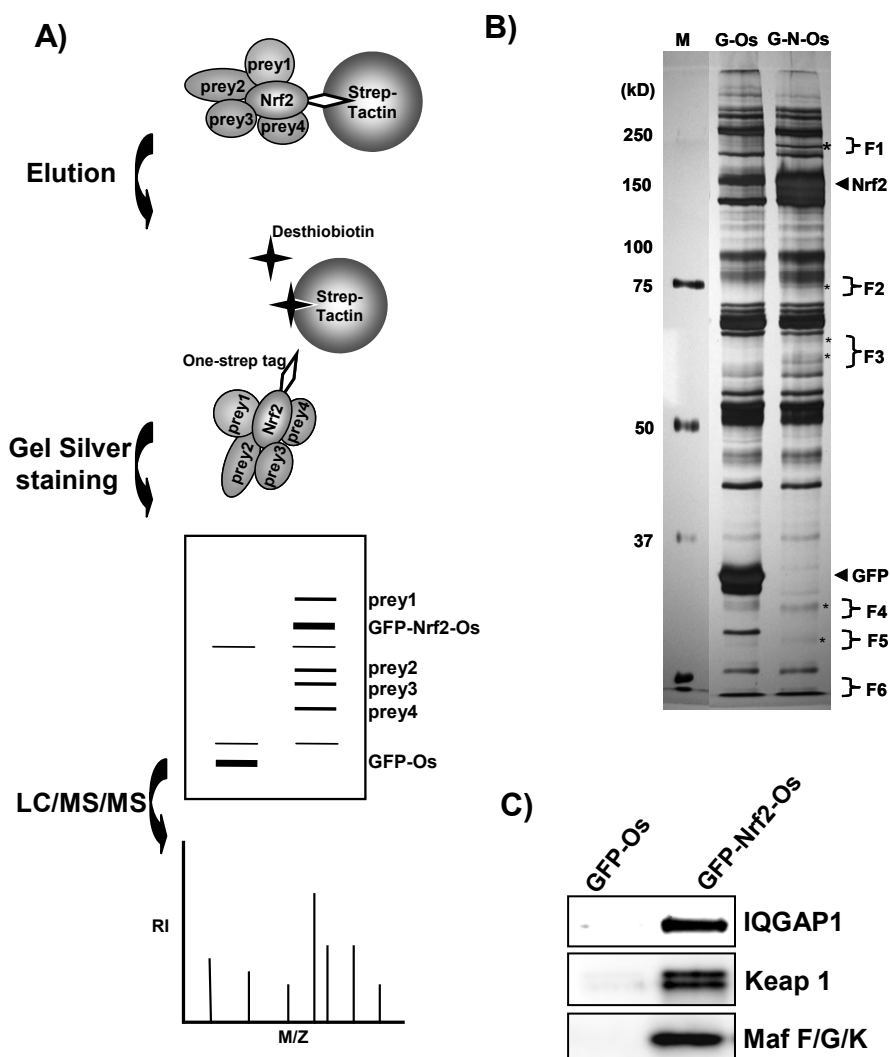
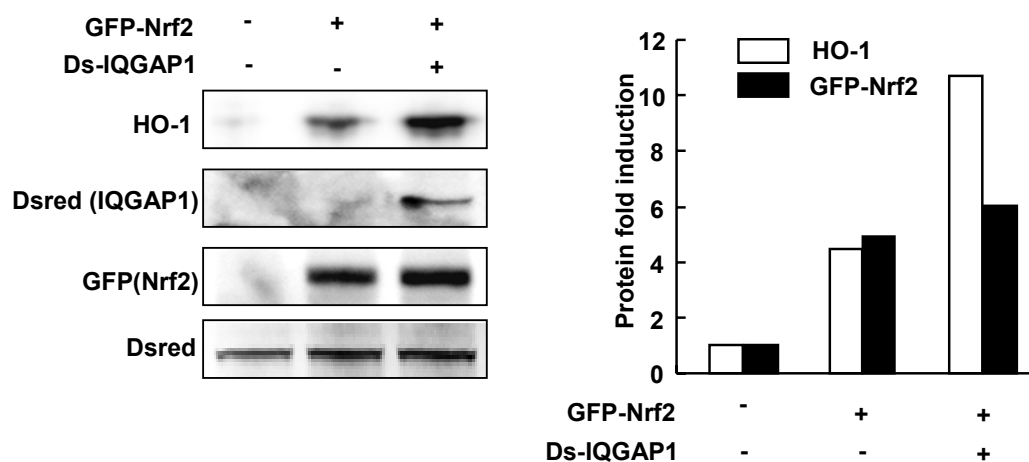


Fig.1-13. Purification and identification of novel Nrf2 partners.

(A) Schematic diagram illustrating the identification of Nrf2 partners using One-STREP™ System (IBA GmbH, Germany). Under physiological condition, Nrf2-partner complex could be bound to the Strep-Tactin bead and could be eluted by desthiobiotin. Eluted fractions were then separated on SDS-PAGE gel for silver staining. And then representative protein bands were excised for LC/MS/MS analysis. (B) Eluted Samples from the One-strep pull-down assay were concentrated using Microcon YM-50 (Milipore) and subjected to PAGE gel (6-15% gradient) electrophoresis for silver staining. The

representative protein bands in the lane of GFP-Nrf2-Os (G-N-Os) were excised for LC/MS/MS analysis. To minimize the nonspecific background between GFP-One-strep (G-Os; control) and GFP-Nrf2-One-strep (G-N-Os), same region of G-Os were also cut as a counterpart of G-N-Os. All excised samples were measured by LTQ_Orbitrap LC/MS/MS equipment (<http://cabm-ms.cabm.rutgers.edu>) and all mass data were analyzed using The Global Proteome Machine Organization Proteomics Database (Open Source Software, www.thegpm.org). (C) Based on the mass identification, same samples from (B) were subjected Western blot analysis to check and verify the identified proteins. Newly identified IQGAP1 was blotted using anti-IQGAP1 antibody and four known Nrf2 partners, Keap1 and Maf F/G/K were blotted using anti-Keap1 and anti-Maf F/G/K antibodies respectively.

A)



B)

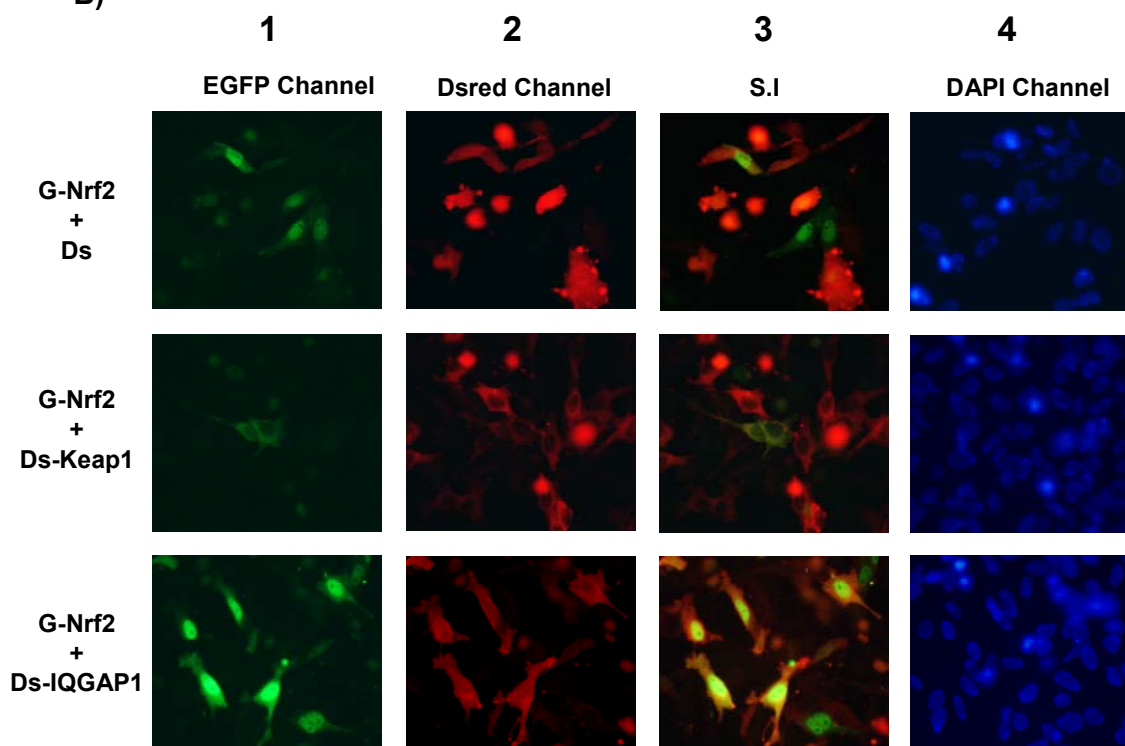


Fig.1-14. IQGAP1 enhances expression of Nrf2 and induction HO-1 expression.

(A) Based on Mass data shown in Table 1, we selected IQGAP1 as a major possible

Nrf2 partner among all the candidates. The newly identified IQGAP1 was then tested whether it could regulate the expression of HO-1, which is regulated by Nrf2. IQGAP1 cDNA was purchased from Invitrogen and subcloned into pDsredm-C1 vector (Clontech). HeLa cells were co-transfected with pDsredm-IQGAP1 and pEGFP-Nrf2 plasmids for 24 h using jetPEI reagent. After transfection, cells were lysed with RIPA lysis buffer and 20 g of sample proteins were subjected to Western blot analysis. Samples were blotted against anti-HO-1, or anti-Dsred for Dsredm-IQGAP1, and anti-GFP for GFP-Nrf2 (left panel). For equal transfection control, same amount of pDsredm-C1 empty vector was transfected to each group and blotted against anti-Dsred antibody. Densitometric data shows the relative fold of induction of HO-1 and GFP-Nrf2 protein (right panel). pCDNA3.1 vector was used for equal amount of transfection. GFP-Nrf2, EGFP-Nrf2; Ds-IQGAP1, Dsredm-IQGAP1. (B) HeLa cells were plated in glass bottom culture dishes and transfected with G-Nrf2 and Ds-IQGAP1 using jetPEI transfection reagent. After 24 h transfection, cells were fixed with 4% paraformaldehyde and the images were taken by fluorescent microscopy. Channel 1 shows EGFP fluorescence, channel 2 shows DsRed fluorescence and channel 3 shows superimposed image (S.I) between channel EGFP and DsRed to show co-localization (yellow). Channel 4 shows Nucleus images stained with DAPI (blue). Ds-Keap1 was transfected with G-Nrf2 as control data. G-Nrf2, pEGFP-Nrf2; Ds-keap1, pDsredm-keap1; Ds-IQGAP1, pDsredm-IQGAP1; S.I, superimposed image, magnification (10 x 40)

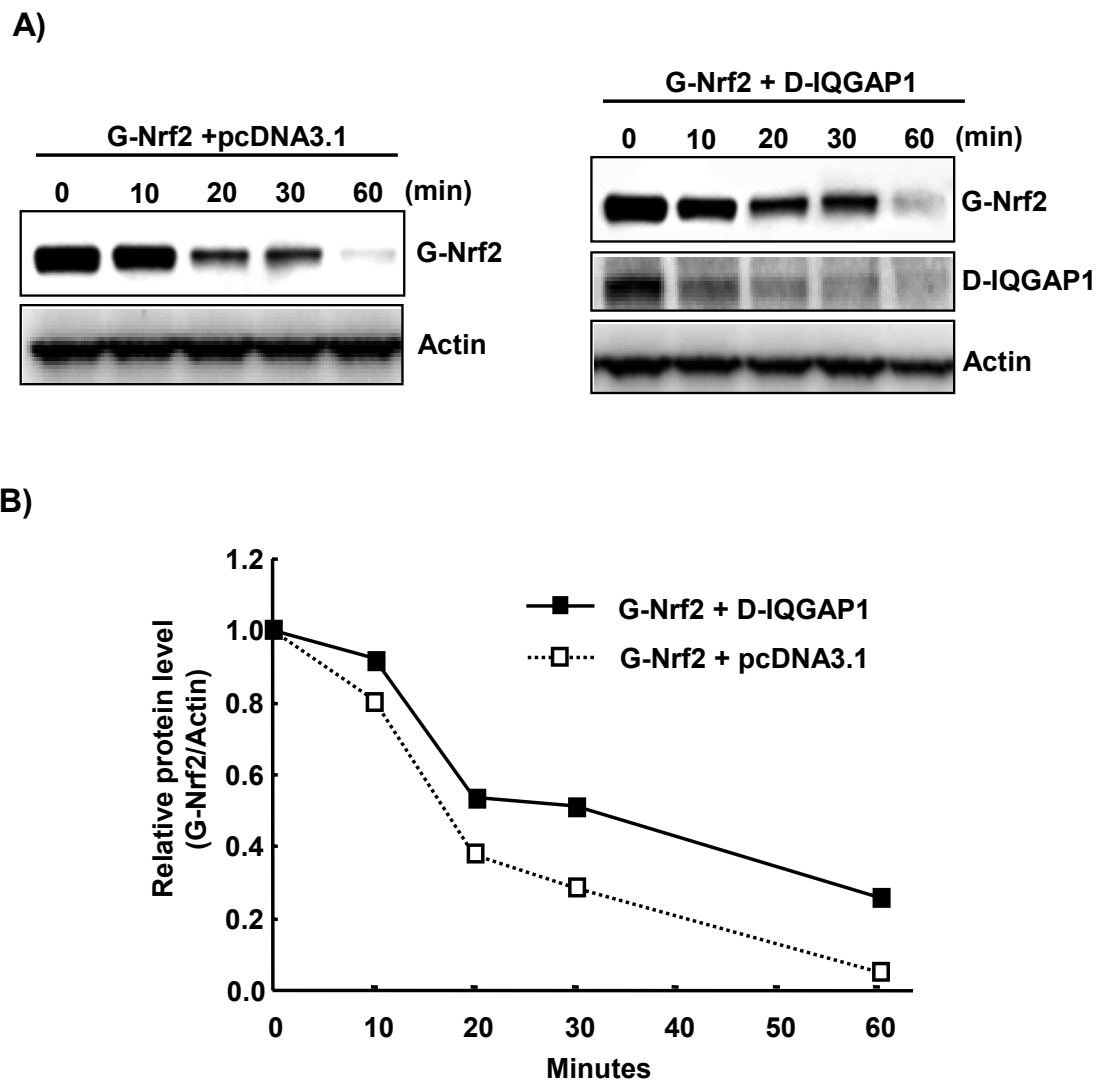


Fig.1-15. The stability of Nrf2 is increased by IQGAP1.

(A) To measure the stability of Nrf2 by IQGAP1, HeLa cells were co-transfected with GFP-Nrf2 (500 ng) and pcDNA3.1 500 ng) or Dsredm-IQGAP1 (500 ng) constructs using jetPEI reagent for 24 h. Then, cells were treated with cycloheximide (5 μ g/ml) for different time intervals as indicated above. Next, cell lysates (20 μ g) were subjected to immunoblotting against GFP-Nrf2 or Dsrednono-IQGAP1 using anti-Nrf2 (C-20) or anti-Dsred (C-20) antibodies respectively. Actin was used for the equal loading control. B)

Densitometric analysis shows the relative protein levels from the experiments in (A). G-Nrf2, EGFP-Nrf2;D-IQGAP1, Dsredm-IQGAP1.

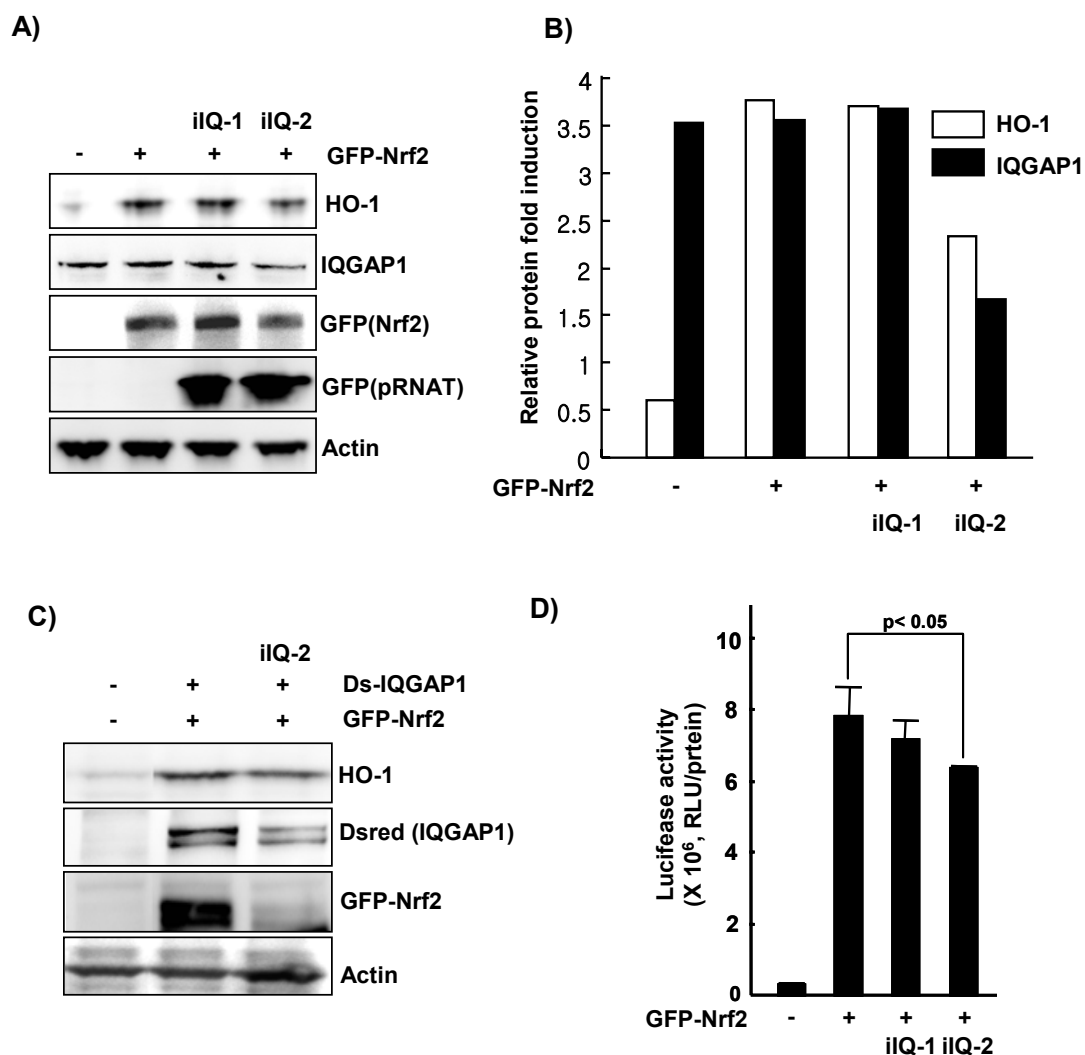


Fig.1-16. silIQGAP1 suppresses HO-1 expression and ARE-luciferase activity.

(A) HeLa cells were co-transfected with pRNAT-silIQGAP1-1 or -2 and pEGFP-Nrf2 (G-Nrf2) for 24 h using jetPEI reagent to silence or knockdown the endogenous IQGAP1 gene expression. The expression level of HO-1 and endogenous IQGAP1 were measured by Western blot analysis. After transfection, cells were lysed with RIPA lysis buffer and 20 mg of sample proteins were subjected to Western blot analysis. Samples

were blotted against anti-HO-1, anti-IQGAP1, and anti-GFP for GFP-Nrf2 or GFP in pRNAT vector. (B) Densitometric data shows the relative fold of induction of HO-1 and endogenous IQGAP1 protein expression from samples described in A. (C) HeLa cells were co-transfected with three different plasmids (ilQ-1 or ilQ-2, G-Nrf2, and pGL2-ARE-Luci). Ten microliter of samples was measured for the ARE luciferase activity. (D) HeLa cells were co-transfected with three different plasmids (pEGFP-Nrf2, pDsredm-IQGAP1, and pRNAT-silIQGAP1) for 24 h using jetPEI transfection reagent. Cell lysates (20 μ g) were subjected to Western blot analysis to examine the silencing of Dsred-IQGAP1 and of GFP-Nrf2 after silIQGAP1 plasmid transfection. Actin was used as control for equal protein loading. pCDNA3.1 vector was used for equal amount of plasmid transfection. GFP-Nrf2, EGFP-Nrf2; ilQ1, pRNAT-silIQGAP1-1; ilQ-2, pRNAT-silIQGAP1-2; Ds-IQGAP1, Dsredm-IQGAP1.

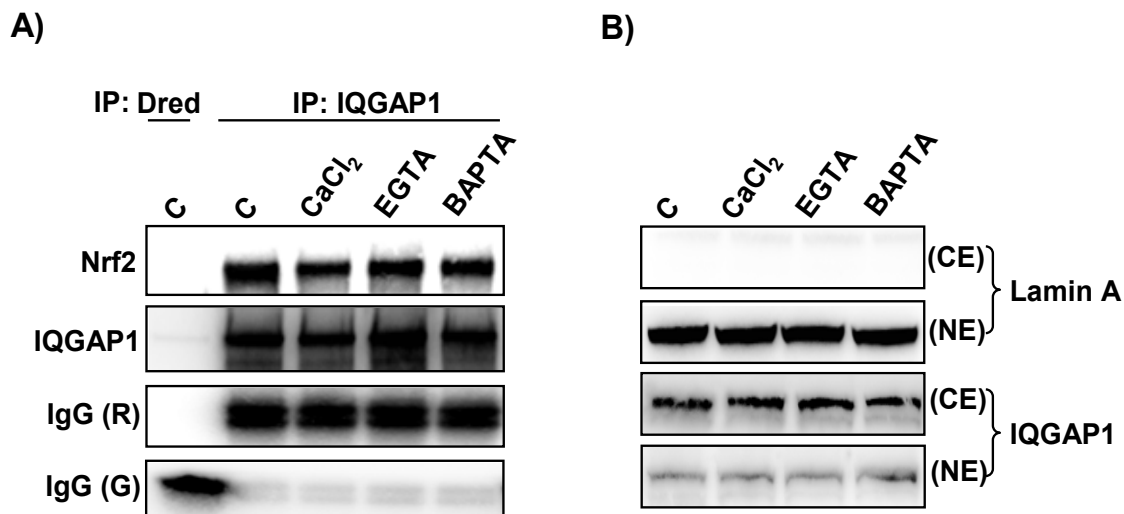


Fig.1-17. Nrf2 escapes from the IQGAP1 by calcium.

(A) To verify the function of calcium in two endogenous Nrf2-IQGAP1 complex, HeLa cells were cultured in 100 mm dishes and treated with DMSO (0.1%) or CaCl₂ (3.8 mM) or EGTA (5 mM) or BAPTA (10 μ M) for 30 min. The final concentration of CaCl₂ in maintained medium is 1.8 mM. After incubation, cells were lysed with M-PER (Pierce) buffer for cytosolic extraction. Next, cytosolic proteins (400 μ g) were subjected to immunoprecipitation (IP) with Dsred or IQGAP1 antibody using Dynabead G (Invitrogen) beads. The procedure of this experiment is described in Materials and Methods. The IP samples were immunoblotted against endogenous Nrf2 using anti-Nrf2 (C-20) or IQGAP1 (H-109) antibody. Rabbit IgG (R) and Goat IgG (G) were used for equal loading.

B) To verify the use of cytosolic extracts in (A), each fractionated extracts were immunoblotted against IQGAP1 (cytosol) and Lamin A (nucleus). The cytosolic extraction shows no contamination with nuclear protein. CE, cytosolic extract; NE, nuclear extract.

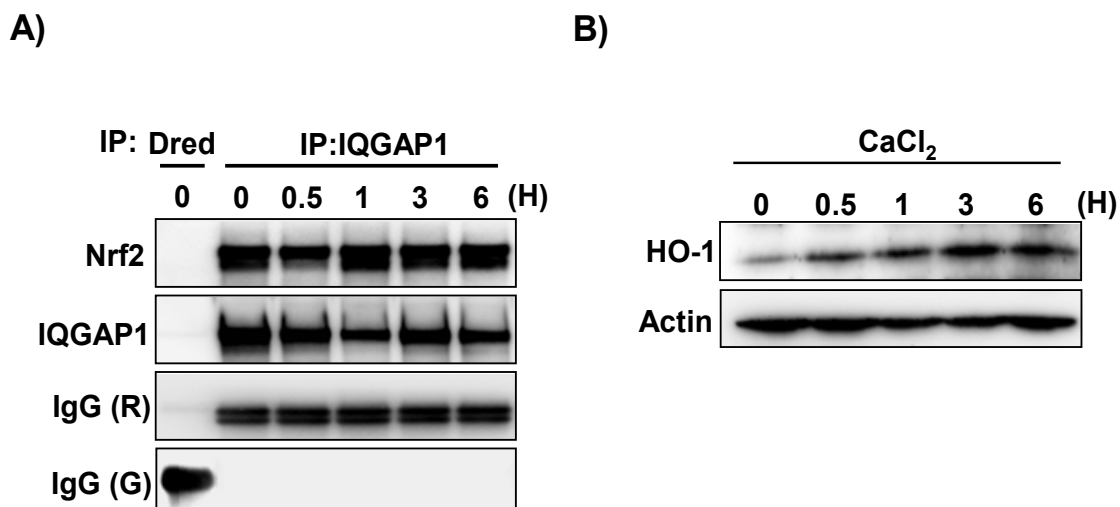


Fig.1-18. Calcium, in early time, stimulates the expression of HO-1 protein.

A) To see the time course release of Nrf2 from IQGPA1, HeLa cells were treated with CaCl₂ (3.8 mM) for different time intervals as indicated above. After incubation, cells were lysed with M-PER (Pierce) buffer for cytosolic extraction. Next, cytosolic proteins (400 µg) were subjected to immunoprecipitation (IP) with Dsred or IQGAP1 antibody using Dynabead G (Invitrogen) beads. The procedure of this experiment is described in Materials and Methods. The IP samples were immunoblotted against endogenous Nrf2 using anti-Nrf2 (C-20) or IQGAP1 (H-109) antibody. Rabbit IgG (R) and Goat IgG (G) were used for equal loading. B) The same samples from (A) were subjected to Immunoblotting against HO-1 using anti-HO-1 (C-20) antibody. Actin was used for the equal loading control.

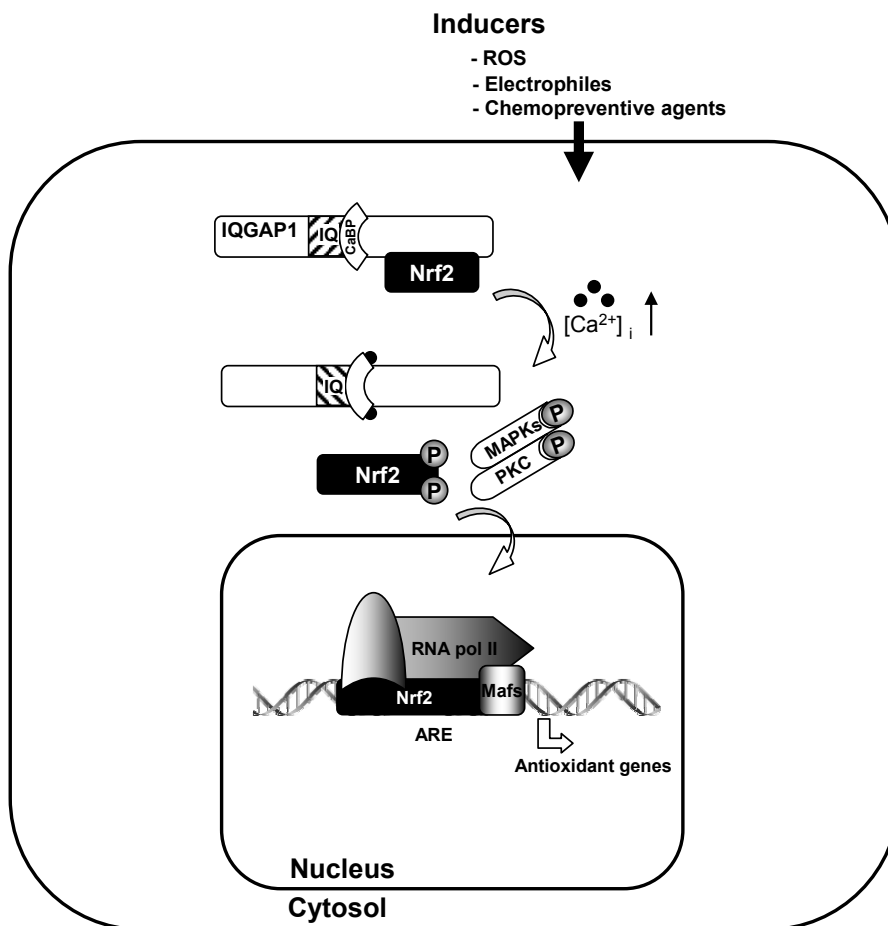


Fig.1-19. A schematic representation of possible mechanisms of Nrf2 activation through IQGAP1 protein in the presence of calcium.

Nrf2 protein can be released from the Nrf2-IQGAP1 complex as a result of increased intracellular calcium level. Calcium binding protein (CaBP, such as calmodulin and myosin) in IQ region of IQGAP1 can be the critical factor for affinity change between Nrf2 and IQGAP1. As a result, liberated Nrf2 from IQGAP1 may undergo for post-translational modification including phosphorylation by MAP kinases or PKC, resulting in induction of phase II or antioxidant genes.

Table 1. Identified Nrf2 partners from LC/MS/MS

Silver-stained excised gel samples were applied to mass LC/MS/MS spectroscopy using LTQ_Orbitrap equipment. Ten of Nrf2 protein partners were newly identified including four previous known partners. The abbreviations used are as follows: F, excised gel fraction number; log(I), base-10 log of the sum of the Intensities of the fragment ion spectra; log(e), based-10 of the expectation that this assignment is stochastic; rl, number of peptides found from this sequence only; Mr, protein molecular mass. Newly identified Proteins are indicated with bold letter.

F	Identifier	log(I)	rl	log(e)	Mr (kDa)	Description	Source
1	ENSP00000268182	6.13	59	-424.6	189.1	Ras GTPase-activating-like protein IQGAP1 (p195)	Uniprot/SWISSPROT P46940
2	ENSP00000345771	4.99	7	-54.1	93.2	6-phosphofructokinase, muscle type (EC 2.7.1.11) (Phosphofructokinase 1)	Uniprot/SWISSPROT P08237
2	ENSP00000370517	4.9	10	-89.1	85.5	6-phosphofructokinase type C (EC 2.7.1.11)	Uniprot/SWISSPROT Q01813
3	ENSP00000171111	5.27	11	-74.5	69.6	Kelch-like ECH-associated protein 1 (Cytosolic inhibitor of Nrf2)	Uniprot/SWISSPROT Q14145
3	ENSP00000368031	5.88	27	-138.9	66.2	ATPase family AAA domain-containing protein 3A	Uniprot/SWISSPROT Q9NVI7
5	ENSP00000370808	5.71	15	-74.9	32.8	ADP/ATP translocase 3 (Adenine nucleotide translocator 2) (ANT 3)	Uniprot/SWISSPROT P12236
5	ENSP00000360671	5.98	23	-88.5	32.8	ADP/ATP translocase 2 (Adenine nucleotide translocator 2) (ANT 2)	Uniprot/SWISSPROT P05141
5	ENSP00000306330	5.37	9	-42.6	28.3	14-3-3 protein gamma (Protein kinase C inhibitor protein 1) (KCIP-1)	Uniprot/SWISSPROT P61981
5	ENSP00000300161	4.94	6	-24.1	28.1	14-3-3 protein beta/alpha (Protein kinase C inhibitor protein 1) (KCIP-1)	Uniprot/SWISSPROT P31946
5	ENSP00000309503	5.38	11	-42.4	27.7	14-3-3 protein zeta/delta (Protein kinase C inhibitor protein 1) (KCIP-1)	Uniprot/SWISSPROT P63104
5	ENSP00000371267	5.16	6	-21.7	27.7	14-3-3 protein theta (14-3-3 protein tau) (14-3-3 protein T-cell) (HS1 protein)	Uniprot/SWISSPROT P27348
6	ENSP00000350369	6.05	13	-69.5	17.8	Transcription factor MafG	Uniprot/SWISSPROT O15525
6	ENSP00000345393	5.62	8	-41.0	17.7	Transcription factor MafF	Uniprot/SWISSPROT Q9ULX9
6	ENSP00000344903	6.25	17	-80.1	17.5	Transcription factor MafK	Uniprot/SWISSPROT O60675

1.5. Summary

In summary, we show that RAC3 binds to Nrf2 protein directly in the nucleus to simulate Nrf2 activity in HeLa cells (Fig. 1-11). Furthermore, we also delineated the interacting regions between Nrf2 and RAC3. The results indicate that the PasB and R3B3 regions of RAC3 interacts with the Neh4 and Neh5 transactivation domains of Nrf2. Therefore, combinatorial understanding of RAC3 and Nrf2 underlying their molecular mechanisms would be useful for cancer or chemoprevention research.

In addition, we isolated and identified ten new Nrf2 partners using One-step tag purification system. Among the candidates, a representative IQGAP1 is investigated on Nrf2 signaling. Transfection of IQGAP1 enhances the stability or expression of Nrf2, resulting in enhanced induction of Heme oxygenase-1 expression. Whereas, siIQGAP1-2 transfection suppresses the stability or expression of Nrf2, resulting in the inhibition of Heme oxygenase-1 expression. Furthermore, Nrf2-IQGAP1 complex was disrupted by the increased intracellular calcium concentration resulted in HO-1 induction. These results suggest that IQGAP1 may play a pivotal role in Nrf2 activation in conjunction with intracellular calcium level.

Taken together, in this study, we elucidated the functional role of RAC3 on Nrf2 signaling as well as their possible functional domains. In addition, we identified ten of novel Nrf2 binding partners and investigated IQGAP1, one of the identified Nrf2 partners, on calcium-involved Nrf2 signaling. Fig. 1-20 shows the possible Nrf2 pathways with RAC3 and IQGAP1 based on the results from this study.

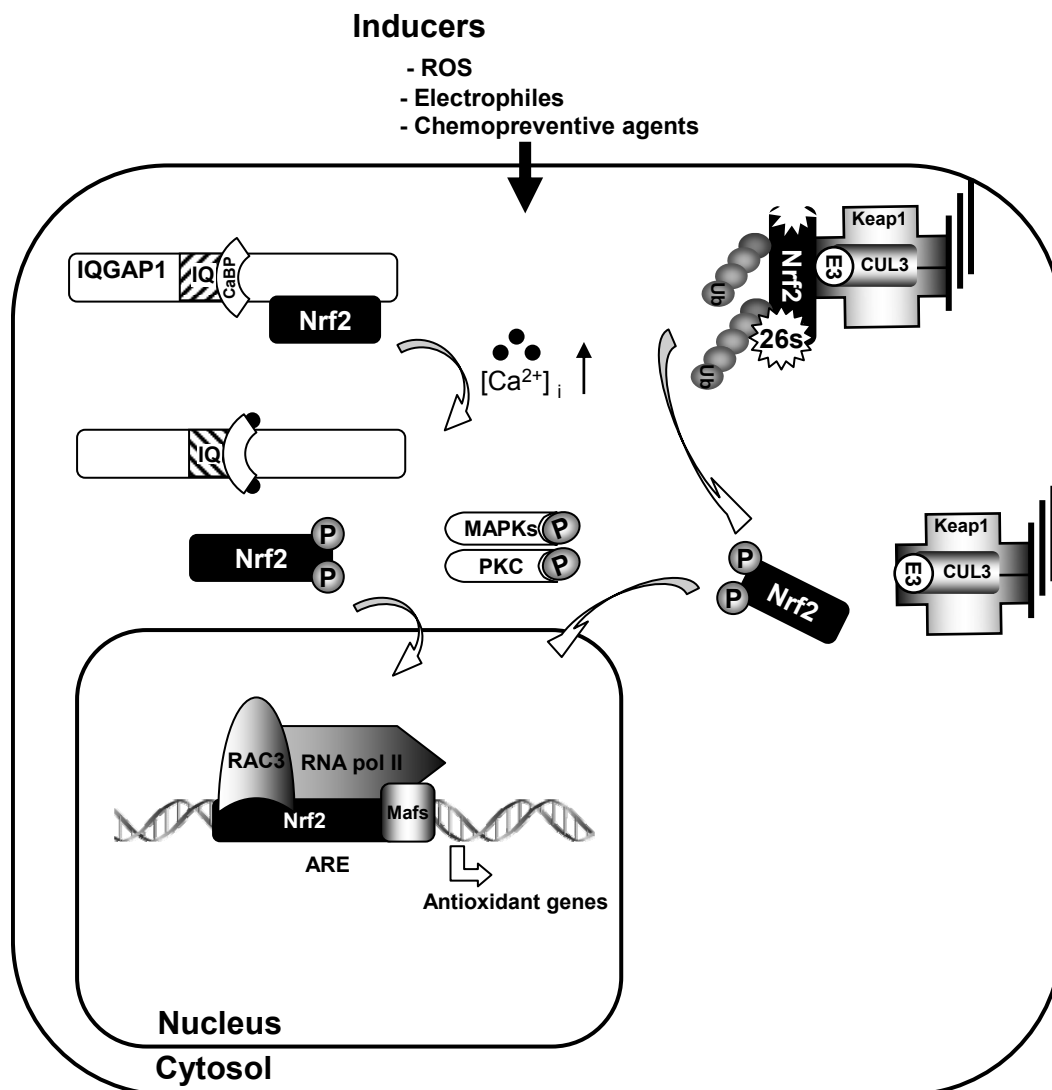


Fig.1-20. The schematic representation shows the summary for the possible mechanisms of Nrf2 activation through RAC3 and IQGAP1 protein.

Supplementary 1

Inhibition of EGFR signaling in human prostate cancer PC-3 cells by combination treatment with beta-phenylethyl isothiocyanate and curcumin¹

KEY WORDS: Curcumin; Phenethyl isothiocyanate; EGFR, NF- κ B; Akt ; cell death

ABBREVIATION: PEITC, phenethyl isothiocyanate; EGFR, epidermal growth factor receptor; PARP, poly (ADP-Ribose) polymerase

¹ This chapter has been published in *Carcinogenesis*, 27(3):475-82, 2006

2.1 Abstract

Many naturally occurring compounds, including β -phenylethyl isothiocyanate (PEITC) and curcumin, exhibit significant anti-cancer chemopreventive effects. In this study, we investigated the combined effects of PEITC and curcumin in PC-3 human prostate cancer cells and in PC-3 cells that were stably transfected with an NF- κ B luciferase plasmid (PC-3 C4). We found an additive effect of PEITC and curcumin for the induction of apoptosis. To elucidate the potential mechanisms of this effect, we studied several critical cellular signaling pathways, including the critical NF- κ B cell survival signal that is hyper-activated in PC-3 cells and many other cancers. PEITC and curcumin additively inhibited NF- κ B-luciferase activity. Furthermore, the combined treatment significantly increased the activity of poly (ADP-Ribose) polymerase (PARP) and cleavage of caspase-3 in correlation with apoptotic cell death. Studying upstream signaling events, we found that the phosphorylations of I κ B α and Akt (Ser473, Thr308) were significantly attenuated by the combination of PEITC and curcumin. As these events can be downstream of the activation of epidermal growth factor receptor (EGFR), we pretreated PC-3 cells with PEITC and curcumin and then stimulated them with EGF. EGFR phosphorylations (Y845 and Y1068) were dramatically suppressed by PEITC or curcumin, and more so by the combination. Importantly, the degree of Akt and PI3K phosphorylations induced by EGF were also significantly suppressed. We conclude that the simultaneous targeting of EGFR, Akt, and NF- κ B signaling pathways by PEITC and curcumin could be the molecular targets by which PEITC and curcumin exert their additive inhibitory effects on cell proliferation and ultimately lead to programmed cell death of tumor cells.

2.2 Introduction

Prostate adenocarcinoma is one of the most common cancers, and it is the second leading cause of death among men in the United States (68). The major cause of death from prostate cancer is the metastasis to the bone and lymph nodes of cancer cells that ultimately resist conventional androgen-deprivation therapy (90). Because androgen ablation of advanced prostate cancer is often unsuccessful, new therapeutic strategies are needed for its treatment and prevention. Prostate cancer commonly overexpresses several growth factors and their receptors, including epidermal growth factor (EGF) receptor (EGFR).

EGFR plays a critical role in tumor growth, and the prostate tissue becomes more susceptible to the growth-promoting action of EGF family growth factors during androgen withdrawal (32, 153). The general inhibition of tyrosine kinase signaling pathways provides therapeutic advantage against prostate cancer metastasis (40). Therefore, inhibiting the activation of growth factor receptors, especially EGFR, may be a promising strategy for the treatment of prostate cancer. Recent studies have shown that several dietary cancer chemopreventive agents could provide promising strategies for reducing the incidence of prostate cancer (23).

The present study, we selected two potent chemopreventive agents to investigate various critical cellular signaling pathways, including EGFR signaling, in human prostate cancer PC-3 cells. Curcumin (from turmeric) is one of the most well-known naturally occurring compounds. It has cancer chemopreventive potential against many types of cancerous cells, including prostate cancer. It is a potent nuclear factor-kappaB (NF- κ B) inhibitor as well as an inducer of apoptosis. Recent data show that curcumin also has an

inhibitory effect on EGFR phosphorylation in PC-3 cells (36). β -phenylethyl isothiocyanate (PEITC), from cruciferous vegetables, is also a highly potent chemopreventive agent that induces apoptosis in prostate cancer cells (178) as well as other cell types (180). In addition, human epidemiological studies show a statistically significant inverse correlation between dietary intake of vegetables that contain isothiocyanates (ITCs) and the risk for prostate cancer (26, 86). We undertook the present study to investigate the effects of PEITC and curcumin on critical cellular signaling pathways, including the possible inhibition of EGFR phosphorylation and its downstream cell survival Akt signaling pathway.

There is increasing interest in the combined use of low doses of chemopreventive agents with differing modes of action, rather than the administration of a single agent at a higher dose, as a means of obtaining increased efficacy and minimized toxicity. This approach is extremely important when a promising chemopreventive agent demonstrates significant efficacy but may produce some untoward side effects at higher effective doses. For example, piroxicam, a non-steroidal anti-inflammatory drug (NSAID) and difluoromethylornithine (DFMO), an ornithine decarboxylase (ODC) inhibitor, were evaluated in preclinical models for their chemopreventive efficacy when administered individually at high doses and in combination at very low dose levels (138). Lowest dose levels of piroxicam and DFMO administered together were more effective in inhibiting the incidence and multiplicity of colon adenocarcinomas than the individual compounds even at higher levels.

We therefore examined the combination of PEITC and curcumin in PC-3 cells for the potential treatment and prevention of prostate cancer. We focused on cell survival

signaling pathways inhibited by PEITC and curcumin. Our results clearly show that combination treatment of PC-3 cells with PEITC and curcumin had a very potent inhibitory effect on the phosphorylation and activation of EGFR and Akt, and on the NF- κ B pathway, when compared with single compound treatment. The concerted inhibitory effect of the combination on EGFR and NF- κ B led to enhanced apoptotic cell death when compared with the effects of the individual compounds. The combination may thus offer therapeutic advantages in the treatment and prevention of human prostate cancer.

2.3 Materials and methods

2.3.1. Materials

PEITC was purchased from Sigma (St Louis, MO). Curcumin ($\geq 98.5\%$) was obtained from Alexis (San Diego, CA). Rabbit polyclonal antibodies against p-EGFR (Y845, Y992 and Y1068), total EGFR, total poly(ADP-Ribose) polymerase (PARP), cleaved PARP, caspase 3, cleaved caspase 3, p-Akt (S473, S308), total Akt, p-PDK1, p-I κ B α , total I κ B α and p-phosphatidylinositol 3-kinase (PI3K) (p85) were purchased from Cell Signaling (Beverly, MA). The rabbit polyclonal antibody for p-EGFR (1086) and secondary antibody were purchased from Zymed (South San Francisco, CA). Anti-actin was a product of Santa Cruz Biotechnology (Santa Cruz, CA).

2.3.2. Cell Lines

PC-3 and PC-3 C4 (a derivative of PC-3, stably transfected with an NF- κ B luciferase gene construct) were maintained in minimum essential medium (MEM) supplemented with 10% heat-inactivated fetal bovine serum (FBS) and 50 U/ml of penicillin/streptomycin mixture (Gibco BRL, Grand Island, NY), in a humidified

atmosphere of 5% CO₂/95% air at 37°C. When cells were 80% confluent, they were serum starved for 24 h with MEM medium without FBS; the cells were subsequently treated with PEITC and/or curcumin.

2.3.3. MTT Assay

The MTT [3-(4,5-dimethylthiazolyl-2)-2,5-diphenyltetrazolium bromide] assay was performed to determine cell proliferation. Briefly, PC-3 C4 cells were plated in 48-well plates at a density of 4×10^4 /well. After incubating for 24 h, cells were serum starved overnight. Cells were then treated with different concentrations of curcumin and/or PEITC for 24 and 48 h, at which time, 20 µg of 5 mg/ml MTT solution was added to each well. After 2 h incubation, medium was removed and dimethyl sulfoxide (DMSO) was applied to the plates. Color intensity of the solubilized formazan was measured at 570 nm with an enzyme linked immunosorbent assay (ELISA) plate reader (Bio-TEK Instruments, CA).

2.3.4. Luciferase Assay

PC-3 C4 cells were plated overnight in 6-well plates at a density of 5×10^5 /well and then serum starved for 24 h. The cells were then treated with the compounds for 24 h. After treatment, the cells were washed twice with ice-cold phosphate-buffered saline (PBS) and harvested in reporter lysis buffer (Promega, Madison, WI). After brief centrifugation at 12,000 rpm, a 10 µl aliquot of the supernatant was assayed for luciferase activity with a luciferase kit from Promega, according to the manufacturer's instructions. The luciferase activity was normalized for protein concentration.

2.3.5. Determination of DNA Fragmentation

The detection of nuclear DNA fragmentation was performed as described previously (145) with some modifications. Briefly, PC-3 C4 cells cultured in 100 mm dishes were resuspended in 200 μ l of hypotonic lysis buffer (0.2% Triton X-100, 1 mM EDTA, 10 mM Tris-HCl, pH 7.5) and incubated for 20 min at 4°C. After centrifugation for 5 min at 14 000 g, the supernatant was collected and incubated with RNase A (400 μ g/ml) for 30 min at 37°C, followed by a digestion with proteinase K (200 μ g/ml) for 30 min at 50°C. The fragmented DNA was then precipitated overnight at -20°C in 50% isopropanol and 0.5 M NaCl and centrifuged for 10 min at 14 000 g. Dried pellets were dissolved in 20 μ l of ultra-pure water, and the DNA was separated by electrophoresis on a 2% agarose gel at 50 V for 1 h.

2.3.6. Western Blotting

PC-3 or PC-3 C4 cells were treated with dimethyl sulfoxide (DMSO; 0.2%), PEITC, curcumin or a combination of PEITC and curcumin in the absence or presence of EGF for various time periods. After treatment, the cells were washed twice with ice-cold PBS and treated with RIPA buffer [50 mM NaCl, 0.5% Triton X-100, 50 mM Tris-HCl (pH 7.4), 25 mM NaF, 20 mM EGTA, 1 mM DTT, 1 mM Na_3VO_4 and protease inhibitor cocktail tablet (Roche, Mannheim, Germany)] for 40 min on ice, followed by centrifugation at 14,800 g for 15 min. The protein concentrations of the supernatants were measured by using bicinchoninic acid (BCA) solution (Pierce, Rockford, IL). Protein (20 μ g) was separated on NuPAGE 4–12% electrophoresis gels (Invitrogen, Carlsbad, CA) and transferred to polyvinylidene difluoride membranes. Membranes were probed with primary antibodies and horseradish peroxidase-conjugated secondary antibody by

standard western blot procedures. The proteins were visualized with the Super Signal Chemiluminescent Substrate (Pierce). The intensity of visualized bands was measured with Quantity One software (Ver 4.4.0, Bio-Rad, Hercules, CA).

2.3.7. Immunofluorescence

PC-3 cells grown on cover glass were fixed in 3% paraformaldehyde in PBS (pH 7.4), for 10 min, permeabilized with 0.5% Triton X-100 for 5 min, blocked with 10% goat serum for 1 h and then incubated with primary antibodies overnight at 4°C. This was followed by incubation with TRITC-conjugated goat anti-rabbit (Zymed) and DAPI (Molecular Probes) for 1 h. Sample images were taken with a fluorescence microscope (Nikon, ECLIPSE E 600 system), and the images were processed using Photoshop 8.0 (Adobe Systems, San Jose, CA).

2.4 Results

2.4.1. Combination treatment with curcumin and PEITC has an additive inhibitory effect on cell survival signaling pathways in PC-3 C4 cells

To determine the effects of PEITC (10 μ M), curcumin (25 μ M) and their combination on cell viability, the MTT assay was performed on PC-3 C4 cells at two selected time points (24 and 48 h). Treatment of the cells with 25 μ M curcumin for 24 or 48 h did not cause significant cell death, whereas treatment with 10 μ M PEITC caused significant cell death. The viability of PEITC-treated cells was 83% and that of the control was 65% at 24 h and 48 h, respectively (Fig. 2-1A). Notably, the combination treatment had a more potent inhibitory effect on cell viability than PEITC alone, with

viability at 60 and 44% of control at 24 and 48 h, respectively (Fig. 2-1A). We next examined the effects of these two compounds on NF- κ B signaling. We measured NF- κ B luciferase activity after a 24 h incubation of PC-3 C4 cells, which are stably transfected with an NF- κ B luciferase plasmid as we have described previously (180) with the compounds. As shown in Fig. 2-1B, NF- κ B luciferase activity was inhibited down to 80, 54 and 21% of control values ($P < 0.05$) when the cells were treated with 25 μ M curcumin, 10 μ M PEITC and their combination, respectively. These data show that the combination treatment has a more potent inhibitory effect than each drug separately. To determine the type of cell death of PC-3 C4 cells induced by the drug combination, we measured the cleavage of PARP, cleavage of caspase 3 and DNA fragmentation as markers of apoptosis. Fig. 2-1C and D shows that the combination treatment has a potent effect on these apoptotic markers with enhanced cleavage of PARP and caspase 3, as well as fragmentation of DNA. These results suggest that the treatment of PC-3 cells with PEITC and curcumin causes cell death by the induction of apoptosis.

We next examined pro-survival signals. The western blotting data in Fig. 2-1E show that the combination treatment is more effective than single drug treatment at inhibiting phosphorylation of Akt, its upstream target PDK1 and inhibitor of NF- κ B alpha ($\text{I}\kappa\text{B}\alpha$). The combined effect of 25 μ M curcumin and 10 μ M PEITC was the most potent compared with combinations of different concentrations tested.

2.4.2. EGFR signaling and NF- κ B signaling are activated by EGF

To investigate the effects of EGF on PC-3 C4 cells, we analyzed signaling molecules related to the EGFR pathway. The phosphorylation of EGFR, PI3K (p85) and Akt were detected by western blotting with antibodies specific to phosphorylated proteins.

As shown in Fig. 2-2, all of these proteins were activated after EGF treatment. Two EGFR phosphorylations (Y845 and Y1068) were detected at 2 min after EGF administration and gradually decreased with time. However, EGFR phosphorylated at Y992 was constitutive even in control cells not treated with EGF. PI3K (p85), a functional subunit of PI3K, was activated within 2 min of EGF administration and gradually decreased by 30 min. One of the downstream targets of EGFR-PI3K is Akt, and phosphorylated Akt (S473) gradually increased and peaked at 30 min. Previously, it has been shown that NF- κ B is activated by EGFR signaling (20, 48). Consistent with this observation, we found that treatment of PC-3 cells with EGF activated the phosphorylation of I κ B α as early as 2 min after treatment, and the increased phosphorylation persisted for up to 30 min.

2.4.3. PEITC has an enhanced inhibitory effect on EGFR phosphorylation when it is combined with curcumin in EGF-stimulated PC-3 C4 cells

EGF signaling might be one of the most critical signaling mechanisms for cancer cells, including prostate cancer cells (35, 36, 40, 153). We therefore focused on PEITC and its combination effect with curcumin on EGFR signaling in PC-3 C4 cells. The cells were pretreated with the single agents or with their combination for 5 min. Then, EGF (100 ng/ml) was added for 10 min. As shown in Fig. 2-3A, curcumin had an inhibitory effect on EGFR phosphorylation as reported previously (36). However, PEITC and the combination treatments show a much greater inhibitory effect than curcumin alone on the inhibition of EGFR phosphorylation (Y845, Y992, Y1068 and Y1086). Among the four types of phosphorylated EGFR, p-EGFR (1086) shows the largest additive inhibition by

combination treatment in PC-3 C4 cells. Similar results were also obtained in parental PC-3 cells (data not shown). We next examined a downstream target of the EGFR signaling pathway, Akt, and found that EGF-stimulated Akt phosphorylation was dramatically inhibited by the combination treatment (Fig. 2-3B).

2.4.4. Combination treatment with PEITC and curcumin significantly inhibits

EGFR signaling in PC-3 cells

To corroborate the above observations obtained in PC-3 C4 cells and to further examine the inhibitory effects of the drugs on EGFR signaling pathway, parental PC-3 cells were treated with PEITC alone or in combination with curcumin. Parental PC-3 cells were pretreated for 5 min, followed by EGF (100 ng/ml) treatment for 10 min. As shown in Fig. 2-4A, EGF-stimulated EGFR activation was attenuated by treatments with PEITC or curcumin. Importantly, the combination treatment showed much more significant inhibition of EGFR phosphorylation than the single treatment, especially with respect to the p-EGFR (Y1068) protein. Densitometry analysis of p-EGFR (Y1068) protein levels (right panel of Fig. 2-4A) shows that EGF-stimulated EGFR phosphorylation was inhibited by 19, 53 and 86% when the cells were treated with curcumin, PEITC and the combination, respectively.

To analyze the downstream signaling events of the EGFR pathway, we next examined EGF-stimulated phosphorylation of PI3K (p85), which also showed significant inhibition by the combination treatment (Fig. 2-4A). In addition, when we examined the downstream signaling molecules Akt and I κ B α , levels of p-Akt (S473), p-Akt(T308) and I κ B α were all significantly inhibited by the combination treatment in PC-3 cells (Fig. 2-

4B). Densitometry analysis shows that p-Akt (S473) protein levels are decreased by curcumin, PEITC and combination by 7, 53 and 69%, respectively, as compared with EGF alone. Immunofluorescence studies after PEITC treatment confirmed that PEITC significantly inhibits EGF-stimulated EGFR phosphorylation (Fig. 2-4C).

These data corroborate very well with that of the PC-3 C4 cells and suggest that both PEITC and curcumin can inhibit EGFR-mediated cell survival signals such as PI3K, Akt and NF- κ B. Furthermore, the combination of PEITC and curcumin demonstrated additive inhibitory effects on these critical cell survival signaling proteins and, importantly, in cell survival.

2.5. Discussion

Prostate cancer is the second leading cause of death among men in the USA. While the incidence of prostate cancer has increased steadily over the years, its etiology is still not completely understood. Factors contributing to prostate cancer may involve genetic changes, activated oncogenes, growth factors, hormones and/or dietary factors. Both the EGFR and NF- κ B signaling pathways are implicated in the survival of androgen insensitive human prostate cell lines such as PC-3 and in advanced prostate cancer in humans (153). Recent studies have indicated that naturally occurring compounds, such as PEITC and curcumin, are potential therapeutics for the prevention and treatment of human prostate cancer (26, 86, 125). Therefore, in the present study we asked whether PEITC and curcumin could interfere with the EGFR and NF- κ B pathways.

We utilized both parental PC-3 cells as well as PC-3 C4 cells, which have a stably transfected NF- κ B luciferase gene (180). These cell lines provide a model system to study signaling mechanisms and pharmacological effects. Our results demonstrate that

PEITC significantly inhibits EGFR activation and, moreover, PEITC displays additive effects in combination with curcumin in both PC-3 C4 and its parental PC-3 cells.

It is well known that EGFR and other growth factor receptors are frequently overexpressed in several types of cancers, including prostate. In fact, the progressive and metastatic growth of prostate cancer has been associated with a significant increase in the expression of EGFR and one of its ligands (25, 62). Similarly, NF- κ B activation in cancer cells has been intensively studied by many groups, and constitutive or improper activation of NF- κ B in prostate cancer cells in vitro and in vivo has been recently recognized(157). Moreover, it has recently been shown that the enzyme NF- κ B inducing kinase (NIK), which preferentially phosphorylates I κ B kinase (IKK)s during the activation of the IKK complex, can regulate the function of NF- κ B through I κ B α phosphorylation following activation of EGFR (20, 48). Importantly, isothiocyanates such as PEITC and sulforaphane can directly inhibit NF- κ B via the direct inhibition of IKK α / β / γ , as we have shown recently (180).

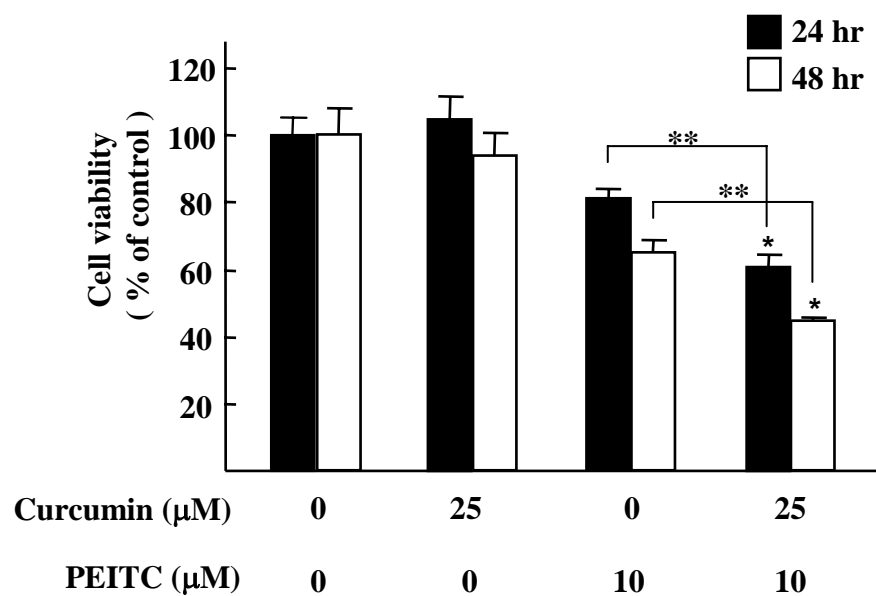
Akt is another important regulator of cell survival and cell proliferation that significantly contributes to tumor growth and progression by promoting cell invasiveness and angiogenesis. Overexpression of Akt has been reported in a variety of human cancers including prostate cancer (31, 56). Loss of PTEN in cancer cells such as PC-3 cells (160) leads to constitutive activation of the PI3K/Akt signal transduction pathway (31).

The combination effect of PEITC and curcumin may thus be explained by their dual roles with positive impact on cell death in prostate cancer: the inhibition of NF- κ B activity and the inhibition of the EGFR activity. Intervention in these signaling pathways by these molecules can culminate in the execution of the apoptotic cell death program, as

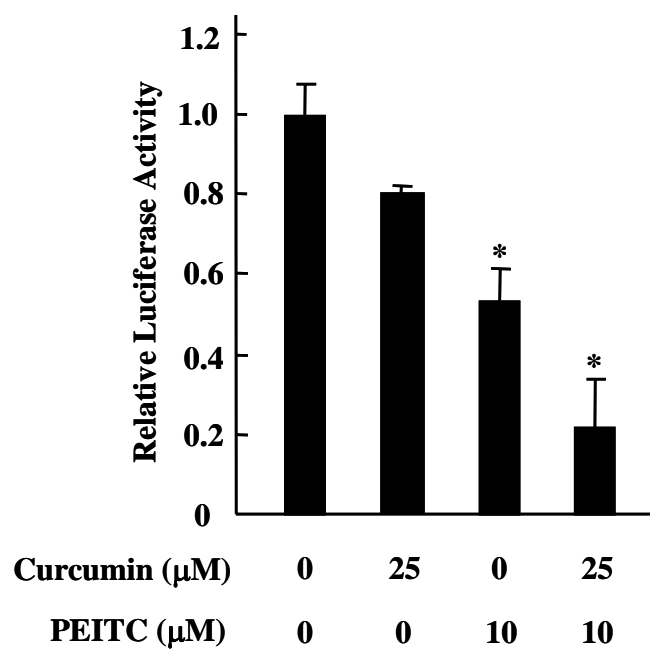
demonstrated by measuring apoptotic biomarkers such as PARP and caspase 3. Thus, the ultimate effect of inhibition of NF- κ B and EGFR activation by PEITC and curcumin is multifactorial, a result which could explain in part their pro-apoptotic properties and could potentially be exploited for prostate cancer prevention. The exact chemical or biochemical mechanisms by which PEITC and curcumin exhibit their additive effects could be related to the combination of their signaling mechanisms, including direct inhibition of IKKs by PEITC (180); direct inhibition of tyrosine kinases by curcumin (101); direct inhibition of JNK phosphatases leading to sustained JNK activation (22); inhibition of histone deacetylases (HDACs) (126) and/or other as yet to be discovered signaling molecules.

In summary, we have demonstrated that PEITC in combination with curcumin inhibits Akt and NF- κ B cell survival signal mechanisms by blocking of EGFR activation in PC-3 cells. Our results suggest that PEITC in combination with curcumin could induce programmed cell death by inhibiting the EGFR/Akt/NF- κ B signaling pathways (Figure 2-5), which are critical for maintaining cell survival. These mechanisms may be exploited for the prevention and/or treatment of human prostate cancer.

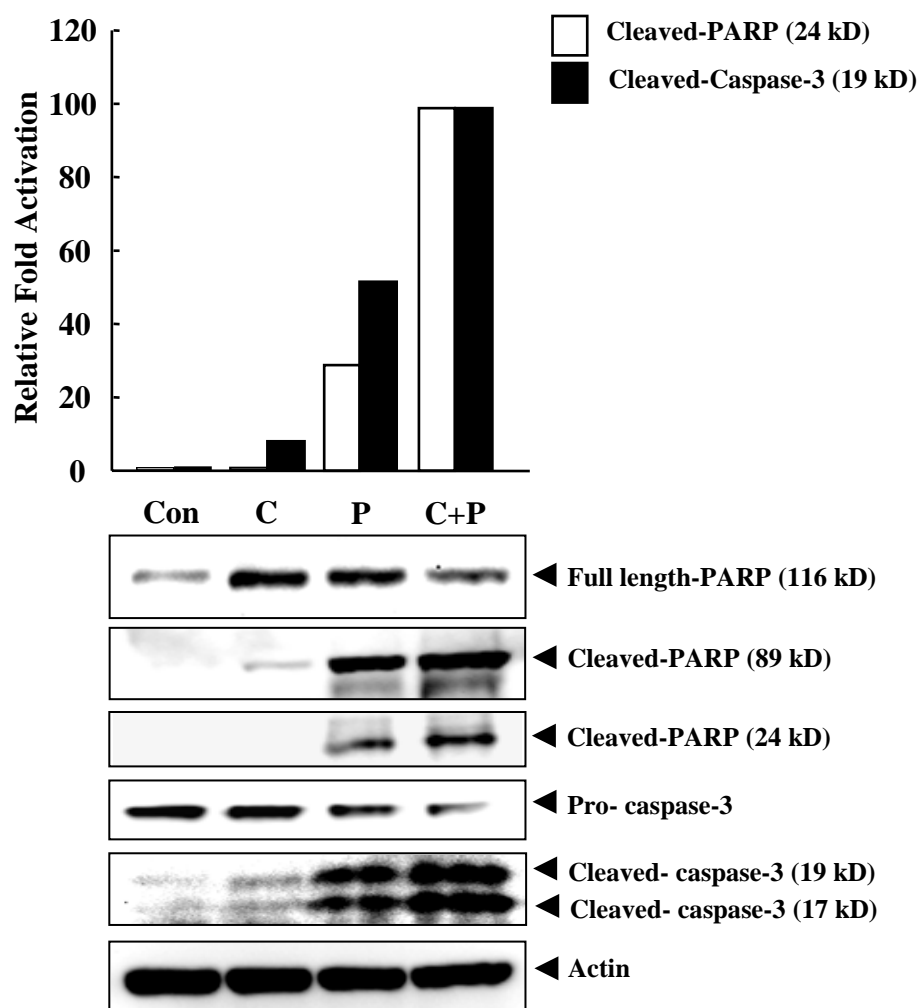
A)



B)



C)



D)

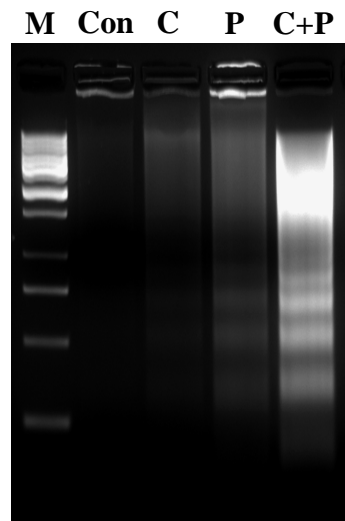


Fig. 2-1. Combined effects of PEITC and curcumin on cell death and NF- κ B signaling pathways in PC-3 human prostate cancer cells.

(A) Cell viability of PC-3 C4 cells was measured by MTT assay after treatment with curcumin, PEITC or a combination of both for 24 or 48 h. Data are shown as mean \pm SD ($n = 3$). For t -tests, $^*P < 0.05$ compared with control; $^{**}P < 0.05$ compared with two groups. (B) NF- κ B luciferase activity was measured after treatment of PC-3 C4 cells with curcumin, PEITC or combination for 24 h. Data are shown as mean \pm SD ($n = 3$). For t -tests, $^*P < 0.05$ compared with control (0.2% DMSO). Cleavage of PARP and caspase 3 (C) and DNA fragmentation (D) as apoptotic markers were measured by western blot analysis and DNA electrophoresis, respectively, after 24 h treatment of PC-3 C4 cells with curcumin, PEITC or a combination (lower panel in C and D). The upper panel in C shows the relative fold activation of cleaved PARP or cleaved caspase 3 by

densitometry. The results are presented as mean \pm SD ($n = 3$). M, DNA marker; Con, control; C, curcumin; P, PEITC. (E) PC-3 C4 cells were treated with different concentrations of curcumin and PEITC in serum-free media for 1 h. Activation levels of Akt signaling proteins (PDK1 and Akt) and NF- κ B signaling protein (I κ B α) were measured using their phospho-specific antibodies by western blotting. Actin was used to ensure equal protein loading. All experiments in this study were performed at least three times.

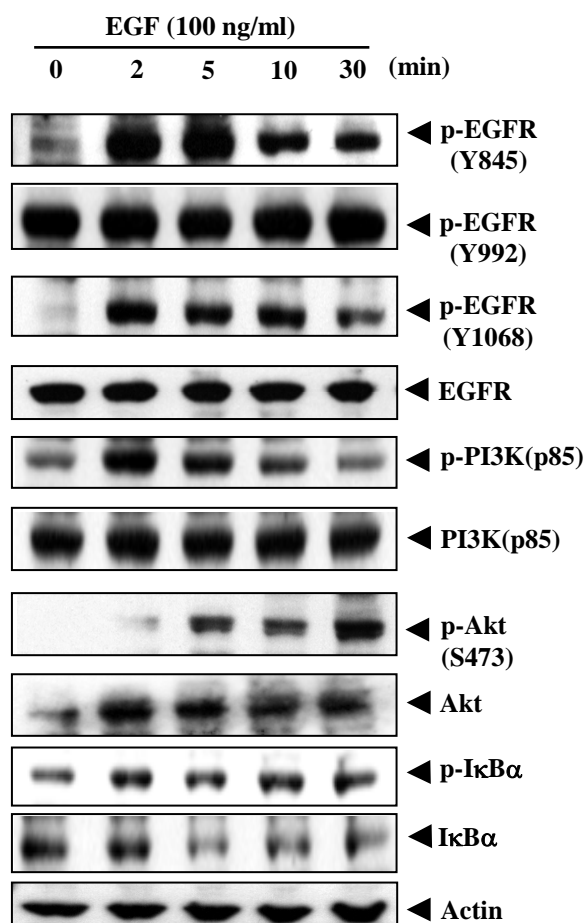
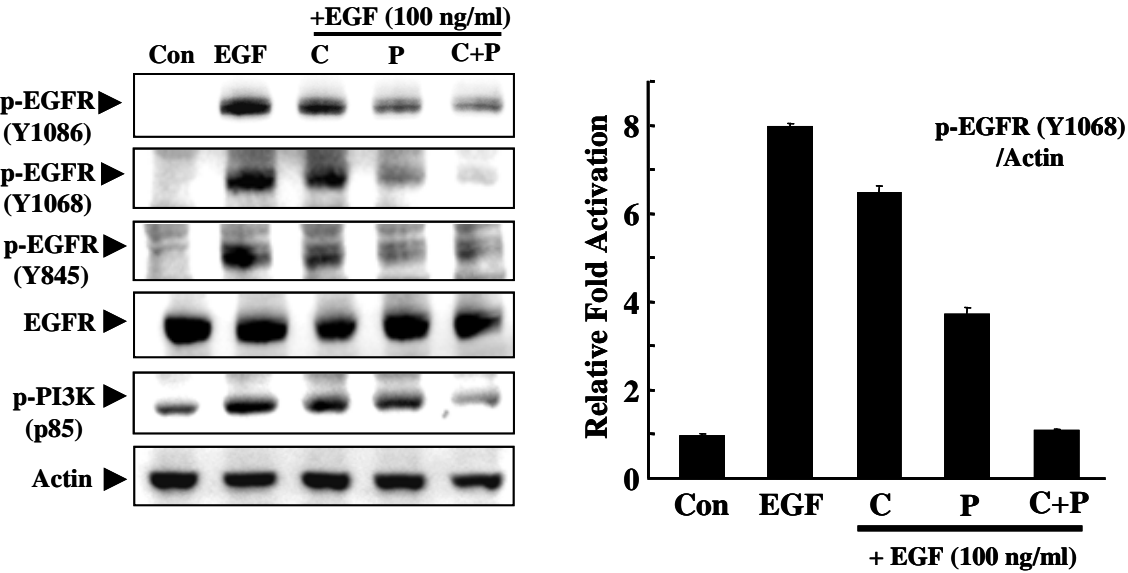


Fig. 2-2. Effects of EGF on EGFR signaling in PC-3 C4 cells.

PC-3 C4 cells were incubated with EGF (100 ng/ml) in serum-free media for the indicated times. Representative EGFR signaling proteins (p-EGFR, p-PI3K (p85), p-Akt and p-IκBα) were measured using phospho-specific antibodies, which detect phosphorylation at specific residue. Anti-EGFR, anti-PI3K (p85), anti-Akt and anti-IκBα antibodies were used to determine the total expression levels of each protein. Actin was used to ensure equal protein loading.

A)



B)

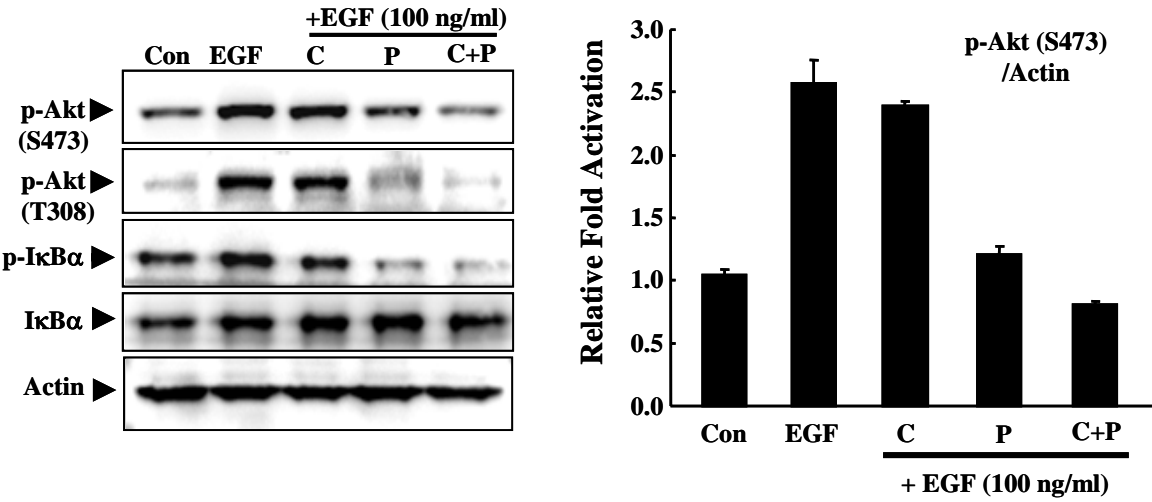
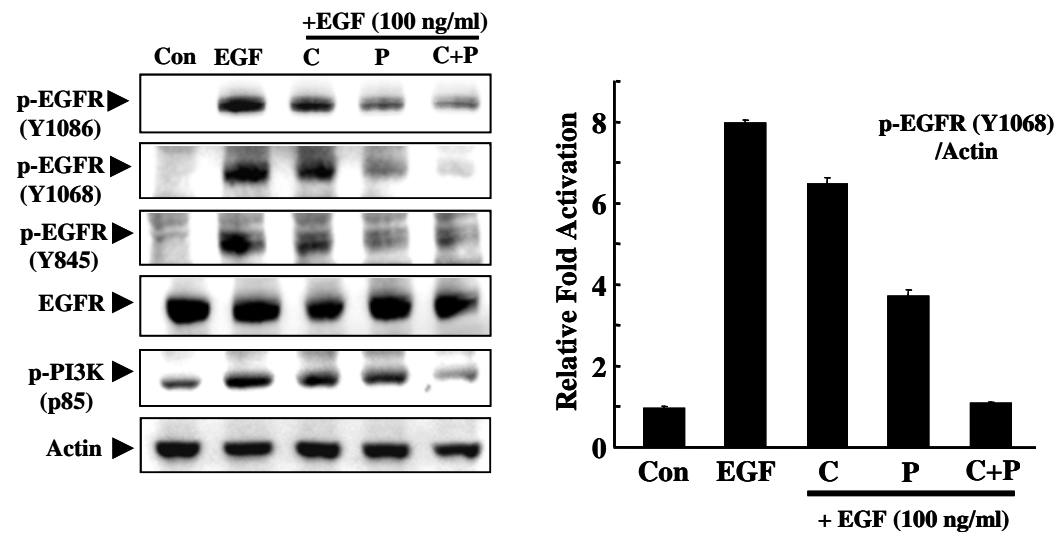


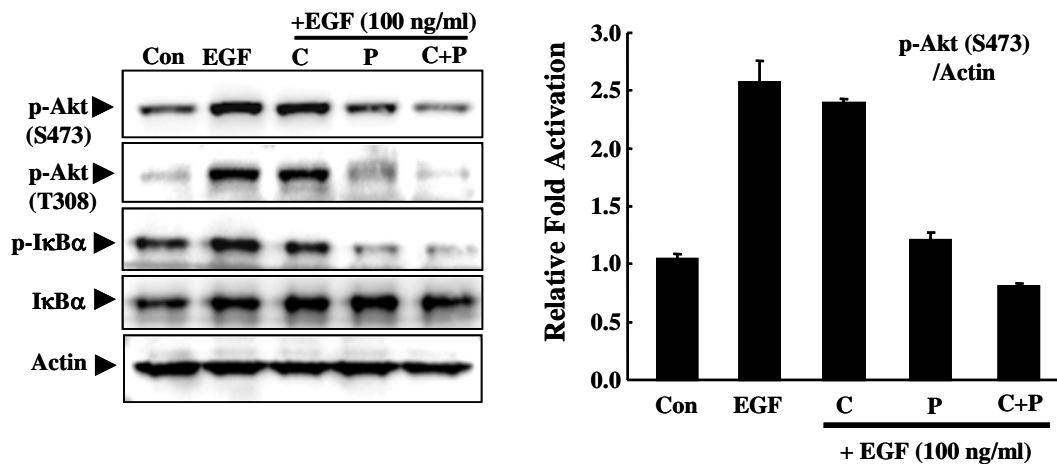
Fig. 2-3. Inhibition of EGFR phosphorylation by PEITC, curcumin, and their combination after stimulation of PC-3 C4 cells with EGF.

(A) PC-3 C4 cells were stimulated with EGF (100 ng/ml) for 10 min after a 5 min pretreatment with compounds (curcumin, 25 μ M; PEITC, 10 μ M; or their combination) in serum-free media. Activated EGFR proteins were measured using four different types of phospho-specific antibodies, which recognize specific phosphorylation sites on tyrosine residues, by western blotting. Con, control; C, curcumin; P, PEITC. (B) PC-3 C4 cells were pretreated with compounds (curcumin, 25 μ M; PEITC, 10 μ M; or their combination) for 5 min and then challenged with EGF (100 ng/ml) for 1 h in serum-free media. Activated Akt proteins were measured by western blotting using phospho-specific antibodies that detect specific phosphorylation sites in Akt. Actin was used to ensure equal protein loading. Con, control; C, curcumin; P, PEITC.

A)



B)



C)

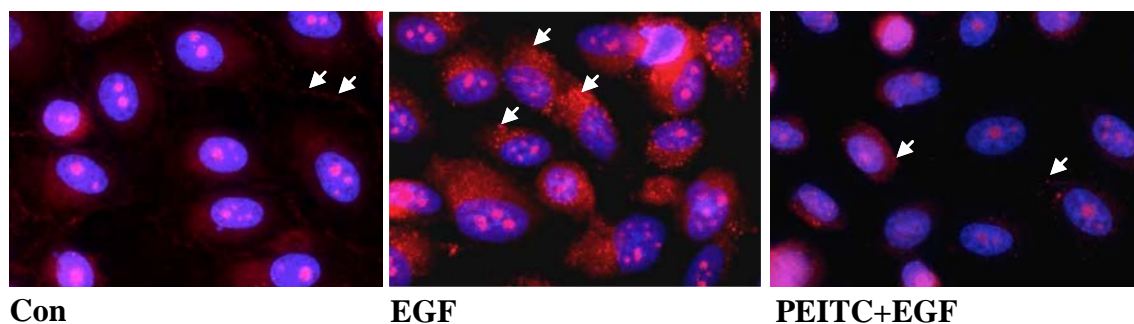


Fig. 2-4. Additive inhibition of EGFR signaling in PC-3 parental cells by combination of PEITC and curcumin.

(A) PC-3 cells were pretreated with compounds (curcumin, 25 μ M; PEITC, 10 μ M; or their combination) for 5 min and then stimulated with EGF (100 ng/ml). For evaluation of the EGFR signaling proteins, phospho-specific antibodies against the phosphorylated tyrosine residues (Y845, Y992 and Y1068) of EGFR were used. Phospho-p85, a subunit PI3K, was detected using a specific antibody, which can detect p-YXXM motif (Y, tyrosine; X, amino acid; M, methionine). Actin was used as an equal loading control. Relative fold of activation of p-EGFR (Y1068) was measured by densitometry analysis (right). Con, control; C, curcumin; P, PEITC. (B) PC-3 cells were pretreated with compounds for 5 min and then incubated with EGF (100 ng/ml) for 2 h. Phosphorylation of Akt was measured using specific antibody detecting phosphorylation of S473 or T308, by western blotting. Relative fold activation of p-Akt was measured by densitometry (right). Total protein levels of Akt and actin were used for the Akt expression level and protein equal loading controls, respectively. Phosphorylation of I κ B α was

also measured by western blotting using a phospho-specific antibody. Con, control; C, curcumin; P, PEITC. (C) PC-3 cells were treated with 0.2% DMSO or 10 μ M PEITC for 5 min followed by a 10 min incubation with EGF (100 ng/ml). Phosphorylated EGFR (red) and nuclei (blue) were detected by immunofluorescence analysis using anti-p-EGFR (Y1086) and DAPI dye, respectively. Pictures with red and blue color were merged. Magnitude: 400-fold; Con, control.

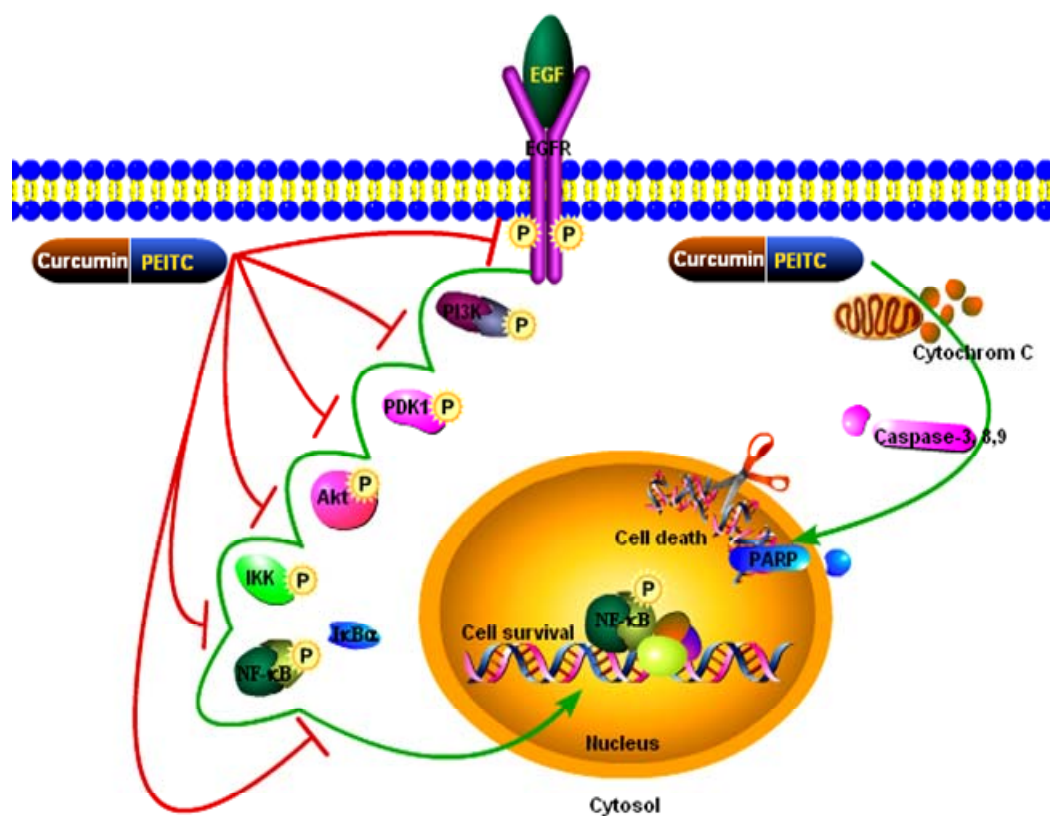


Fig. 2-5. A schematic representation of possible mechanisms for the combined effect of PEITC and curcumin on EGFR signaling and apoptosis in PC-3 cells.

Signaling pathways and blocking mechanisms are indicated with green and red colored line, respectively.

Supplementary 2

Resveratrol inhibits Genistein-induced Multi-drug Resistance Protein 2 (MRP2) expression in HepG2 cells²

KEY WORDS: MRP2; Genistein; Resveratrol, RXR

ABBREVIATIONS: MRP2, multidrug resistance-associated protein 2; cMOAT, canalicular multispecific organic anion transporter; ABC, ATP-binding cassette; cMRP, canalicular MRP2; RXR α , retinoid X receptor alpha; FXR, farnesoid X receptor; CAR, constitutive androstane receptor; PXR, pregnane X receptor

² This chapter is in preparation for journal publication

3.1. Abstract

In this study, we investigated the effects of genistein and resveratrol on MRP2 (multidrug resistance protein 2) expression and their molecular mechanism in HepG2-C3 cells which were stably transfected with human MRP-2 promoter and luciferase reporter gene construct. The results showed that a 3-fold induction of MRP2 luciferase activity was observed with treatment of genistein (50 μ M) and this was inhibition by resveratrol (50 μ M) treatment in 24 h cultured HepG2-C3 cells. Furthermore, Western blot analysis and RT-PCR analysis showed that resveratrol inhibited genistein-induced MRP2 protein synthesis well as mRNA expression. In addition, immunocytochemistry data showed that genistein-induced formation of MRP2 vacuoles were dramatically reduced by treatment with resveratrol. Next we investigated the binding affinity between RXR α (retinoid X receptor alpha) and MRP2 promoter using DNA-protein pull-down assay. The results showed that resveratrol inhibited the genistein-induced binding activity of RXR α . Taken together, we surmise that resveratrol inhibits the genistein-induced MRP2 expression by blocking the binding activity between RXR α transcription factor and MRP2 promoter in HepG2 cells. This study suggests that naturally occurring chemopreventive agents can inhibit the activity of drug transporters such as MRP2 which can play an important role in modulating the efficacy of interventive chemopreventive strategies.

3.2. Introduction

Human multidrug resistance-associated protein 2 (MRP2/ABCC2/cMOAT/cMRP), a subfamily C of member of the ATP-binding cassette (ABC) transporter family, plays an important role in elimination of diverse organic anions including reduced glutathione, glutathione conjugates, bilirubin glucuronides, sulfated, glucuronidated bile salts and non-conjugated organic anions from hepatocytes into bile or from intestinal epithelial cells into the intestinal lumen, or from kidney proximal tubules into urine (77, 158).

MRP2 is an efflux pump protein, which is localized to the apical (canalicular) membrane of hepatocytes (76, 133) and other apical membrane of the polarized cells including the small intestine (41), colon (150), gallbladder (141), bronchi (150, 155) and placenta (155). To date, the twelve members (ABCC1-12) have been identified [reviewed in ref. (129)]. Among these, MRP1 (27), MRP2 (13, 132) and MRP3 (79, 88, 89) have been well characterized as conjugate export pump. Unlike apical localization of MRP2, MRP1 and MRP3 are localized in basolateral membrane of polarized cells (39, 88, 89, 114). Since MRP2 plays a critical role in the elimination of bilirubin glucuronosides from hepatocytes into bile, MRP2 deficient in canalicular membrane can cause the conjugated hyperbilirubinemia as observed in Dubin-Johnson syndrome in humans (133, 164, 169).

The modulation of MRP2 expression has been studied by identifying the critical region of MRP2 promoter. The critical region for the transcription is span between -517 and -197 from the initial codon (154). Recently, hormone response elements for the transcriptional regulation were also identified in rat *Mrp2* promoter region. *Mrp2* expression is regulated by heterodimers of the retinoid X receptor α (RXR α) with

pregnane X receptor (PXR) or with farnesoid X receptor (FXR) or with constitutive androstane receptor (CAR) with high affinity to its promoter region (72). Recent studies were shown that MRP2 expression was induced by bile acid via FXR (131), or by antibiotic rifampicin, the synthetic glucocorticoid dexamethasone and pregnenolone 16 α -carbonitrile via PXR (10, 46, 80), or by Phenobarbital via CAR(156). Vollrath *et al.* proposed that Nrf2 (nuclear factor-erythroid 2 p45-related factor 2) might also regulate the expression of Mrp2 gene via antioxidant response element (ARE) in Mrp2 promoter region (168). Furthermore, not only the transcriptional regulation, but also post-translational regulation has been suggested to explain the modification in the transport activity of Mrp2. And some protein kinase C (PKC) also have been reported to change the transport activity and/or localization of MRP2/Mrp2 (92, 139).

It has been considered that MRPs may also play an important role in progression in cancer. Since tumor cells showed a resistance to different anticancer drugs due to the increased expression of MRP2, or activity of efflux pump which leads to a decrease in drug accumulation in the cells (121). Also aberrant expression of MRP2 was observed by tissue microarrays in some malignant tumor samples from renal cell, breast, ovarian, stomach, lung and colon (150).

Some naturally occurring dietary phytochemicals, such as resveratrol and genistein, have been studied for the chemopreventive effect on different cancers. These dietary agents are believed to repress the inflammatory processes that lead to tumorigenesis by inhibition of variety of molecular signals which induced by various environmental stresses. Their inhibitory effects on initial tumorigenesis may eventually suppress the final steps of carcinogenesis as well, namely angiogenesis and metastasis(1).

Genistein (4,5,7-hydroxyisoflavone, Fig. 3-1), a isoflavone from soybeans, chickpea, and kudzu root, is known as a tyrosine kinase inhibitor (2), antioxidant (109), and chemopreventive agent for cancers (1). Genistein plays a role in attenuation of the growth of cancer cells by inhibiting the protein-tyrosine kinase (PTK)-mediated signaling mechanisms (2). Recent report showed that genistein inhibited the phosphorylation of tyrosine in proto-oncogene HER-2 protein in breast cancer cells and delays the onset of tumor in transgenic mice expressing the HER-2 gene (148). Also, genistein has antioxidant effects to protect the cells against reactive oxygen species by scavenging free radicals which can stimulate the expression of genes relating to stress-mediated carcinogenesis (143, 193). In addition, genistein has been shown to have inhibitory effect on the growth of breast cancer and prostate cancer which have estrogen and androgen receptor positive and negative respectively as well as on estrogen-stimulated growth of breast cancer cells *in vitro* culture systems (134, 135). Further more, genistein showed its powerful inhibition on cell survival signaling pathway such as nuclear factor-kappa B (NF- κ B) and Akt (105).

Resveratrol (trans-3,5,4'-trihydroxystilbene, Fig. 3-1), a phytoalexin from the skin and seeds of grapes or red wine, has been reported to have antioxidant (75), anti-inflammatory (34, 112) and cancer chemopreventive (47, 67, 191) properties. In addition epidemiological study suggests that resveratrol may have protective effect on the cardiovascular disease (167). Many groups have been extensively studied the effects of resveratrol especially on cancer related molecular targets, and revealed its effects on many molecular targets, such as NF- κ B signaling, activator protein-1 (AP-1), cell cycle, cell survival kinase Akt, tumor-suppressor gene p53, growth factors signaling pathways,

chemokines and metastasis, tumor necrosis factor (TNF), signal transducer and activator of transcription, cyclooxygenase (COX-2), inducible nitric oxide synthase (iNOS), mitogen-activated protein (MAP) kinases, and angiogenesis (1).

Recent studies have shown that the consumption of non- or less-toxic dietary chemopreventive agents could be a promising strategy to reduce the incidence of many cancers. Moreover, consumption or treatment with MRP2 inhibitors from natural compounds could be expected to enhance the effect of drug for the chemoprevention or chemotherapy in cancer patients. In this study, we chose two different chemopreventive agents (geistein and resveratrol) for investigating the MRP2 expression as well as mechanism in human hepatocarcinoma HepG2-C3 cells.

3.3. Materials and Methods

3.3.1. Materials

F12 medium, fetal bovine serum (FBS) and penicillin/streptomycin antibiotics mixture, and Trizol[®] reagent were obtained from Invitrogen. Genistein, *trans*-resveratrol and monoclonal MRP2 (M2III-6) antibody were purchased from Alexis (San Diego, CA). RXR α (N197) antibody was purchased from Santa Cruz biotechnology (Santa Cruz, CA). ECL femto signal substrate was purchased from Pierce Biotech Inc. Polyvinylidene difluoride (PVDF) membrane was obtained from Millipore. Protease inhibitor cocktail was from Roche Molecular Biochemicals. And all other chemicals used were of analytical grade or the highest grade available.

3.3.2. Cell culture

HepG2-C3 (which was stably transfected with human MRP2 promoter-luciferase

gene construct; pGL2-*MRP2* (1229bp)-luciferase) were maintained at 37 °C in a humidified atmosphere of 5% CO₂/95% air in F12 medium supplemented with 10% heat-inactivated fetal bovine serum (FBS), 0.1% insulin, 1% MEM amino acid, and 50 U/ml of penicillin/streptomycin mixture (Gibco BRL, Grand Island, NY). Cells were grown to 60–80% confluence and trypsinized with 0.05% trypsin containing 2 mM EDTA.

3.3.3. Cell proliferation assay

Cell proliferation was measured by MTT (3-(4,5-dimethylthiazolyl)-2,5-diphenyltetrazolium bromide) assay. Briefly, HepG2-C3 cells were plated in 48-well plates at a density of 4×10^4 /well. After overnight culture, cells were treated with different concentrations of genistein or resveratrol or their combination for 24 h and 48 h. All stock compounds were dissolved in DMSO which was maintained in 0.2% for drug treatments. After treatment with the compounds, 20 µg of 5 mg/ml MTT solution was added to each well and incubated for 2 h. Formazan grain in cells was dissolved in DMSO after removal of the medium. Solubilized formazan was measured at 570 nm with an ELISA plate reader (Bio-TEK instrument, CA).

3.3.4. Luciferase assay

HepG2-C3 cells were plated in 6-well plate at a density of 5×10^5 /well and cultured overnight. The cells were then treated with the compounds for 24 h. After treatment, the cells were washed twice with ice-cold PBS and harvested in 200 µl of 1xreporter lysis buffer (Promega). After brief centrifugation at 12,000 rpm, a 10 µl of the supernatant was assayed for luciferase activity. Luciferase activity was measured with a

luciferase kit from promega (Madison, WI) according to the manufacturer's instructions. The luciferase activity was normalized with protein concentration.

3.3.5. Western blotting

HepG2-C3 cells were cultured in 60 mm dishes at 60% confluency prior to drug treatment. Cells were treated with DMSO (0.2 %) or drugs with desired concentration for different time intervals. Whole cell proteins were extracted with RIPA lysis buffer (150 mM NaCl, 0.5% Triton X-100, 50 mM Tris-HCl, pH 7.4, 25 mM NaF, 20 mM EGTA, 1 mM DTT, 1 mM Na₃VO₄, 0.1% SDS, and protease inhibitors cocktail) for 30 min on ice followed by centrifugation at 12,000 rpm for 15 min. The protein concentration of the supernatant was measured by using the BCA reagent. Protein (45 µg) was electrophoresed on 4-15% gradient Tris-HCl gel (Biorad) and electrotransferred onto polyvinylidene difluoride (PVDF) membrane in Tris-glycine buffer (pH 8.4) containing 20% methanol. The membrane was then blocked in 5% fat-free dry milk in phosphate-buffered saline with 0.1% Tween-20 (PBS-T) for 1 h. Membranes were probed with monoclonal anti-MRP2 (M2III-6) antibody and horseradish peroxidase-conjugated secondary antibody by standard western blot procedures. The proteins were visualized with the Femto Signal Chemiluminescent Substrate (Pierce) under the image analyzer (Biorad).

3.3.6. RNA extraction and RT-PCR

Total RNA from HepG2-C3 cells was isolated using Trizol (Invitrogen, Carlsbad, CA). Total RNA (1 µg) was subjected to RT-PCR using one-step RT-PCR kit (Qiagen) by following the manufacturer's instructions. To amplify the MRP2 mRNA, primers were

used as follow: forward, 5'-CTG GAG GAG ATT TGG CTG AG-3', and reverse, 5'-GGC GGG AGG TAG ACA CAT AA-3'. For control, actin was used as an internal standard using the primers as follow: forward, 5'-TCG TGC GTG ACA TTA AGG AG-3', and reverse, 5'-TGA TCC ACA TCT GCT GGA AG-3'. PCR products were resolved on 1.2% agarose gels and visualized under UV lamps. PCR conditions are as follows: 50°C for 30 min for reverse transcription, 95°C for 15 min for initial PCR activation step, 94°C for 30 sec, 55°C for 30 sec, 72°C for 1.5 min for 25 cycles of amplification step, and 72°C for 10 min for a final extension. To prevent the saturation of internal standard, β -actin was amplified in 20 cycles. The PCR sizes for MRP2 and β -actin are 1.2 kb and 450 bp respectively.

3.3.7. Immunofluorescence

HepG2-C3 cells were cultured on cover glass (thickness 0.15 mm) and treated with genistein with/or resveratrol for 24 h. After drug treatment, cells were washed with ice-cold PBS solution twice and fixed with 3% paraformaldehyde in PBS, pH 7.4, for 20 min. Then cells were underwent permeabilization using fresh prepared 0.1% Triton X-100 in PBS at room temperature for 5 min and washed with PBS. This step was repeated for three times. To block the nonspecific binding, cells were pre-incubated with 5% goat serum solution (Zymed) at room temperature for 1 h. And cells were incubated with anti-MRP2 (M2III-6) antibody in 2.5% goat serum solution overnight at 4 °C. After 4 times of washing with PBS, cells were incubated with TRITC-conjugated goat anti-mouse (Zymed, San Francisco, CA) for MRP2 and DAPI (Molecular Probes) for nucleus for 1 h and followed by washing the samples with PBS. Mounted samples were examined under the fluorescence microscopy. Apical MRP2 vacuoles were counted and normalized with

DAPI stained cells.

3.3.8. DNA-Protein pull-down assay

To obtain the biotin labeled MRP2 promoter DNA (1.2 kb), template DNA from pGL2-MRP2-luc was amplified by PCR method using platinum taq DNA polymerase kit (Invitrogen) with primers as follow: forward, 5'-dual biotin-CCT AGA ATT TGA CCA GAT TT-3' and reverse 5'-GTT CTG CAA CTC TAC TTT T-3'. PCR conditions are as follow: 94°C for 5 min for initial PCR activation step, 94°C for 30 sec, 55°C for 30 sec, 72°C for 1.5 min for 35 cycles of amplification step, and 72°C for 10 min for a final extension. Single band of PCR products were checked by DNA electrophoresis. To link biotinylated DNA to immobilized streptavidin beads, PCR DNA (8 µg) was mixed with PBS-washed 400 µl (50% slurry) of Ultralink Immobilized streptavidin beads (Pierce) and filled up with 600 µl of PBS to make 1 ml reaction volume. The mixture was incubated for 24 h at 4°C in a rotary shaker. After washing twice with cold PBS, DNA-bead mixtures (80 µl, 640 ng DNA/32 µl bead) were incubated with 100 µg of nuclear protein samples in 500 µl of incubation buffer (5 mM Tris-HCl, pH 7.5, 50 mM NaCl, 0.5 mM DTT, 0.5 mM EDTA, 2% glycerol, 0.5 mM PMSF, 50 µg/ml sonicated salmon sperm DNA) for 24 h at 4°C in a rotary shaker. After washing the samples 3 times with 1ml of incubation buffer, samples were boiled with 2xSDS sample buffer for 5 min and followed by Western blot analysis against RXRα using anti-RXRα (N-197) antibody. For non-specific binding control, DNA non-bound beads were mixed with protein samples. To check the linkage between biotinylated DNA and streptavidin beads, the complex was digested with BglII restriction enzyme and followed by gel electrophoresis.

3.4 Results

3.4.1. Toxicity of genistein and resveratrol in HepG2-C3 cells

To measure the cytotoxicity of genistein and/or resveratrol in HepG2-C3 cells, each drug or their combination was treated in HepG2-C3 cells with different concentrations or times and subjected to MTT assay to measure the cell viability. The results show that single treatment of genistein and resveratrol has less or no toxic in concentration up to 100 μ M for 24h or 48 h incubation. Also combination of same concentration (up to 50 μ M) from two drugs has no effect on cell toxicity. However combination treatment by these two drugs at 100 μ M dramatically increased cell toxicity up to 30% and 40% for 24 h and 48 h incubation, respectively. The higher concentration at 200 μ M from the each single or combination treatment shows high toxicity in both 24 h and 48 h incubation times (Fig. 3-2A and 2B). In this study, we used non- or less toxic range of each drug concentration for the evaluation on MRP2 expression.

3.4.2. Effects of genistein and resveratrol on MRP2-Luciferase activity

To measure the MRP-2 luciferase activity, HepG2-C3 cells were treated with 50 μ M or 100 μ M of genistein or resveratrol for various times. The results showed that genistein induced the MRP2-luciferase activity at both 50 μ M and 100 μ M and peaked in 10 h (4-fold induction) and gradually decreased. However, resveratrol, at 50 μ M, has no effect on the induction of MRP2-luciferase activity for different times but only 2-fold induction of MRP2 luciferase activity was measured in 10 h incubation (Fig. 3-3A).

To show the intervention effect by resveratrol on genistein-induced MRP2-luciferase activity, HepG2-C3 cells were treated with 50 μ M of genistein with various

concentration of resveratrol (up to 100 μ M) for 24 h. The results showed that resveratrol inhibited the genistein-induced MRP2-luciferase activity (Fig. 3-3B).

3.4.3. Inhibition of genistein-induced MRP2 protein by resveratrol

To see the inhibitory effect of resveratrol on genistein-induced MRP2 expression, HepG2-C3 cells were first treated with 50 μ M of genistein and/or 50 μ M of resveratrol for various times and subjected to Western blot analysis to measure the MRP2 protein level. The results showed that MRP2 protein induction (\sim 2.5 fold) was peaked in 24 h by genistein and suppressed by resveratrol (Fig. 3-4A). We also measured MRP2 protein level by single treatment of resveratrol with two different concentrations (50 μ M and 100 μ M) at various time points. The results showed that MRP2 protein was slightly induced (\sim 1.5 fold) in 10 h by resveratrol (50 μ M) and decreased gradually to under basal level by 48 h. Furthermore, high concentration of resveratrol (100 μ M) potently inhibited the expression of MRP2 protein (Fig. 3-4B). To see the dose dependent manner by resveratrol treatment in genistein-induced MRP2 expression, cells were treated with genistein (50 μ M) and different concentration of resveratrol for 24 h and subjected to Western blot analysis to measure the MRP2 protein. The results showed that resveratrol inhibited the genistein-stimulated MRP2 induction with dose dependent manner (Fig. 3-4C).

3.4.4. Suppression of genistein-induced *MRP2* mRNA by resveratrol

To see the effect of genistein on expression of *MRP2* mRNA, HepG2-C3 cells were cultured with 50 μ M of genistein for various times and conducted RT-PCR. The results showed that induction of *MRP2* mRNA was peaked in 12 h (2-fold) and 24 h (1.5-

fold) by genistein (Fig. 3-5A). Based upon these results, we investigated the effect of resveratrol on genistein-induced *MRP2* mRNA. HepG2-C3 cells were treated with 50 μ M of genistein and various concentrations of resveratrol for 24 h and subjected to RT-PCR. The results showed that resveratrol was suppressed the genistein-stimulated *MRP2* mRNA with dose dependent manner (Fig. 3-5B).

3.4.5. Inhibition of genistein-induced MRP2 vacuoles by resveratrol

Formation of MRP2 vacuoles may refer to the efflux activity of MRP2. Based on this, we investigated the inhibitory effect of resveratrol on genistein-induced MRP2 vacuole formation. HepG2-C3 cells were treated with 50 μ M of genistein and 50 μ M or 100 μ M of resveratrol for 24 h. MRP2 vacuoles were detected by immunocytochemistry using anti-MRP2 (M2III-6) and TRITC-conjugated secondary antibody and measured under the fluorescence microscopy. The results showed that resveratrol was significantly inhibited the formation of genistein-mediated MRP2 vacuoles (Fig. 3-6A). Also, MRP2 vacuoles were counted from three different pictures to analyze the inhibitory effect of resveratrol in this study. As shown in Fig. 3-6B, genistein induced 5-fold of MRP2 vacuole formation and that was decreased down to 3-fold or 1-fold by 50 μ M or 100 μ M of resveratrol, respectively.

3.4.6. Inhibitory effect of resveratrol on genistein- or rifampicin-induced binding activity between RXR α and MRP2 promoter DNA

To investigate whether resveratrol interfere the binding activity of RXR α in the MRP2 promoter region, protein-DNA pull-down assay was conducted. HepG2-C3 cells were treated with 50 μ M of genistein or 10 μ M of rifampicin (positive control as a PXR

ligand) with 50 μ M of resveratrol for 24 h. Next, the nuclear samples were incubated with MRP2 promoter DNA-biotin-streptavidin bead complex and subjected to Western blot analysis to detect RXR α protein. The results showed that resveratrol significantly inhibited genistein- or rifampicin-stimulated RXR α binding activity in the MRP2 promoter (Fig. 3-7A). We also confirmed the complex formation between biotinylated MRP2 promoter DNA and streptavidin bead by digestion with BglII restriction enzyme (Fig. 3-7B).

3.5 Discussion

As an aspect of potential for drug resistance by chemopreventive agents, here, we investigated the effects of genistein and resveratrol on MRP2 expression in HepG2-C3 cells. In this study, the results showed that genistein-mediated MRP2 protein and mRNA were inhibited by resveratrol. The approach of this study was based on investigation of drug-drug interaction between chemopreventive agents. This may provide a new idea in chemopreventive or chemotherapeutic approach to intensify the drug effect in cancer treatment. It is a well-known fact that prolonged cancer treatment using chemotherapeutic agent may increase the resistance against chemotherapeutic drug, resulting in difficult treatment of cancer.

In this study, drug concentration for the treatment is based on the non-toxic range tested by MTT assay. As an indirect method for the MRP2 expression, we first tested the MRP2-luciferase activity. Genistein strongly induced MRP2-luciferase activity ranging from 6 h to 24 h at both 50 μ M and 100 μ M with similar fold-induction. However, resveratrol slightly induced MRP2-luciferase activity at 50 μ M but not at 100 μ M in 10 h (Fig. 3-3). Likewise, we found that resveratrol also slightly induced MRP2 protein at 50

μM in 10 h but not at 100 μM (Fig. 3-4). Despite of the early induction of MRP2 by 50 μM of resveratrol, it inhibited genistein-stimulated MRP2 induction for 24 h at the same dose. It is possible that functionally active form of resveratrol on MRP2 expression may depend on incubation time and concentration resulting from the metabolism process.

Recently, metabolism of resveratrol has been studied using *in vitro*, *ex vivo*, and *in vivo* model systems. Yu *et al.* (186) reported that resveratrol was not underwent by phase I enzyme reaction, such as oxidation, reduction, and hydrolysis, in the microsomal incubation. However, the major resveratrol metabolites, trans-resveratrol-3-*O*-glucuronide and trans-resveratrol-3-*O*-sulfate, were identified in rat urine, mouse serum as well as rat and human hepatocytes, whereas, no free-resveratrol was detected in urine and serum samples. In this aspect of MRP2 transport of resveratrol and its metabolites, Maier-Salamon *et al.* (111) reported that biliary excretion of resveratrol glucuronides were significantly decreased in Mrp2-deficient rats. In contrast, biliary secretion of the sulfates was not much changed in the same system. These results suggest that Mrp2 mainly mediates the biliary excretion of resveratrol glucuronides but not for resveratrol sulfates. In addition, Transport of unconjugated resveratrol is not affected by MRP2 from Caco-2 cells and rats models (106, 111). Presumably, resveratrol glucuronides, as a result of fast metabolism in early time, can act as a MRP2 substrate or inducer of MRP2 in HepG2 cells, however, different metabolites, such as sulfate conjugates or combined conjugates, may play a critical role in MRP2 regulation. Apart from the expression of MRP2 by resveratrol, activity of MRP2 efflux against other MRP2 substrates may be affected by resveratrol.

Recent data showed that biliary excretion of organic anion BSP

(bromosulphophthalein) glucuronide, a specific Mrp2 specific substrate, was competed with resveratrol or its glucuronide metabolites, resulting in the inhibition of biliary secretion of BSP glucuronide in Wister rats (111). Likewise, resveratrol or its metabolites may affect the MRP2-mediated efflux of genistein or its metabolites (glucuronides or sulfates) (151) by competition for this transporter. The inhibition of Mrp2-mediated canalicular transport by the resveratrol glucuronides may also take place in human, resulting in a decrease of the biliary elimination and a subsequent accumulation of MRP2 specific drugs, such as anthracyclines, vinca alkaloids, etoposide, as well as camptothecins and methotrexate in target organs (29, 59, 74, 85). Thus, resveratrol or its metabolites may play a different role in MRP2 regulation and its transporter activity as well as other targeted biological activity.

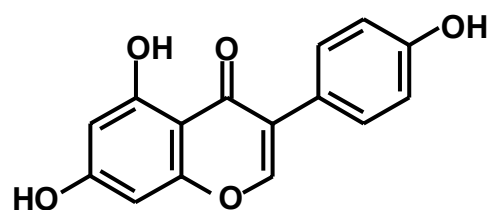
In this study, we also showed that genistein induced MRP mRNA and protein level at 50 μ M for 24 h. Genistein or its metabolites were regarded as MRP2 substrate (65). Recently Hanet *et al.* reported the effects of genistein, as an endocrine disruptor, on MRP2 gene associated with 17 β -estradiol metabolism in HepG2 cells. Although real-time PCR data for the MRP2 expression was appeared to be down-regulated, however, protein level of MRP2 was appeared to be increased by 70 μ M of genistein in the Western blotting analysis (50). The discrepancy between the two groups was based on mRNA expression of MRP2 in HepG2 cells. However, the formation of MRP2 vacuoles could be explained by the induction of MRP2 protein by genistein in this study.

The inhibition of MRP2 activity may be explained by reduced number of MRP2 vacuole which is responsible for the efflux of detoxified foreign substances. Although, efflux activity of MRP2 was not monitored in this study, inhibitory effect of resveratrol

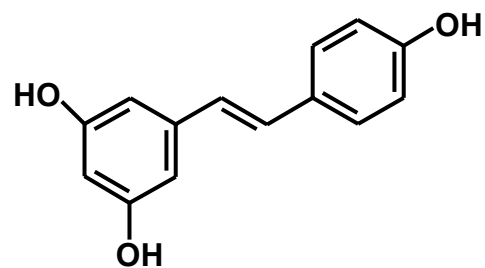
on genistein-mediated MRP2 efflux activity could be measured by counting the number of MRP2 apical vacuoles. Human hepatoma HepG2 cells have hepatic polarity and form bile canaliculus-like structures, called apical vacuoles (14), which can be monitored by fluorescent amphiphilic anions such as glutathionylmethylfluorescein (140). In this study, we counted the number of immunostained MRP2 vacuoles under the fluorescence microscopy after drug treatments since immunofluorescence microscopy showed mainly human MRP2 vacuoles in apical membrane of polarized HepG2 cells. HepG2 cells may be useful to study the function of human MRP2 and to explore the action of inhibitors of MRP2-mediated transport.

RXR α (retinoid X receptor alpha) may play a critical role in transcriptional regulation of MRP2 by heterodimerizing with pregnane X receptor (PXR) or with farnesoid X receptor (FXR) or with constitutive androstane receptor (CAR) in MRP2 promoter region (72). In this study, we showed that genistein- or rifampicin-induced RXR α affinity in the MRP2 promoter was inhibited by resveratrol. This suggests that resveratrol may affect hormone receptor related gene expressions.

In summary, this study shows that resveratrol inhibits the genistein-induced MRP2 expression by blocking the binding activity of RXR α in the MRP2 promoter in HepG2 cells, suggesting naturally occurring chemopreventive agents can inhibit the activity of drug transporters such as MRP2 which can play an important role in modulating the efficacy of interventive chemopreventive strategies.



Genistein



Resveratrol

Fig. 3-1. Chemical structures of genistein and resveratrol

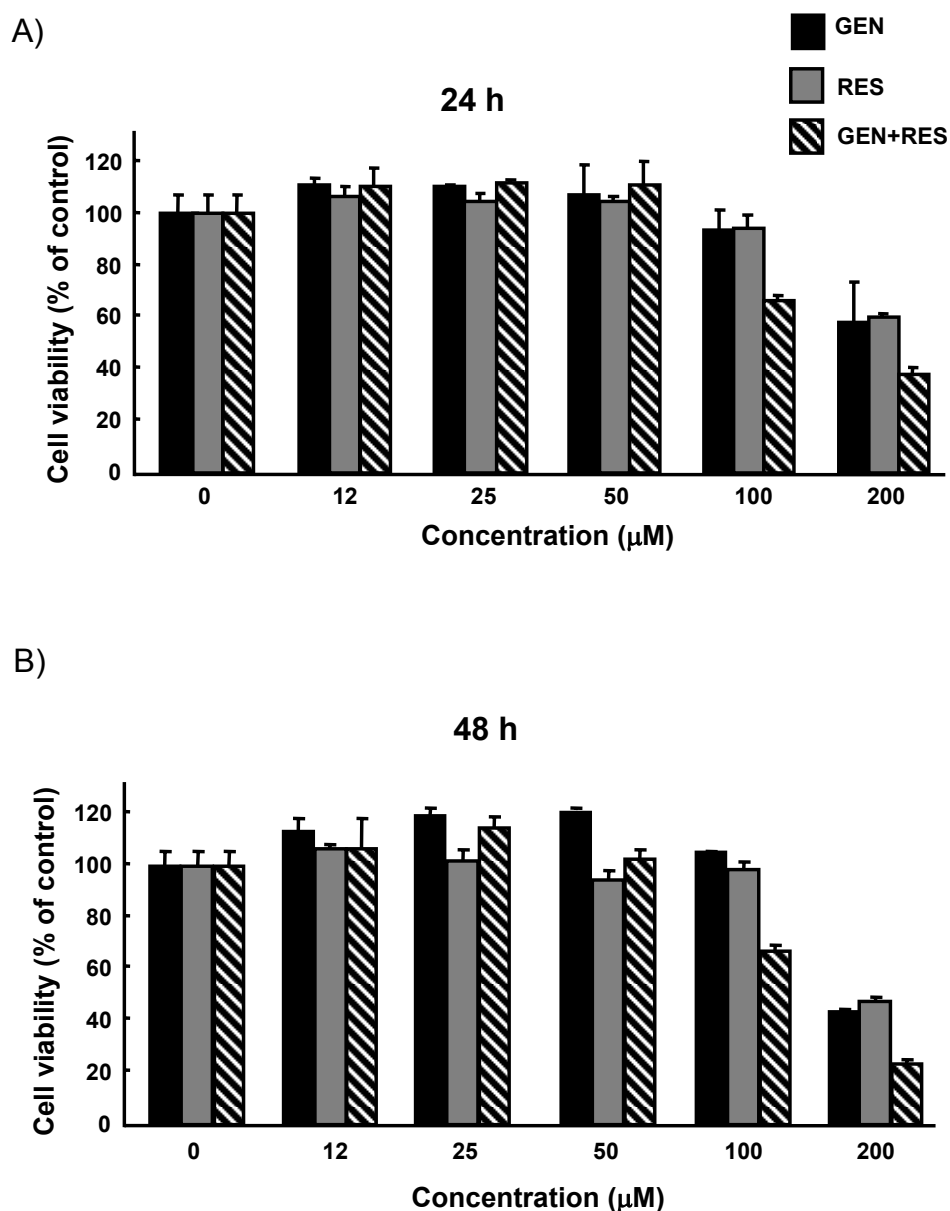


Fig. 3-2. Cytotoxicity of genistein and resveratrol in HepG2-C3 cells

HepG2-C3 cells were plated in 48 well dishes and treated various concentration of genistein or resveratrol or their combination for A) 24 hr or B) 48 h. Cell viability of HepG2-C3 cells was measured by MTT assay. The procedures of MTT assay are described in Methods. GEN, genestein; RES, resveratrol.

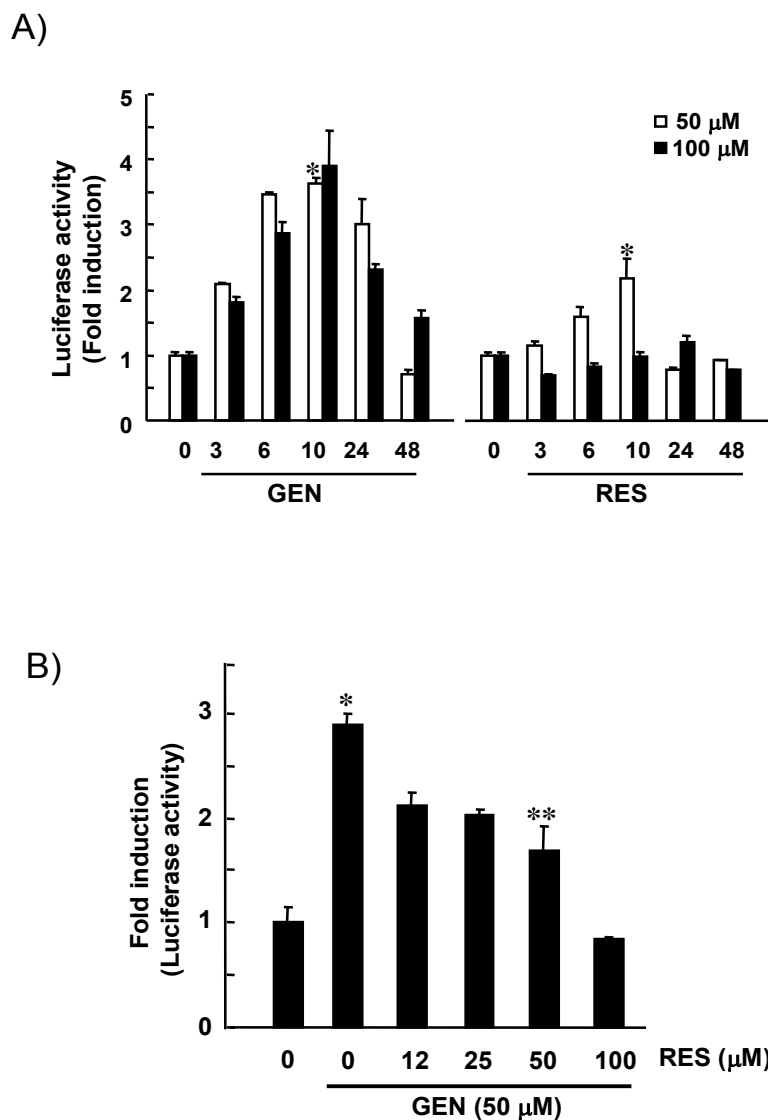
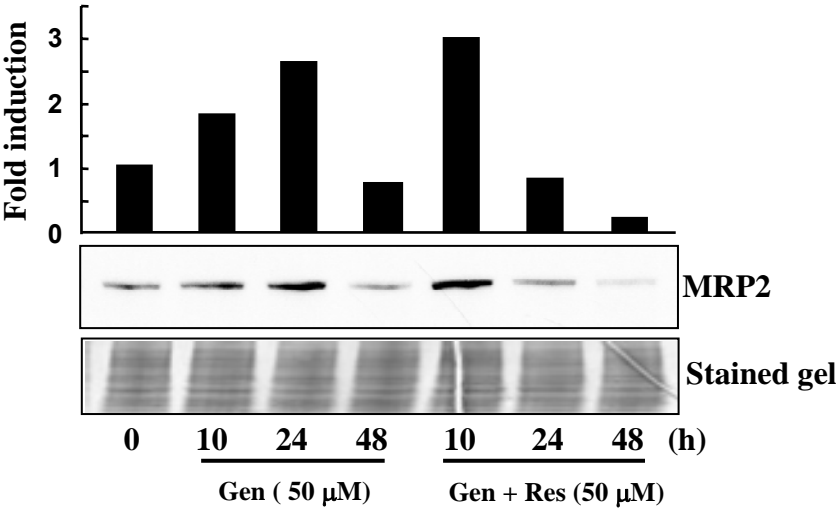


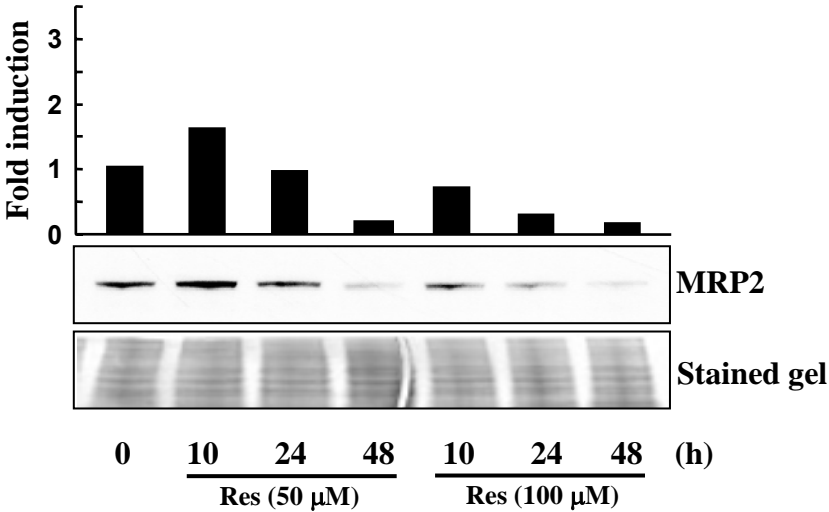
Fig. 3-3. Resveratrol inhibits genistein-induced MRP2-luciferase activity.

A) To check whether genistein could induce the MRP2 protein in HepG2-C3 cells, HepG2-C3 were treated with various concentrations for different time intervals and followed by luciferase reporter assay. B) MRP2-luciferase activities were measured after treatment with genistein and/or resveratrol for 24 h in HepG2-C3 cells. The results are presented as mean \pm S.D(n=3). *, $p < 0.05$ compared with control (0.2 % DMSO). **, $p < 0.05$ compared with GEN (50 μ M). GEN, genistein; RES, resveratrol. **,

A)



B)



C)

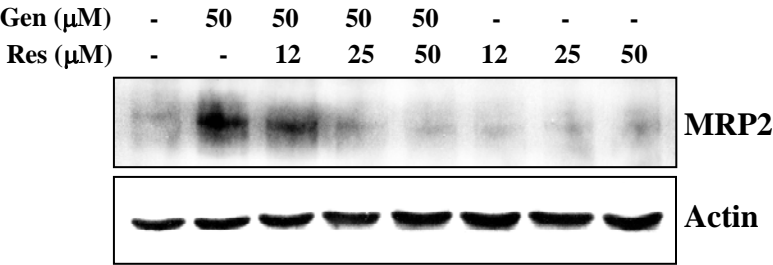
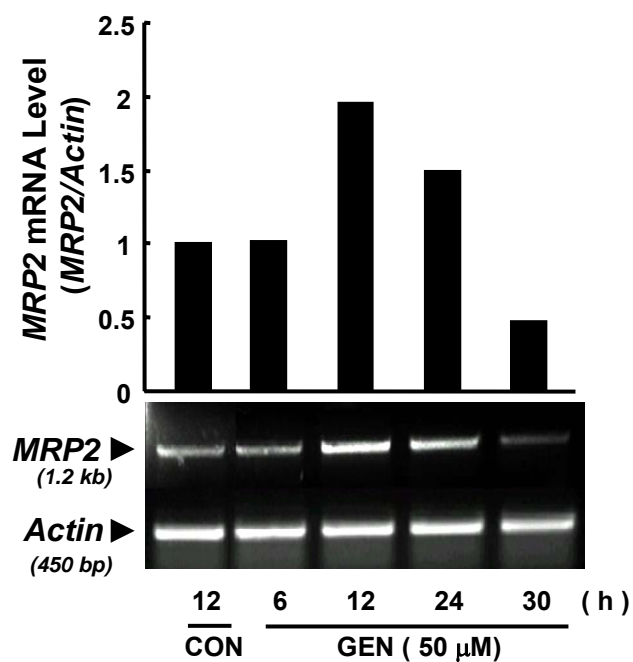


Fig. 3-4. Resveratrol inhibits genistein-induced MRP2 protein.

A) For time course study MRP2 protein expression, HepG2-C3 cells were treated with genistein (50 μ M) or genistein (50 μ M) plus resveratrol (50 μ M) for different times and concentrations. To measure the MRP2 expression, cell lysates were subjected to Western blot analysis using MRP2 (M2III-6) antibody. Fold induction of MRP2 protein was represented by densitometric analysis (*upper*). B) HepG2-C3 cells were incubated with various concentrations of resveratrol for different time intervals. MRP2 protein levels were detected by Western blotting using (M2III-6) antibody. Fold induction of MRP2 protein was represented by densitometric analysis (*upper*). For equal loading control, samples were run on SDS-PAGE gel and stained with commassie brilliant blue (*bottom*). C) HepG2-C3 cells were treated with genistein (50 μ M) and various concentration of resveratrol for 24 h. The protein samples were subjected to Western blotting against MRP2. Actin was used as an internal control. GEN, genistein; RES, resveratrol.

A)



B)

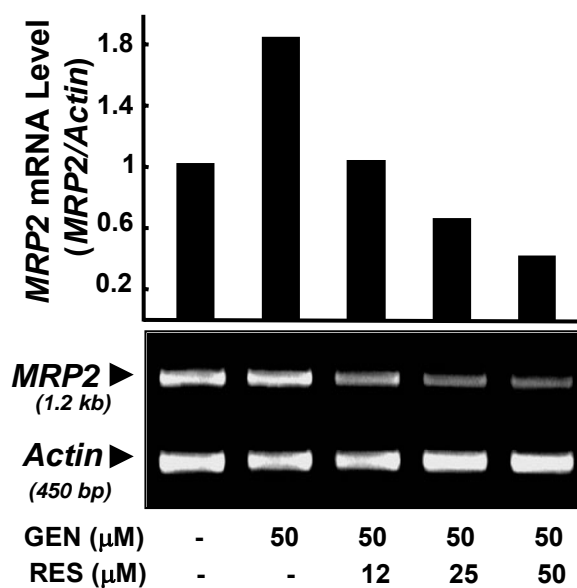


Fig. 3-5. Resveratrol suppresses genistein-induced *MRP2* mRNA.

A) HepG2-C3 cells were cultured in 100 mm dishes and treated with genistein (50 μ M) by time course manner. And B) cells were treated with 50 μ M of

genistein and different concentration of resveratrol for 24 h. Total RNA was isolated using Trizol reagent (Invitrogen) followed by RT-PCR reaction with 1 µg of samples. *Actin* mRNA was used for controls. Total RNA isolation and RT-PCR methods are described in Methods. Fold induction of *MRP2* mRNA was measured by densitometric analysis (*upper*). GEN, genistein; RES, resveratrol.

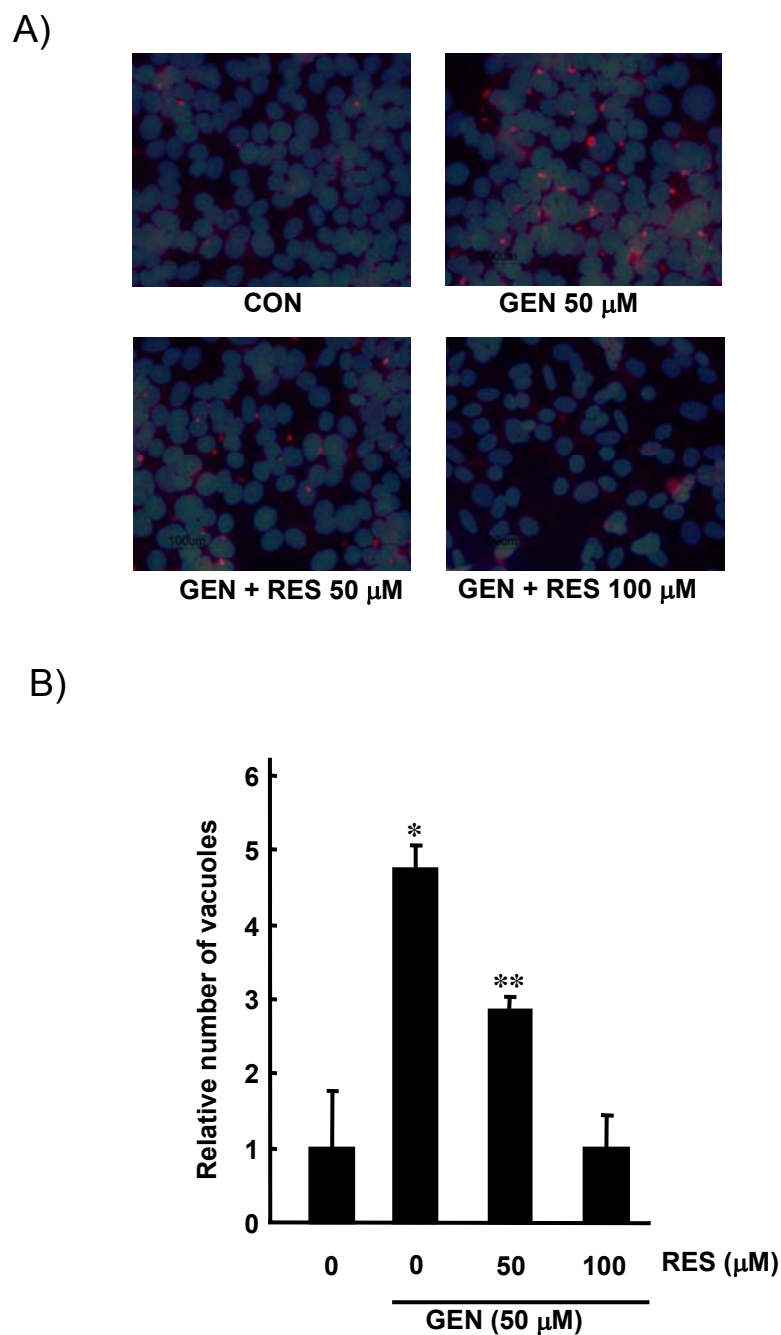


Fig. 3-6. Genistein-induced apical MRP2 vacuoles were repressed by Resveratrol.

A) HepG2-C3 cells were plated on cover glasses and treated with genistein (50 μ M) and/or resveratrol (50 or 100 μ M) for 24 h. MRP2 vacuoles were detected by immunocytochemistry using anti-MRP2 (M2III-6) and TRITC-conjugated

secondary antibody. The procedures of immunocytochemistry were described in Methods. The numbers of MRP2 vacuoles were counted with three different pictures to generate the graph (*B*). Red, MRP2 vacuole; blue, nucleus stained by DAPI. The results are presented as mean \pm S.D (n=3). *, $p < 0.05$ compared with control (0.2 % DMSO). **, $p < 0.05$ compared with GEN (50 μ M). GEN, genistein; RES, resveratrol.

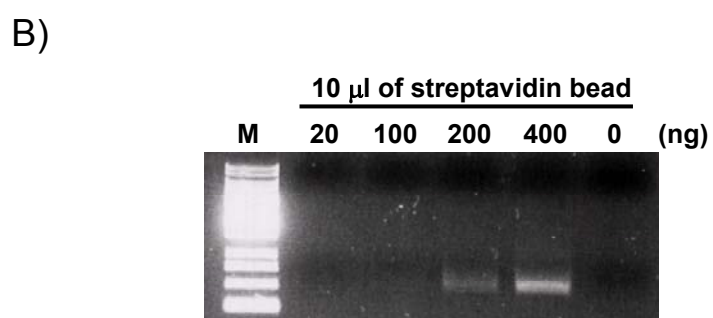
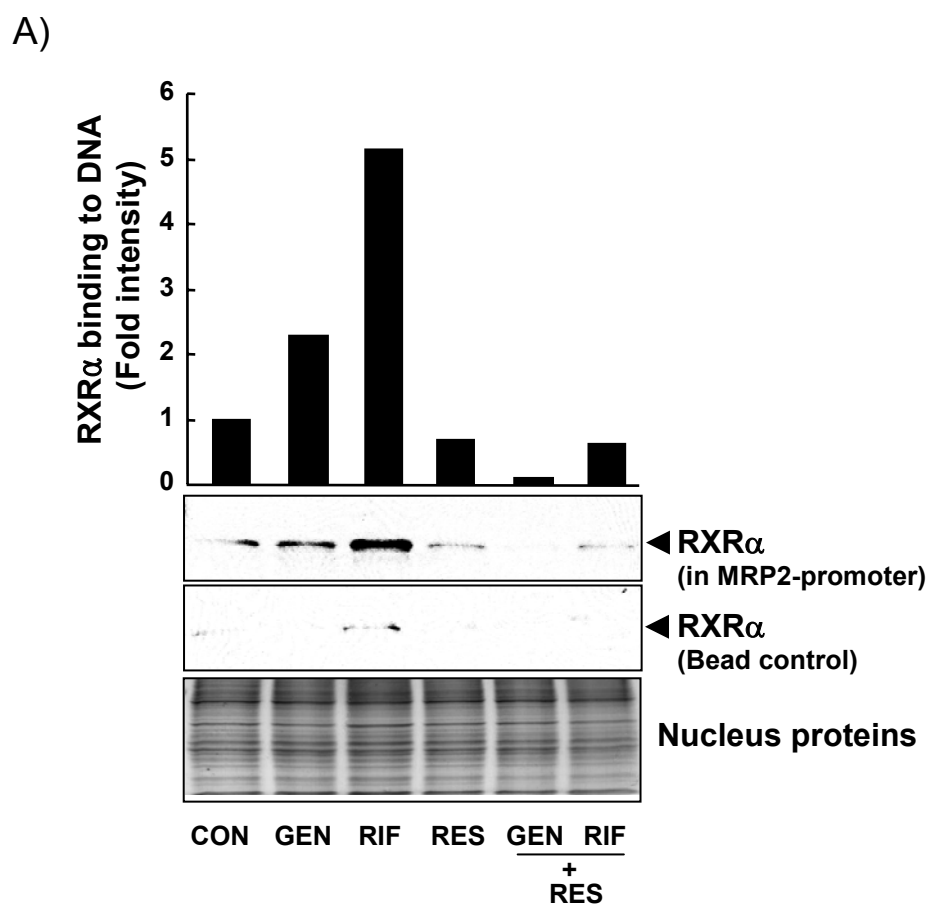


Fig. 3-7. Resveratrol suppresses RXR α binding in the MRP2 promoter.

A) HepG2-C3 cells were cultured in 100 mm dishes at 80% confluency and treated with genistein (50 μ M), resveratrol (50 μ M), and rifampicin (10 μ M) by

different combinations for 24 h. The nuclear proteins were extracted using NE-PER kit (Pierce). One hundred micrograms of nuclear samples were incubated with streptavidin beads (conjugated with biotinylated MRP2 promoter) for 24 h at 4°C. Samples were then washed and subjected to Western blot analysis against RXR α using anti-RXR α (N197) antibody. Nucleus fractions were run on SDS-PAGE gel for equal input for the reactions. CON, 0.2% DMSO; GEN, genistein; RIF, rifampicin; RES, resveratrol. B) To check whether biotinylated MRP2 promoter could conjugate with streptavidin on beads, various amounts of biotinylated PCR Product was incubated with 10 μ l (50% slurry) of streptavidin beads for 24 h at 4°C. Then reaction mixtures were washed with PBS and digested with BglII restriction Enzyme and followed by DNA electrophoresis. The size of digested DNA is 460 bp from the 3' of MRP2 promoter. M, 1 kb ladder marker (Fermentas).

References

1. Aggarwal, B. B., and S. Shishodia. 2006. Molecular targets of dietary agents for prevention and therapy of cancer. *Biochem Pharmacol* 71:1397-421.
2. Akiyama, T., J. Ishida, S. Nakagawa, H. Ogawara, S. Watanabe, N. Itoh, M. Shibuya, and Y. Fukami. 1987. Genistein, a specific inhibitor of tyrosine-specific protein kinases. *J Biol Chem* 262:5592-5.
3. Alam, J., D. Stewart, C. Touchard, S. Boinapally, A. M. Choi, and J. L. Cook. 1999. Nrf2, a Cap'n'Collar transcription factor, regulates induction of the heme oxygenase-1 gene. *J Biol Chem* 274:26071-8.
4. Anzick, S. L., J. Kononen, R. L. Walker, D. O. Azorsa, M. M. Tanner, X. Y. Guan, G. Sauter, O. P. Kallioniemi, J. M. Trent, and P. S. Meltzer. 1997. AIB1, a steroid receptor coactivator amplified in breast and ovarian cancer. *Science* 277:965-8.
5. Arimura, A., M. vn Peer, A. J. Schroder, and P. B. Rothman. 2004. The transcriptional co-activator p/CIP (NCoA-3) is up-regulated by STAT6 and serves as a positive regulator of transcriptional activation by STAT6. *J Biol Chem* 279:31105-12.
6. Balogun, E., M. Hoque, P. Gong, E. Killeen, C. J. Green, R. Foresti, J. Alam, and R. Motterlini. 2003. Curcumin activates the haem oxygenase-1 gene via regulation of Nrf2 and the antioxidant-responsive element. *Biochem J* 371:887-95.
7. Berridge, M. J., P. Lipp, and M. D. Bootman. 2000. The versatility and universality of calcium signalling. *Nat Rev Mol Cell Biol* 1:11-21.
8. Blank, V. 2008. Small Maf proteins in mammalian gene control: mere dimerization partners or dynamic transcriptional regulators? *J Mol Biol* 376:913-25.
9. Bloom, D. A., and A. K. Jaiswal. 2003. Phosphorylation of Nrf2 at Ser40 by protein kinase C in response to antioxidants leads to the release of Nrf2 from INrf2, but is not required for Nrf2 stabilization/accumulation in the nucleus and transcriptional activation of antioxidant response element-mediated NAD(P)H:quinone oxidoreductase-1 gene expression. *J Biol Chem* 278:44675-82.
10. Blumberg, B., W. Sabbagh, Jr., H. Juguilon, J. Bolado, Jr., C. M. van Meter, E. S. Ong, and R. M. Evans. 1998. SXR, a novel steroid and xenobiotic-sensing nuclear receptor. *Genes Dev* 12:3195-205.
11. Briggs, M. W., and D. B. Sacks. 2003. IQGAP1 as signal integrator: Ca²⁺, calmodulin, Cdc42 and the cytoskeleton. *FEBS Lett* 542:7-11.
12. Brill, S., S. Li, C. W. Lyman, D. M. Church, J. J. Wasmuth, L. Weissbach, A. Bernards, and A. J. Snijders. 1996. The Ras GTPase-activating-protein-related human protein IQGAP2 harbors a potential actin binding domain and interacts with calmodulin and Rho family GTPases. *Mol Cell Biol* 16:4869-78.
13. Buchler, M., J. Konig, M. Brom, J. Kartenbeck, H. Spring, T. Horie, and D. Keppler. 1996. cDNA cloning of the hepatocyte canalicular isoform of the multidrug resistance protein, cMrp, reveals a novel conjugate export pump deficient in hyperbilirubinemic mutant rats. *J Biol Chem* 271:15091-8.
14. Cantz, T., A. T. Nies, M. Brom, A. F. Hofmann, and D. Keppler. 2000. MRP2, a human conjugate export pump, is present and transports fluo 3 into apical vacuoles of Hep G2 cells. *Am J Physiol Gastrointest Liver Physiol* 278:G522-31.

15. Chan, K., X. D. Han, and Y. W. Kan. 2001. An important function of Nrf2 in combating oxidative stress: detoxification of acetaminophen. *Proc Natl Acad Sci U S A* 98:4611-6.
16. Chan, K., and Y. W. Kan. 1999. Nrf2 is essential for protection against acute pulmonary injury in mice. *Proc Natl Acad Sci U S A* 96:12731-6.
17. Chen, C., and A. N. Kong. 2004. Dietary chemopreventive compounds and ARE/EpRE signaling. *Free Radic Biol Med* 36:1505-16.
18. Chen, C., D. Pung, V. Leong, V. Hebbar, G. Shen, S. Nair, W. Li, and A. N. Kong. 2004. Induction of detoxifying enzymes by garlic organosulfur compounds through transcription factor Nrf2: effect of chemical structure and stress signals. *Free Radic Biol Med* 37:1578-90.
19. Chen, D., H. Ma, H. Hong, S. S. Koh, S. M. Huang, B. T. Schurter, D. W. Aswad, and M. R. Stallcup. 1999. Regulation of transcription by a protein methyltransferase. *Science* 284:2174-7.
20. Chen, D., L. G. Xu, L. Chen, L. Li, Z. Zhai, and H. B. Shu. 2003. NIK is a component of the EGF/heregulin receptor signaling complexes. *Oncogene* 22:4348-55.
21. Chen, H., R. J. Lin, R. L. Schiltz, D. Chakravarti, A. Nash, L. Nagy, M. L. Privalsky, Y. Nakatani, and R. M. Evans. 1997. Nuclear receptor coactivator ACTR is a novel histone acetyltransferase and forms a multimeric activation complex with P/CAF and CBP/p300. *Cell* 90:569-80.
22. Chen, Y. R., J. Han, R. Kori, A. N. Kong, and T. H. Tan. 2002. Phenylethyl isothiocyanate induces apoptotic signaling via suppressing phosphatase activity against c-Jun N-terminal kinase. *J Biol Chem* 277:39334-42.
23. Chiao, J. W., F. L. Chung, R. Kancherla, T. Ahmed, A. Mittelman, and C. C. Conaway. 2002. Sulforaphane and its metabolite mediate growth arrest and apoptosis in human prostate cancer cells. *Int J Oncol* 20:631-6.
24. Chin, D., and A. R. Means. 2000. Calmodulin: a prototypical calcium sensor. *Trends Cell Biol* 10:322-8.
25. Chott, A., Z. Sun, D. Morganstern, J. Pan, T. Li, M. Susani, I. Mosberger, M. P. Upton, G. J. Bubley, and S. P. Balk. 1999. Tyrosine kinases expressed in vivo by human prostate cancer bone marrow metastases and loss of the type 1 insulin-like growth factor receptor. *Am J Pathol* 155:1271-9.
26. Cohen, J. H., A. R. Kristal, and J. L. Stanford. 2000. Fruit and vegetable intakes and prostate cancer risk. *J Natl Cancer Inst* 92:61-8.
27. Cole, S. P., G. Bhardwaj, J. H. Gerlach, J. E. Mackie, C. E. Grant, K. C. Almquist, A. J. Stewart, E. U. Kurz, A. M. Duncan, and R. G. Deeley. 1992. Overexpression of a transporter gene in a multidrug-resistant human lung cancer cell line. *Science* 258:1650-4.
28. Cope, G. A., and R. J. Deshaies. 2003. COP9 signalosome: a multifunctional regulator of SCF and other cullin-based ubiquitin ligases. *Cell* 114:663-71.
29. Cui, Y., J. Konig, J. K. Buchholz, H. Spring, I. Leier, and D. Keppler. 1999. Drug resistance and ATP-dependent conjugate transport mediated by the apical multidrug resistance protein, MRP2, permanently expressed in human and canine cells. *Mol Pharmacol* 55:929-37.
30. Cullinan, S. B., J. D. Gordan, J. Jin, J. W. Harper, and J. A. Diehl. 2004. The

- Keap1-BTB protein is an adaptor that bridges Nrf2 to a Cul3-based E3 ligase: oxidative stress sensing by a Cul3-Keap1 ligase. *Mol Cell Biol* 24:8477-86.
31. Datta, S. R., A. Brunet, and M. E. Greenberg. 1999. Cellular survival: a play in three Akts. *Genes Dev* 13:2905-27.
 32. Davies, P., C. L. Eaton, T. D. France, and M. E. Phillips. 1988. Growth factor receptors and oncogene expression in prostate cells. *Am J Clin Oncol* 11 Suppl 2:S1-7.
 33. Dinkova-Kostova, A. T., W. D. Holtzclaw, R. N. Cole, K. Itoh, N. Wakabayashi, Y. Katoh, M. Yamamoto, and P. Talalay. 2002. Direct evidence that sulfhydryl groups of Keap1 are the sensors regulating induction of phase 2 enzymes that protect against carcinogens and oxidants. *Proc Natl Acad Sci U S A* 99:11908-13.
 34. Donnelly, L. E., R. Newton, G. E. Kennedy, P. S. Fenwick, R. H. Leung, K. Ito, R. E. Russell, and P. J. Barnes. 2004. Anti-inflammatory effects of resveratrol in lung epithelial cells: molecular mechanisms. *Am J Physiol Lung Cell Mol Physiol* 287:L774-83.
 35. Dorai, T., J. P. Dutcher, D. W. Dempster, and P. H. Wiernik. 2004. Therapeutic potential of curcumin in prostate cancer--V: Interference with the osteomimetic properties of hormone refractory C4-2B prostate cancer cells. *Prostate* 60:1-17.
 36. Dorai, T., N. Gehani, and A. Katz. 2000. Therapeutic potential of curcumin in human prostate cancer. II. Curcumin inhibits tyrosine kinase activity of epidermal growth factor receptor and depletes the protein. *Mol Urol* 4:1-6.
 37. Eggler, A. L., Y. Luo, R. B. van Breemen, and A. D. Mesecar. 2007. Identification of the highly reactive cysteine 151 in the chemopreventive agent-sensor Keap1 protein is method-dependent. *Chem Res Toxicol* 20:1878-84.
 38. Enomoto, A., K. Itoh, E. Nagayoshi, J. Haruta, T. Kimura, T. O'Connor, T. Harada, and M. Yamamoto. 2001. High sensitivity of Nrf2 knockout mice to acetaminophen hepatotoxicity associated with decreased expression of ARE-regulated drug metabolizing enzymes and antioxidant genes. *Toxicol Sci* 59:169-77.
 39. Evers, R., G. J. Zaman, L. van Deemter, H. Jansen, J. Calafat, L. C. Oomen, R. P. Oude Elferink, P. Borst, and A. H. Schinkel. 1996. Basolateral localization and export activity of the human multidrug resistance-associated protein in polarized pig kidney cells. *J Clin Invest* 97:1211-8.
 40. Festuccia, C., G. L. Gravina, A. Angelucci, D. Millimaggi, P. Muzi, C. Vicentini, and M. Bologna. 2005. Additive antitumor effects of the epidermal growth factor receptor tyrosine kinase inhibitor, gefitinib (Iressa), and the nonsteroidal antiandrogen, bicalutamide (Casodex), in prostate cancer cells in vitro. *Int J Cancer* 115:630-40.
 41. Fromm, M. F., H. M. Kauffmann, P. Fritz, O. Burk, H. K. Kroemer, R. W. Warzok, M. Eichelbaum, W. Siegmund, and D. Schrenk. 2000. The effect of rifampin treatment on intestinal expression of human MRP transporters. *Am J Pathol* 157:1575-80.
 42. Fukata, M., S. Kuroda, K. Fujii, T. Nakamura, I. Shoji, Y. Matsuura, K. Okawa, A. Iwamatsu, A. Kikuchi, and K. Kaibuchi. 1997. Regulation of cross-linking of actin filament by IQGAP1, a target for Cdc42. *J Biol Chem* 272:29579-83.
 43. Fukata, M., T. Watanabe, J. Noritake, M. Nakagawa, M. Yamaga, S. Kuroda, Y.

- Matsuura, A. Iwamatsu, F. Perez, and K. Kaibuchi. 2002. Rac1 and Cdc42 capture microtubules through IQGAP1 and CLIP-170. *Cell* 109:873-85.
44. Furukawa, M., and Y. Xiong. 2005. BTB protein Keap1 targets antioxidant transcription factor Nrf2 for ubiquitination by the Cullin 3-Roc1 ligase. *Mol Cell Biol* 25:162-71.
 45. Gnanapragasam, V. J., H. Y. Leung, A. S. Pulimood, D. E. Neal, and C. N. Robson. 2001. Expression of RAC 3, a steroid hormone receptor co-activator in prostate cancer. *Br J Cancer* 85:1928-36.
 46. Goodwin, B., E. Hodgson, and C. Liddle. 1999. The orphan human pregnane X receptor mediates the transcriptional activation of CYP3A4 by rifampicin through a distal enhancer module. *Mol Pharmacol* 56:1329-39.
 47. Gusman, J., H. Malonne, and G. Atassi. 2001. A reappraisal of the potential chemopreventive and chemotherapeutic properties of resveratrol. *Carcinogenesis* 22:1111-7.
 48. Habib, A. A., S. Chatterjee, S. K. Park, R. R. Ratan, S. Lefebvre, and T. Vartanian. 2001. The epidermal growth factor receptor engages receptor interacting protein and nuclear factor-kappa B (NF-kappa B)-inducing kinase to activate NF-kappa B. Identification of a novel receptor-tyrosine kinase signalosome. *J Biol Chem* 276:8865-74.
 49. Han, S. J., F. J. DeMayo, J. Xu, S. Y. Tsai, M. J. Tsai, and B. W. O'Malley. 2006. Steroid receptor coactivator (SRC)-1 and SRC-3 differentially modulate tissue-specific activation functions of the progesterone receptor. *Mol Endocrinol* 20:45-55.
 50. Hanet, N., A. Lancon, D. Delmas, B. Jannin, M. C. Chagnon, M. Cherkaoui-Malki, N. Latruffe, Y. Artur, and J. M. Heydel. 2008. Effects of endocrine disruptors on genes associated with 17beta-estradiol metabolism and excretion. *Steroids* 73:1242-51.
 51. Hart, M. J., M. G. Callow, B. Souza, and P. Polakis. 1996. IQGAP1, a calmodulin-binding protein with a rasGAP-related domain, is a potential effector for cdc42Hs. *Embo J* 15:2997-3005.
 52. Hayashi, A., H. Suzuki, K. Itoh, M. Yamamoto, and Y. Sugiyama. 2003. Transcription factor Nrf2 is required for the constitutive and inducible expression of multidrug resistance-associated protein 1 in mouse embryo fibroblasts. *Biochem Biophys Res Commun* 310:824-9.
 53. Hayes, J. D., S. A. Chanas, C. J. Henderson, M. McMahon, C. Sun, G. J. Moffat, C. R. Wolf, and M. Yamamoto. 2000. The Nrf2 transcription factor contributes both to the basal expression of glutathione S-transferases in mouse liver and to their induction by the chemopreventive synthetic antioxidants, butylated hydroxyanisole and ethoxyquin. *Biochem Soc Trans* 28:33-41.
 54. Heery, D. M., E. Kalkhoven, S. Hoare, and M. G. Parker. 1997. A signature motif in transcriptional co-activators mediates binding to nuclear receptors. *Nature* 387:733-6.
 55. Henke, R. T., B. R. Haddad, S. E. Kim, J. D. Rone, A. Mani, J. M. Jessup, A. Wellstein, A. Maitra, and A. T. Riegel. 2004. Overexpression of the nuclear receptor coactivator AIB1 (SRC-3) during progression of pancreatic adenocarcinoma. *Clin Cancer Res* 10:6134-42.

56. Hill, M. M., and B. A. Hemmings. 2002. Inhibition of protein kinase B/Akt. implications for cancer therapy. *Pharmacol Ther* 93:243-51.
57. Ho, Y. D., J. L. Joyal, Z. Li, and D. B. Sacks. 1999. IQGAP1 integrates Ca^{2+} /calmodulin and Cdc42 signaling. *J Biol Chem* 274:464-70.
58. Hochstrasser, M. 1996. Ubiquitin-dependent protein degradation. *Annu Rev Genet* 30:405-39.
59. Hooijberg, J. H., H. J. Broxterman, M. Kool, Y. G. Assaraf, G. J. Peters, P. Noordhuis, R. J. Scheper, P. Borst, H. M. Pinedo, and G. Jansen. 1999. Antifolate resistance mediated by the multidrug resistance proteins MRP1 and MRP2. *Cancer Res* 59:2532-5.
60. Howe, C. J., M. M. LaHair, J. A. Maxwell, J. T. Lee, P. J. Robinson, O. Rodriguez-Mora, J. A. McCubrey, and R. A. Franklin. 2002. Participation of the calcium/calmodulin-dependent kinases in hydrogen peroxide-induced Ikappa B phosphorylation in human T lymphocytes. *J Biol Chem* 277:30469-76.
61. Huang, H. C., T. Nguyen, and C. B. Pickett. 2002. Phosphorylation of Nrf2 at Ser-40 by protein kinase C regulates antioxidant response element-mediated transcription. *J Biol Chem* 277:42769-74.
62. Huang, S. M., J. Li, and P. M. Harari. 2002. Molecular inhibition of angiogenesis and metastatic potential in human squamous cell carcinomas after epidermal growth factor receptor blockade. *Mol Cancer Ther* 1:507-14.
63. Itoh, K., T. Chiba, S. Takahashi, T. Ishii, K. Igarashi, Y. Katoh, T. Oyake, N. Hayashi, K. Satoh, I. Hatayama, M. Yamamoto, and Y. Nabeshima. 1997. An Nrf2/small Maf heterodimer mediates the induction of phase II detoxifying enzyme genes through antioxidant response elements. *Biochem Biophys Res Commun* 236:313-22.
64. Itoh, K., N. Wakabayashi, Y. Katoh, T. Ishii, K. Igarashi, J. D. Engel, and M. Yamamoto. 1999. Keap1 represses nuclear activation of antioxidant responsive elements by Nrf2 through binding to the amino-terminal Neh2 domain. *Genes Dev* 13:76-86.
65. Jager, W., O. Winter, B. Halper, A. Salamon, M. Sartori, L. Gajdzik, G. Hamilton, G. Theyer, J. Graf, and T. Thalhammer. 1997. Modulation of liver canalicular transport processes by the tyrosine-kinase inhibitor genistein: implications of genistein metabolism in the rat. *Hepatology* 26:1467-76.
66. Jain, A. K., D. A. Bloom, and A. K. Jaiswal. 2005. Nuclear import and export signals in control of Nrf2. *J Biol Chem* 280:29158-68.
67. Jang, M., L. Cai, G. O. Udeani, K. V. Slowing, C. F. Thomas, C. W. Beecher, H. H. Fong, N. R. Farnsworth, A. D. Kinghorn, R. G. Mehta, R. C. Moon, and J. M. Pezzuto. 1997. Cancer chemopreventive activity of resveratrol, a natural product derived from grapes. *Science* 275:218-20.
68. Jemal, A., R. Siegel, E. Ward, T. Murray, J. Xu, and M. J. Thun. 2007. Cancer statistics, 2007. *CA Cancer J Clin* 57:43-66.
69. Joyal, J. L., R. S. Annan, Y. D. Ho, M. E. Huddleston, S. A. Carr, M. J. Hart, and D. B. Sacks. 1997. Calmodulin modulates the interaction between IQGAP1 and Cdc42. Identification of IQGAP1 by nanoelectrospray tandem mass spectrometry. *J Biol Chem* 272:15419-25.
70. Jurma, O. P., D. G. Hom, and J. K. Andersen. 1997. Decreased glutathione results

- in calcium-mediated cell death in PC12. *Free Radic Biol Med* 23:1055-66.
71. Kang, M. I., A. Kobayashi, N. Wakabayashi, S. G. Kim, and M. Yamamoto. 2004. Scaffolding of Keap1 to the actin cytoskeleton controls the function of Nrf2 as key regulator of cytoprotective phase 2 genes. *Proc Natl Acad Sci U S A* 101:2046-51.
 72. Kast, H. R., B. Goodwin, P. T. Tarr, S. A. Jones, A. M. Anisfeld, C. M. Stoltz, P. Tontonoz, S. Kliewer, T. M. Willson, and P. A. Edwards. 2002. Regulation of multidrug resistance-associated protein 2 (ABCC2) by the nuclear receptors pregnane X receptor, farnesoid X-activated receptor, and constitutive androstane receptor. *J Biol Chem* 277:2908-15.
 73. Katoh, Y., K. Itoh, E. Yoshida, M. Miyagishi, A. Fukamizu, and M. Yamamoto. 2001. Two domains of Nrf2 cooperatively bind CBP, a CREB binding protein, and synergistically activate transcription. *Genes Cells* 6:857-68.
 74. Kawabe, T., Z. S. Chen, M. Wada, T. Uchiumi, M. Ono, S. Akiyama, and M. Kuwano. 1999. Enhanced transport of anticancer agents and leukotriene C4 by the human canalicular multispecific organic anion transporter (cMOAT/MRP2). *FEBS Lett* 456:327-31.
 75. Kawada, N., S. Seki, M. Inoue, and T. Kuroki. 1998. Effect of antioxidants, resveratrol, quercetin, and N-acetylcysteine, on the functions of cultured rat hepatic stellate cells and Kupffer cells. *Hepatology* 27:1265-74.
 76. Keppler, D., and J. Kartenbeck. 1996. The canalicular conjugate export pump encoded by the cmrp/cmoat gene. *Prog Liver Dis* 14:55-67.
 77. Keppler, D., and J. Konig. 2000. Hepatic secretion of conjugated drugs and endogenous substances. *Semin Liver Dis* 20:265-72.
 78. Keum, Y. S., S. Yu, P. P. Chang, X. Yuan, J. H. Kim, C. Xu, J. Han, A. Agarwal, and A. N. Kong. 2006. Mechanism of action of sulforaphane: inhibition of p38 mitogen-activated protein kinase isoforms contributing to the induction of antioxidant response element-mediated heme oxygenase-1 in human hepatoma HepG2 cells. *Cancer Res* 66:8804-13.
 79. Kiuchi, Y., H. Suzuki, T. Hirohashi, C. A. Tyson, and Y. Sugiyama. 1998. cDNA cloning and inducible expression of human multidrug resistance associated protein 3 (MRP3). *FEBS Lett* 433:149-52.
 80. Kliewer, S. A., J. T. Moore, L. Wade, J. L. Staudinger, M. A. Watson, S. A. Jones, D. D. McKee, B. B. Oliver, T. M. Willson, R. H. Zetterstrom, T. Perlmann, and J. M. Lehmann. 1998. An orphan nuclear receptor activated by pregnanes defines a novel steroid signaling pathway. *Cell* 92:73-82.
 81. Kobayashi, A., M. I. Kang, H. Okawa, M. Ohtsuji, Y. Zenke, T. Chiba, K. Igarashi, and M. Yamamoto. 2004. Oxidative stress sensor Keap1 functions as an adaptor for Cul3-based E3 ligase to regulate proteasomal degradation of Nrf2. *Mol Cell Biol* 24:7130-9.
 82. Kobayashi, M., K. Itoh, T. Suzuki, H. Osanai, K. Nishikawa, Y. Katoh, Y. Takagi, and M. Yamamoto. 2002. Identification of the interactive interface and phylogenetic conservation of the Nrf2-Keap1 system. *Genes Cells* 7:807-20.
 83. Kobayashi, M., and M. Yamamoto. 2005. Molecular mechanisms activating the Nrf2-Keap1 pathway of antioxidant gene regulation. *Antioxid Redox Signal* 7:385-94.

84. Koh, S. S., D. Chen, Y. H. Lee, and M. R. Stallcup. 2001. Synergistic enhancement of nuclear receptor function by p160 coactivators and two coactivators with protein methyltransferase activities. *J Biol Chem* 276:1089-98.
85. Koike, K., T. Kawabe, T. Tanaka, S. Toh, T. Uchiumi, M. Wada, S. Akiyama, M. Ono, and M. Kuwano. 1997. A canalicular multispecific organic anion transporter (cMOAT) antisense cDNA enhances drug sensitivity in human hepatic cancer cells. *Cancer Res* 57:5475-9.
86. Kolonel, L. N., J. H. Hankin, A. S. Whittemore, A. H. Wu, R. P. Gallagher, L. R. Wilkens, E. M. John, G. R. Howe, D. M. Dreon, D. W. West, and R. S. Paffenbarger, Jr. 2000. Vegetables, fruits, legumes and prostate cancer: a multiethnic case-control study. *Cancer Epidemiol Biomarkers Prev* 9:795-804.
87. Kong, A. N., E. Owuor, R. Yu, V. Hebbar, C. Chen, R. Hu, and S. Mandlekar. 2001. Induction of xenobiotic enzymes by the MAP kinase pathway and the antioxidant or electrophile response element (ARE/EpRE). *Drug Metab Rev* 33:255-71.
88. Konig, J., D. Rost, Y. Cui, and D. Keppler. 1999. Characterization of the human multidrug resistance protein isoform MRP3 localized to the basolateral hepatocyte membrane. *Hepatology* 29:1156-63.
89. Kool, M., M. van der Linden, M. de Haas, G. L. Scheffer, J. M. de Vree, A. J. Smith, G. Jansen, G. J. Peters, N. Ponne, R. J. Scheper, R. P. Elferink, F. Baas, and P. Borst. 1999. MRP3, an organic anion transporter able to transport anti-cancer drugs. *Proc Natl Acad Sci U S A* 96:6914-9.
90. Kreis, W. 1995. Current chemotherapy and future directions in research for the treatment of advanced hormone-refractory prostate cancer. *Cancer Invest* 13:296-312.
91. Kuang, S. Q., L. Liao, H. Zhang, A. V. Lee, B. W. O'Malley, and J. Xu. 2004. AIB1/SRC-3 deficiency affects insulin-like growth factor I signaling pathway and suppresses v-Ha-ras-induced breast cancer initiation and progression in mice. *Cancer Res* 64:1875-85.
92. Kubitz, R., C. Huth, M. Schmitt, A. Horbach, G. Kullak-Ublick, and D. Haussinger. 2001. Protein kinase C-dependent distribution of the multidrug resistance protein 2 from the canalicular to the basolateral membrane in human HepG2 cells. *Hepatology* 34:340-50.
93. Kuroda, S., M. Fukata, M. Nakagawa, K. Fujii, T. Nakamura, T. Ookubo, I. Izawa, T. Nagase, N. Nomura, H. Tani, I. Shoji, Y. Matsuura, S. Yonehara, and K. Kaibuchi. 1998. Role of IQGAP1, a target of the small GTPases Cdc42 and Rac1, in regulation of E-cadherin-mediated cell-cell adhesion. *Science* 281:832-5.
94. Lau, A., N. F. Villeneuve, Z. Sun, P. K. Wong, and D. D. Zhang. 2008. Dual roles of Nrf2 in cancer. *Pharmacol Res* 58:262-70.
95. Lee, J. M., M. J. Calkins, K. Chan, Y. W. Kan, and J. A. Johnson. 2003. Identification of the NF-E2-related factor-2-dependent genes conferring protection against oxidative stress in primary cortical astrocytes using oligonucleotide microarray analysis. *J Biol Chem* 278:12029-38.
96. Lee, J. M., K. Chan, Y. W. Kan, and J. A. Johnson. 2004. Targeted disruption of Nrf2 causes regenerative immune-mediated hemolytic anemia. *Proc Natl Acad Sci U S A* 101:9751-6.

97. Lee, J. M., A. Y. Shih, T. H. Murphy, and J. A. Johnson. 2003. NF-E2-related factor-2 mediates neuroprotection against mitochondrial complex I inhibitors and increased concentrations of intracellular calcium in primary cortical neurons. *J Biol Chem* 278:37948-56.
98. Lee, J. S., and Y. J. Surh. 2005. Nrf2 as a novel molecular target for chemoprevention. *Cancer Lett* 224:171-84.
99. Lee, S. K., H. J. Kim, S. Y. Na, T. S. Kim, H. S. Choi, S. Y. Im, and J. W. Lee. 1998. Steroid receptor coactivator-1 coactivates activating protein-1-mediated transactivations through interaction with the c-Jun and c-Fos subunits. *J Biol Chem* 273:16651-4.
100. Leo, C., and J. D. Chen. 2000. The SRC family of nuclear receptor coactivators. *Gene* 245:1-11.
101. Leu, T. H., S. L. Su, Y. C. Chuang, and M. C. Maa. 2003. Direct inhibitory effect of curcumin on Src and focal adhesion kinase activity. *Biochem Pharmacol* 66:2323-31.
102. Levonen, A. L., A. Landar, A. Ramachandran, E. K. Ceaser, D. A. Dickinson, G. Zanoni, J. D. Morrow, and V. M. Darley-Usmar. 2004. Cellular mechanisms of redox cell signalling: role of cysteine modification in controlling antioxidant defences in response to electrophilic lipid oxidation products. *Biochem J* 378:373-82.
103. Li, C., R. C. Wu, L. Amazit, S. Y. Tsai, M. J. Tsai, and B. W. O'Malley. 2007. Specific amino acid residues in the basic helix-loop-helix domain of SRC-3 are essential for its nuclear localization and proteasome-dependent turnover. *Mol Cell Biol* 27:1296-308.
104. Li, Y., and A. K. Jaiswal. 1993. Regulation of human NAD(P)H:quinone oxidoreductase gene. Role of AP1 binding site contained within human antioxidant response element. *J Biol Chem* 268:21454.
105. Li, Y., and F. H. Sarkar. 2002. Inhibition of nuclear factor kappaB activation in PC3 cells by genistein is mediated via Akt signaling pathway. *Clin Cancer Res* 8:2369-77.
106. Li, Y., Y. G. Shin, C. Yu, J. W. Kosmeder, W. H. Hirschelman, J. M. Pezzuto, and R. B. van Breemen. 2003. Increasing the throughput and productivity of Caco-2 cell permeability assays using liquid chromatography-mass spectrometry: application to resveratrol absorption and metabolism. *Comb Chem High Throughput Screen* 6:757-67.
107. Li, Z., and D. B. Sacks. 2003. Elucidation of the interaction of calmodulin with the IQ motifs of IQGAP1. *J Biol Chem* 278:4347-52.
108. Lin, W., G. Shen, X. Yuan, M. R. Jain, S. Yu, A. Zhang, J. D. Chen, and A. N. Kong. 2006. Regulation of Nrf2 transactivation domain activity by p160 RAC3/SRC3 and other nuclear co-regulators. *J Biochem Mol Biol* 39:304-10.
109. Liu, D., L. L. Homan, and J. S. Dillon. 2004. Genistein acutely stimulates nitric oxide synthesis in vascular endothelial cells by a cyclic adenosine 5'-monophosphate-dependent mechanism. *Endocrinology* 145:5532-9.
110. Luo, Y., A. L. Eggler, D. Liu, G. Liu, A. D. Mesecar, and R. B. van Breemen. 2007. Sites of alkylation of human Keap1 by natural chemoprevention agents. *J Am Soc Mass Spectrom* 18:2226-32.

111. Maier-Salamon, A., B. Hagenauer, G. Reznicek, T. Szekeres, T. Thalhammer, and W. Jager. 2008. Metabolism and disposition of resveratrol in the isolated perfused rat liver: role of Mrp2 in the biliary excretion of glucuronides. *J Pharm Sci* 97:1615-28.
112. Manna, S. K., A. Mukhopadhyay, and B. B. Aggarwal. 2000. Resveratrol suppresses TNF-induced activation of nuclear transcription factors NF-kappa B, activator protein-1, and apoptosis: potential role of reactive oxygen intermediates and lipid peroxidation. *J Immunol* 164:6509-19.
113. Mateer, S. C., A. E. McDaniel, V. Nicolas, G. M. Habermacher, M. J. Lin, D. A. Cromer, M. E. King, and G. S. Bloom. 2002. The mechanism for regulation of the F-actin binding activity of IQGAP1 by calcium/calmodulin. *J Biol Chem* 277:12324-33.
114. Mayer, R., J. Kartenbeck, M. Buchler, G. Jedlitschky, I. Leier, and D. Keppler. 1995. Expression of the MRP gene-encoded conjugate export pump in liver and its selective absence from the canalicular membrane in transport-deficient mutant hepatocytes. *J Cell Biol* 131:137-50.
115. Mbele, G. O., J. C. Deloulme, B. J. Gentil, C. Delphin, M. Ferro, J. Garin, M. Takahashi, and J. Baudier. 2002. The zinc- and calcium-binding S100B interacts and co-localizes with IQGAP1 during dynamic rearrangement of cell membranes. *J Biol Chem* 277:49998-50007.
116. McCallum, S. J., W. J. Wu, and R. A. Cerione. 1996. Identification of a putative effector for Cdc42Hs with high sequence similarity to the RasGAP-related protein IQGAP1 and a Cdc42Hs binding partner with similarity to IQGAP2. *J Biol Chem* 271:21732-7.
117. McKenna, N. J., R. B. Lanz, and B. W. O'Malley. 1999. Nuclear receptor coregulators: cellular and molecular biology. *Endocr Rev* 20:321-44.
118. McKenna, N. J., and B. W. O'Malley. 2002. Combinatorial control of gene expression by nuclear receptors and coregulators. *Cell* 108:465-74.
119. McMahon, M., K. Itoh, M. Yamamoto, S. A. Chanas, C. J. Henderson, L. I. McLellan, C. R. Wolf, C. Cavin, and J. D. Hayes. 2001. The Cap'n'Collar basic leucine zipper transcription factor Nrf2 (NF-E2 p45-related factor 2) controls both constitutive and inducible expression of intestinal detoxification and glutathione biosynthetic enzymes. *Cancer Res* 61:3299-307.
120. McMahon, M., N. Thomas, K. Itoh, M. Yamamoto, and J. D. Hayes. 2004. Redox-regulated turnover of Nrf2 is determined by at least two separate protein domains, the redox-sensitive Neh2 degron and the redox-insensitive Neh6 degron. *J Biol Chem* 279:31556-67.
121. Meijerman, I., J. H. Beijnen, and J. H. Schellens. 2008. Combined action and regulation of phase II enzymes and multidrug resistance proteins in multidrug resistance in cancer. *Cancer Treat Rev*.
122. Moi, P., K. Chan, I. Asunis, A. Cao, and Y. W. Kan. 1994. Isolation of NF-E2-related factor 2 (Nrf2), a NF-E2-like basic leucine zipper transcriptional activator that binds to the tandem NF-E2/AP1 repeat of the beta-globin locus control region. *Proc Natl Acad Sci U S A* 91:9926-30.
123. Morse, M. A., and G. D. Stoner. 1993. Cancer chemoprevention: principles and prospects. *Carcinogenesis* 14:1737-46.

124. Motohashi, H., and M. Yamamoto. 2004. Nrf2-Keap1 defines a physiologically important stress response mechanism. *Trends Mol Med* 10:549-57.
125. Mukhopadhyay, A., C. Bueso-Ramos, D. Chatterjee, P. Pantazis, and B. B. Aggarwal. 2001. Curcumin downregulates cell survival mechanisms in human prostate cancer cell lines. *Oncogene* 20:7597-609.
126. Myzak, M. C., P. A. Karplus, F. L. Chung, and R. H. Dashwood. 2004. A novel mechanism of chemoprotection by sulforaphane: inhibition of histone deacetylase. *Cancer Res* 64:5767-74.
127. Nakaso, K., H. Yano, Y. Fukuhara, T. Takeshima, K. Wada-Isoe, and K. Nakashima. 2003. PI3K is a key molecule in the Nrf2-mediated regulation of antioxidative proteins by hemin in human neuroblastoma cells. *FEBS Lett* 546:181-4.
128. Nguyen, T., P. J. Sherratt, H. C. Huang, C. S. Yang, and C. B. Pickett. 2003. Increased protein stability as a mechanism that enhances Nrf2-mediated transcriptional activation of the antioxidant response element. Degradation of Nrf2 by the 26 S proteasome. *J Biol Chem* 278:4536-41.
129. Nies, A. T., and D. Keppler. 2007. The apical conjugate efflux pump ABCC2 (MRP2). *Pflugers Arch* 453:643-59.
130. Nioi, P., T. Nguyen, P. J. Sherratt, and C. B. Pickett. 2005. The carboxy-terminal Neh3 domain of Nrf2 is required for transcriptional activation. *Mol Cell Biol* 25:10895-906.
131. Parks, D. J., S. G. Blanchard, R. K. Bledsoe, G. Chandra, T. G. Consler, S. A. Kliewer, J. B. Stimmel, T. M. Willson, A. M. Zavacki, D. D. Moore, and J. M. Lehmann. 1999. Bile acids: natural ligands for an orphan nuclear receptor. *Science* 284:1365-8.
132. Paulusma, C. C., P. J. Bosma, G. J. Zaman, C. T. Bakker, M. Otter, G. L. Scheffer, R. J. Scheper, P. Borst, and R. P. Oude Elferink. 1996. Congenital jaundice in rats with a mutation in a multidrug resistance-associated protein gene. *Science* 271:1126-8.
133. Paulusma, C. C., M. Kool, P. J. Bosma, G. L. Scheffer, F. ter Borg, R. J. Scheper, G. N. Tytgat, P. Borst, F. Baas, and R. P. Oude Elferink. 1997. A mutation in the human canalicular multispecific organic anion transporter gene causes the Dubin-Johnson syndrome. *Hepatology* 25:1539-42.
134. Peterson, G., and S. Barnes. 1993. Genistein and biochanin A inhibit the growth of human prostate cancer cells but not epidermal growth factor receptor tyrosine autophosphorylation. *Prostate* 22:335-45.
135. Peterson, G., and S. Barnes. 1996. Genistein inhibits both estrogen and growth factor-stimulated proliferation of human breast cancer cells. *Cell Growth Differ* 7:1345-51.
136. Pickart, C. M. 2001. Mechanisms underlying ubiquitination. *Annu Rev Biochem* 70:503-33.
137. Ramos-Gomez, M., M. K. Kwak, P. M. Dolan, K. Itoh, M. Yamamoto, P. Talalay, and T. W. Kensler. 2001. Sensitivity to carcinogenesis is increased and chemoprotective efficacy of enzyme inducers is lost in nrf2 transcription factor-deficient mice. *Proc Natl Acad Sci U S A* 98:3410-5.
138. Reddy, B. S., J. Nayini, K. Tokumo, J. Rigotty, E. Zang, and G. Kelloff. 1990.

- Chemoprevention of colon carcinogenesis by concurrent administration of piroxicam, a nonsteroidal antiinflammatory drug with D,L-alpha-difluoromethylornithine, an ornithine decarboxylase inhibitor, in diet. *Cancer Res* 50:2562-8.
139. Roelofsen, H., R. Ottenhoff, R. P. Oude Elferink, and P. L. Jansen. 1991. Hepatocanalicular organic-anion transport is regulated by protein kinase C. *Biochem J* 278 (Pt 3):637-41.
 140. Roelofsen, H., T. A. Vos, I. J. Schippers, F. Kuipers, H. Koning, H. Moshage, P. L. Jansen, and M. Muller. 1997. Increased levels of the multidrug resistance protein in lateral membranes of proliferating hepatocyte-derived cells. *Gastroenterology* 112:511-21.
 141. Rost, D., J. Konig, G. Weiss, E. Klar, W. Stremmel, and D. Keppler. 2001. Expression and localization of the multidrug resistance proteins MRP2 and MRP3 in human gallbladder epithelia. *Gastroenterology* 121:1203-8.
 142. Roy, M., Z. Li, and D. B. Sacks. 2004. IQGAP1 binds ERK2 and modulates its activity. *J Biol Chem* 279:17329-37.
 143. Ruiz-Larrea, M. B., A. R. Mohan, G. Paganga, N. J. Miller, G. P. Bolwell, and C. A. Rice-Evans. 1997. Antioxidant activity of phytoestrogenic isoflavones. *Free Radic Res* 26:63-70.
 144. Rushmore, T. H., and C. B. Pickett. 1990. Transcriptional regulation of the rat glutathione S-transferase Ya subunit gene. Characterization of a xenobiotic-responsive element controlling inducible expression by phenolic antioxidants. *J Biol Chem* 265:14648-53.
 145. Saeki, K., N. Kobayashi, Y. Inazawa, H. Zhang, H. Nishitoh, H. Ichijo, M. Isemura, and A. Yuo. 2002. Oxidation-triggered c-Jun N-terminal kinase (JNK) and p38 mitogen-activated protein (MAP) kinase pathways for apoptosis in human leukaemic cells stimulated by epigallocatechin-3-gallate (EGCG): a distinct pathway from those of chemically induced and receptor-mediated apoptosis. *Biochem J* 368:705-20.
 146. Sakakura, C., A. Hagiwara, R. Yasuoka, Y. Fujita, M. Nakanishi, K. Masuda, A. Kimura, Y. Nakamura, J. Inazawa, T. Abe, and H. Yamagishi. 2000. Amplification and over-expression of the AIB1 nuclear receptor co-activator gene in primary gastric cancers. *Int J Cancer* 89:217-23.
 147. Sakamoto, K., L. D. Lawson, and J. A. Milner. 1997. Allyl sulfides from garlic suppress the in vitro proliferation of human A549 lung tumor cells. *Nutr Cancer* 29:152-6.
 148. Sakla, M. S., N. S. Shenouda, P. J. Ansell, R. S. Macdonald, and D. B. Lubahn. 2007. Genistein affects HER2 protein concentration, activation, and promoter regulation in BT-474 human breast cancer cells. *Endocrine* 32:69-78.
 149. Sambrook, J., E. F. Fritsch, and T. Maniatis. 1989. *Molecular Cloning: A Laboratory Manual*, 2nd Ed., pp. 16.66-16.67, Cold Spring Harbor Laboratory, Cold Spring Harbor, NY.
 150. Sandusky, G. E., K. S. Mintze, S. E. Pratt, and A. H. Dantzig. 2002. Expression of multidrug resistance-associated protein 2 (MRP2) in normal human tissues and carcinomas using tissue microarrays. *Histopathology* 41:65-74.
 151. Shelnutt, S. R., C. O. Cimino, P. A. Wiggins, M. J. Ronis, and T. M. Badger. 2002.

- Pharmacokinetics of the glucuronide and sulfate conjugates of genistein and daidzein in men and women after consumption of a soy beverage. *Am J Clin Nutr* 76:588-94.
152. Shen, G., V. Hebbar, S. Nair, C. Xu, W. Li, W. Lin, Y. S. Keum, J. Han, M. A. Gallo, and A. N. Kong. 2004. Regulation of Nrf2 transactivation domain activity. The differential effects of mitogen-activated protein kinase cascades and synergistic stimulatory effect of Raf and CREB-binding protein. *J Biol Chem* 279:23052-60.
 153. Sherwood, E. R., J. L. Van Dongen, C. G. Wood, S. Liao, J. M. Kozlowski, and C. Lee. 1998. Epidermal growth factor receptor activation in androgen-independent but not androgen-stimulated growth of human prostatic carcinoma cells. *Br J Cancer* 77:855-61.
 154. Stockel, B., J. Konig, A. T. Nies, Y. Cui, M. Brom, and D. Keppler. 2000. Characterization of the 5'-flanking region of the human multidrug resistance protein 2 (MRP2) gene and its regulation in comparison with the multidrug resistance protein 3 (MRP3) gene. *Eur J Biochem* 267:1347-58.
 155. St-Pierre, M. V., M. A. Serrano, R. I. Macias, U. Dubs, M. Hoechli, U. Lauper, P. J. Meier, and J. J. Marin. 2000. Expression of members of the multidrug resistance protein family in human term placenta. *Am J Physiol Regul Integr Comp Physiol* 279:R1495-503.
 156. Sueyoshi, T., T. Kawamoto, I. Zelko, P. Honkakoski, and M. Negishi. 1999. The repressed nuclear receptor CAR responds to phenobarbital in activating the human CYP2B6 gene. *J Biol Chem* 274:6043-6.
 157. Suh, J., F. Payvandi, L. C. Edelstein, P. S. Amenta, W. X. Zong, C. Gelinas, and A. B. Rabson. 2002. Mechanisms of constitutive NF-kappaB activation in human prostate cancer cells. *Prostate* 52:183-200.
 158. Suzuki, H., and Y. Sugiyama. 1998. Excretion of GSSG and glutathione conjugates mediated by MRP1 and cMOAT/MRP2. *Semin Liver Dis* 18:359-76.
 159. Takeshita, A., G. R. Cardona, N. Koibuchi, C. S. Suen, and W. W. Chin. 1997. TRAM-1, A novel 160-kDa thyroid hormone receptor activator molecule, exhibits distinct properties from steroid receptor coactivator-1. *J Biol Chem* 272:27629-34.
 160. Teng, D. H., R. Hu, H. Lin, T. Davis, D. Iliev, C. Frye, B. Swedlund, K. L. Hansen, V. L. Vinson, K. L. Gumpfer, L. Ellis, A. El-Naggar, M. Frazier, S. Jasser, L. A. Langford, J. Lee, G. B. Mills, M. A. Pershouse, R. E. Pollack, C. Tornos, P. Troncoso, W. K. Yung, G. Fujii, A. Berson, P. A. Steck, and et al. 1997. MMAC1/PTEN mutations in primary tumor specimens and tumor cell lines. *Cancer Res* 57:5221-5.
 161. Thimmulappa, R. K., K. H. Mai, S. Srisuma, T. W. Kensler, M. Yamamoto, and S. Biswal. 2002. Identification of Nrf2-regulated genes induced by the chemopreventive agent sulforaphane by oligonucleotide microarray. *Cancer Res* 62:5196-203.
 162. Torres-Arzayus, M. I., J. Font de Mora, J. Yuan, F. Vazquez, R. Bronson, M. Rue, W. R. Sellers, and M. Brown. 2004. High tumor incidence and activation of the PI3K/AKT pathway in transgenic mice define AIB1 as an oncogene. *Cancer Cell* 6:263-74.
 163. Trinkle-Mulcahy, L., J. E. Sleeman, and A. I. Lamond. 2001. Dynamic targeting

- of protein phosphatase 1 within the nuclei of living mammalian cells. *J Cell Sci* 114:4219-28.
164. Tsujii, H., J. Konig, D. Rost, B. Stockel, U. Leuschner, and D. Keppler. 1999. Exon-intron organization of the human multidrug-resistance protein 2 (MRP2) gene mutated in Dubin-Johnson syndrome. *Gastroenterology* 117:653-60.
 165. Velichkova, M., and T. Hasson. 2005. Keap1 regulates the oxidation-sensitive shuttling of Nrf2 into and out of the nucleus via a Crm1-dependent nuclear export mechanism. *Mol Cell Biol* 25:4501-13.
 166. Venugopal, R., and A. K. Jaiswal. 1996. Nrf1 and Nrf2 positively and c-Fos and Fra1 negatively regulate the human antioxidant response element-mediated expression of NAD(P)H:quinone oxidoreductase1 gene. *Proc Natl Acad Sci U S A* 93:14960-5.
 167. Vidavalur, R., H. Otani, P. K. Singal, and N. Maulik. 2006. Significance of wine and resveratrol in cardiovascular disease: French paradox revisited. *Exp Clin Cardiol* 11:217-25.
 168. Vollrath, V., A. M. Wielandt, M. Iruretagoyena, and J. Chianale. 2006. Role of Nrf2 in the regulation of the Mrp2 (ABCC2) gene. *Biochem J* 395:599-609.
 169. Wada, M., S. Toh, K. Taniguchi, T. Nakamura, T. Uchiumi, K. Kohno, I. Yoshida, A. Kimura, S. Sakisaka, Y. Adachi, and M. Kuwano. 1998. Mutations in the canalicular multispecific organic anion transporter (cMOAT) gene, a novel ABC transporter, in patients with hyperbilirubinemia II/Dubin-Johnson syndrome. *Hum Mol Genet* 7:203-7.
 170. Wang, Y., M. C. Wu, J. S. Sham, W. Zhang, W. Q. Wu, and X. Y. Guan. 2002. Prognostic significance of c-myc and AIB1 amplification in hepatocellular carcinoma. A broad survey using high-throughput tissue microarray. *Cancer* 95:2346-52.
 171. Wang, Z., D. W. Rose, O. Hermanson, F. Liu, T. Herman, W. Wu, D. Szeto, A. Gleiberman, A. Krones, K. Pratt, R. Rosenfeld, C. K. Glass, and M. G. Rosenfeld. 2000. Regulation of somatic growth by the p160 coactivator p/CIP. *Proc Natl Acad Sci U S A* 97:13549-54.
 172. Wasserman, W. W., and W. E. Fahl. 1997. Functional antioxidant responsive elements. *Proc Natl Acad Sci U S A* 94:5361-6.
 173. Watai, Y., A. Kobayashi, H. Nagase, M. Mizukami, J. McEvoy, J. D. Singer, K. Itoh, and M. Yamamoto. 2007. Subcellular localization and cytoplasmic complex status of endogenous Keap1. *Genes Cells* 12:1163-78.
 174. Weissbach, L., A. Bernards, and D. W. Herion. 1998. Binding of myosin essential light chain to the cytoskeleton-associated protein IQGAP1. *Biochem Biophys Res Commun* 251:269-76.
 175. Weissbach, L., J. Settleman, M. F. Kalady, A. J. Snijders, A. E. Murthy, Y. X. Yan, and A. Bernards. 1994. Identification of a human rasGAP-related protein containing calmodulin-binding motifs. *J Biol Chem* 269:20517-21.
 176. Werbajh, S., I. Nojek, R. Lanz, and M. A. Costas. 2000. RAC-3 is a NF-kappa B coactivator. *FEBS Lett* 485:195-9.
 177. Wu, X., H. Li, and J. D. Chen. 2001. The human homologue of the yeast DNA repair and TFIIH regulator MMS19 is an AF-1-specific coactivator of estrogen receptor. *J Biol Chem* 276:23962-8.

178. Xiao, D., and S. V. Singh. 2002. Phenethyl isothiocyanate-induced apoptosis in p53-deficient PC-3 human prostate cancer cell line is mediated by extracellular signal-regulated kinases. *Cancer Res* 62:3615-9.
179. Xie, D., J. S. Sham, W. F. Zeng, H. L. Lin, J. Bi, L. H. Che, L. Hu, Y. X. Zeng, and X. Y. Guan. 2005. Correlation of AIB1 overexpression with advanced clinical stage of human colorectal carcinoma. *Hum Pathol* 36:777-83.
180. Xu, C., G. Shen, C. Chen, C. Gelinas, and A. N. Kong. 2005. Suppression of NF-kappaB and NF-kappaB-regulated gene expression by sulforaphane and PEITC through IkappaBalpha, IKK pathway in human prostate cancer PC-3 cells. *Oncogene* 24:4486-95.
181. Xu, F. P., D. Xie, J. M. Wen, H. X. Wu, Y. D. Liu, J. Bi, Z. L. Lv, Y. X. Zeng, and X. Y. Guan. 2007. SRC-3/AIB1 protein and gene amplification levels in human esophageal squamous cell carcinomas. *Cancer Lett* 245:69-74.
182. Xu, J., L. Liao, G. Ning, H. Yoshida-Komiya, C. Deng, and B. W. O'Malley. 2000. The steroid receptor coactivator SRC-3 (p/CIP/RAC3/AIB1/ACTR/TRAM-1) is required for normal growth, puberty, female reproductive function, and mammary gland development. *Proc Natl Acad Sci U S A* 97:6379-84.
183. Yan, J., C. T. Yu, M. Ozen, M. Ittmann, S. Y. Tsai, and M. J. Tsai. 2006. Steroid receptor coactivator-3 and activator protein-1 coordinately regulate the transcription of components of the insulin-like growth factor/AKT signaling pathway. *Cancer Res* 66:11039-46.
184. Yao, T. P., G. Ku, N. Zhou, R. Scully, and D. M. Livingston. 1996. The nuclear hormone receptor coactivator SRC-1 is a specific target of p300. *Proc Natl Acad Sci U S A* 93:10626-31.
185. Ying, H., F. Furuya, M. C. Willingham, J. Xu, B. W. O'Malley, and S. Y. Cheng. 2005. Dual functions of the steroid hormone receptor coactivator 3 in modulating resistance to thyroid hormone. *Mol Cell Biol* 25:7687-95.
186. Yu, C., Y. G. Shin, A. Chow, Y. Li, J. W. Kosmeder, Y. S. Lee, W. H. Hirschelman, J. M. Pezzuto, R. G. Mehta, and R. B. van Breemen. 2002. Human, rat, and mouse metabolism of resveratrol. *Pharm Res* 19:1907-14.
187. Zhang, D. D., and M. Hannink. 2003. Distinct cysteine residues in Keap1 are required for Keap1-dependent ubiquitination of Nrf2 and for stabilization of Nrf2 by chemopreventive agents and oxidative stress. *Mol Cell Biol* 23:8137-51.
188. Zhang, D. D., S. C. Lo, J. V. Cross, D. J. Templeton, and M. Hannink. 2004. Keap1 is a redox-regulated substrate adaptor protein for a Cul3-dependent ubiquitin ligase complex. *Mol Cell Biol* 24:10941-53.
189. Zhang, J., T. Ohta, A. Maruyama, T. Hosoya, K. Nishikawa, J. M. Maher, S. Shibahara, K. Itoh, and M. Yamamoto. 2006. BRG1 interacts with Nrf2 to selectively mediate HO-1 induction in response to oxidative stress. *Mol Cell Biol* 26:7942-52.
190. Zhang, Y., P. Talalay, C. G. Cho, and G. H. Posner. 1992. A major inducer of anticarcinogenic protective enzymes from broccoli: isolation and elucidation of structure. *Proc Natl Acad Sci U S A* 89:2399-403.
191. Zhao, J., J. Wang, Y. Chen, and R. Agarwal. 1999. Anti-tumor-promoting activity of a polyphenolic fraction isolated from grape seeds in the mouse skin two-stage initiation-promotion protocol and identification of procyanidin B5-3'-gallate as

- the most effective antioxidant constituent. *Carcinogenesis* 20:1737-45.
192. Zhou, G., Y. Hashimoto, I. Kwak, S. Y. Tsai, and M. J. Tsai. 2003. Role of the steroid receptor coactivator SRC-3 in cell growth. *Mol Cell Biol* 23:7742-55.
 193. Zhou, Y., and A. S. Lee. 1998. Mechanism for the suppression of the mammalian stress response by genistein, an anticancer phytoestrogen from soy. *J Natl Cancer Inst* 90:381-8.
 194. Zhu, M., and W. E. Fahl. 2001. Functional characterization of transcription regulators that interact with the electrophile response element. *Biochem Biophys Res Commun* 289:212-9.
 195. Zipper, L. M., and R. T. Mulcahy. 2003. Erk activation is required for Nrf2 nuclear localization during pyrrolidine dithiocarbamate induction of glutamate cysteine ligase modulatory gene expression in HepG2 cells. *Toxicol Sci* 73:124-34.
 196. Zipper, L. M., and R. T. Mulcahy. 2002. The Keap1 BTB/POZ dimerization function is required to sequester Nrf2 in cytoplasm. *J Biol Chem* 277:36544-52.

CURRICULUM VITAE

Jung-Hwan Kim

EDUCATION

- 2009 Ph.D. in Pharmaceutical Science, Rutgers, the State University of New Jersey
- 2000 M.S. in Pharmacy, Seoul National University, Rep. of KOREA
- 1996 B.S. in Genetic Engineering, Soonchunhyang University, Rep. of KOREA

PROFESSIONAL EXPERIENCE

- 2003 – 2003 Research Specialist, National Creative Research Initiative Center for the Study of CNS Zinc, University of Ulsan College of Medicine, Seoul, KOREA
- 2001 – 2002 Research Specialist, College of Pharmacy at Seoul National University, Seoul, KOREA
- 2000 – 2001 Research Intern, College of Pharmacy at Seoul National University, Seoul, KOREA

PUBLICATION

- 1) Yu S, Shen G, Khor T. O, **Kim J.H.**, Kong AN. (2008) Curcumin inhibits Akt/mammalian target of rapamycin signaling through protein phosphatase-dependent mechanism. *Mol Cancer Ther.* 7: 2609-2620
- 2) Li W, Yu S, Liu T, **Kim JH**, Blank V, Li H, and Kong AN. (2008) Heterodimerization with small Maf proteins enhances nuclear retention of Nrf2 via masking the NESzip motif. *Biochim Biophys Acta.* 1783(10):1847-56
- 3) **Kim, J.H.**, Na, H.K., Pak, Y.K., Lee, Y.S., Lee, S.J., Moon, A. and Surh, Y.J. (2008) Roles of ERK and p38 mitogen-activated protein kinases in phorbol ester-induced NF-kappaB activation and COX-2 expression in human breast epithelial cells. *Chem Biol Interact.* 30;171(2):133-41
- 4) Keum, Y.S., Yu, S., Chang, P.P.J., Yuan, X., **Kim, J.H.**, Xu., C., Han J., Agarwal A. and Kong, A.H. (2006) Mechanism of action of sulforaphane: Inhibition of p38 MAPK isoforms contributing to the induction of antioxidant response element (ARE)-mediated Heme Oxygenase-1 (HO-1) in human hepatoma HepG2 cells. *Cancer Res.* 66(17):8804-13.
- 5) Keum Y.S, Han Y.H, Liew C, **Kim J.H.**, Xu C, Yuan X, Shakarjian M, Chong S and Kong, A.H. (2006) Induction of heme oxygenase-1 (HO-1) and NAD[P]H: quinine oxidoreductase 1 (NQO1) by a phenolic antioxidant, butylated hydroxyanisole (BHA) and its metabolite, tert-butylhydroquinone (tBHQ) in primary cultured human and rat hepatocytes. *Pharm Res.* 23(11):2586-94.
- 6) Xu C, Yuan X, Pan Z, Shen G, **Kim JH**, Yu S, Khor TO, Li W, Ma J, Kong AN. (2006) Mechanism of action of isothiocyanates: the induction of ARE-regulated genes is associated with activation of ERK and JNK and the phosphorylation and nuclear translocation of Nrf2. *Mol Cancer Ther.* 5(8):1918-26

- 7) Khor, T.O., Keum, Y.S., Lin, W., **Kim, J.H.**, Hu, R., Shen, G., Xu, C., Gopalakrishnan, A., Reddy, B., Zheng, X., Conney, A.H. and Kong, A.N. (2006) Combined Inhibitory Effects of Curcumin and Phenethyl Isothiocyanate on the Growth of Human PC-3 Prostate Xenografts in Immunodeficient Mice. *Cancer Res*, **66**, 613-621.
- 8) Yuan X, Xu C, Pan Z, Keum YS, **Kim JH**, Shen G, Yu S, Oo KT, Ma J, Kong AN. (2006) Butylated hydroxyanisole regulates ARE-mediated gene expression via Nrf2 coupled with ERK and JNK signaling pathway in HepG2 cells. *Mol Carcinog*. 45(11):841-50.
- 9) **Kim, J.H.**, Lee, K.W., Lee, M.W., Lee, H.J., Kim, S.H. and Surh, Y.J. (2006) Hirsutenone inhibits phorbol ester-induced upregulation of COX-2 and MMP-9 in cultured human mammary epithelial cells: NF-kappaB as a potential molecular target. *FEBS Lett*. 23;580(2):385-92.
- 10) Xu, C., Shen, G., Yuan, X., **Kim, J.H.**, Gopalakrishnan, A., Keum, Y.S., Nair, S. and Kong, A.N. (2006) ERK and JNK signaling pathways are involved in the regulation of activator protein 1 and cell death elicited by three isothiocyanates in human prostate cancer PC-3 cells. *Carcinogenesis*, 27(3):437-45.
- 11) **J.-H. Kim**, C. Xu, Y.-S. Keum, B. Reddy, A. Conney, and A.-N. T. Kong (2005) Inhibition of EGFR signaling in human prostate cancer PC-3 cells by combination treatment with with phenylethyl isothiocyanate and curcumin. *Carcinogenesis*, 27(3):475-82.
- 12) Jeong, W.S., Keum, Y.S., Chen, C., Jain, M.R., Shen, G., **Kim, J.H.**, Li, W. and Kong, A.N. (2005) Differential expression and stability of endogenous nuclear factor E2-related factor 2 (Nrf2) by natural chemopreventive compounds in HepG2 human hepatoma cells. *J Biochem Mol Biol*, 38, 167-76.
- 13) K.W Lee*, **J.-H. Kim***, H.J. Lee, and Y.-J. Surh. (2005) Curcumin Inhibits Phorbol Ester-Induced Up-Regulation of Cyclooxygenase-2 and Matrixmetalloproteinase-9 by Blocking ERK1/2 Phosphorylation and NF-kB Transcriptional Activity in MCF10A Human Breast Epithelial Cells. *Antioxidants & Redox Signaling*. 7(11): 1612-1620. *, equally contributed
- 14) Z.-H. Chen, Y.-J. Hurh, H.-K. Na, **J.-H. Kim**, Y.-J. Chun, D.-H. Kim, K.-S. Kang, M.-H. Cho, Y.-J. Surh (2004) Resveratrol inhibits TCDD-induced expression of CYP1A1 and CYP1B1 and catechol estrogen-mediated oxidative DNA damage in cultured human mammary epithelial cells, *Carcinogenesis*, 25(10):2005-13.
- 15) Lee, J.-Y., **Kim, J.-H.**, Hong, S. H., Lee, J. Y., Cherny, R. A., Bush, A. I., Palmiter, R. D. and Koh, J.-Y. (2004) Estrogen decreases zinc transporter 3 expression and synaptic vesicle zinc levels in mouse brain. *J. Biol. Chem.*, 279(10):8602-7.
- 16) Yuan L, Wagatsuma C, Sun B, **Kim JH**, Surh YJ. (2003) The role of beta-glucuronidase in induction of apoptosis by genistein combined polysaccharide (GCP) in xenogeneic mice bearing human mammary cancer cells. *Ann NY Acad Sci.*, 1010:347-9.
- 17) Lee, J.-Y., **Kim, J.-H.**, Palmiter, R. D. and Koh, J.-Y. (2003) Zinc released from metallothionein-III may contribute to hippocampal CA1 and thalamic neuronal death following acute brain injury. *Experimental Neurology*, 184:337-347.
- 18) Yuan L, Wagatsuma C., Yoshida M, Miura T., Mukoda T., Fujii H., Sun B., **Kim JH** and Surh YJ. (2003) Inhibition of human breast cancer growth by GCP (genistein combined polysaccharide) in xenogeneic athymic mice: involvement of genistein biotransformation by beta-glucuronidase from tumor tissues. *Mutat Res.*, 523-524:55-62.
- 19) Chung, M.-H., **Kim, J.-H.**, Keum, J.-S., Lee, S. S. and Surh Y.-J. (2003) Genistein inhibits NF- B-dependent COX-2 expression in human breast epithelial cells. *Journal of Korean Association of Cancer Prevention*, 7(4): 229-232

- 20) **Kim, J.-H.**, Na, H.-K. and Surh, Y.-J. (2002) Investigation of Carcinogenic Potential of TCDD in the Human Epithelial Cell Line. *Environmental Mutagens & Carcinogenesis*. 22(4): 312-3
- 21) Lee, M.W., **Kim, J.H.**, Jeong, D.W., Ahn, K.H., Toh, S.H. and Surh Y.J. (2000) Inhibition of cyclooxygenase-2 expression by diarylhetanoids from the bark of *Alnus hirsuta* var. *sibirica* . *Biol. Pharm. Bull.*, 23: 517-518.
- 22) Hurh, Y.- J. **Kim, J.-H.**, Jang, J.-H., Ahn, B.-Z. and Surh, Y.-J (2000) Anticarcinogenic activity of a novel anthraquinone derivative DHAQ-97 : Induction of apoptosis in human breast cancer cell line MCF7. *Environmental Mutagens & Carcinogenesis* 20: 14-20.
- 23) Hurh, Y.- J., **Kim, J.-H.**, Seo, H.-J., Kong, G. and Surh, Y.-J. (1999) Anticarcinogenic activity of resveratrol, a major antioxidant present in red wine: Induction of apoptosis in human cancer cells. *Environmental Mutagens & Carcinogenesis* 19: 56-62.

BOOK REVIEW

- 1) Young-Sam Keum, Seong Su Han, **Jung-Hwan Kim**, Jeong-Hill Park and Young-Joon Surh. Chemopreventive activities of heat-processed ginseng. In dietary anticarcinogens and antimutagens: Chemical and biological aspects (I.T. Johnson and G.R. Fenwick eds.), 274-278, Royal Chemistry of Society, London, 1999.